

Waste Characteristics of Spent Nuclear Fuel from a Pebble Bed Reactor

by

Paul E. Owen

B.S., Aerospace Engineering, United States Military Academy (1990)
M.S., Engineering Management, University of Missouri – Rolla (1995)

SUBMITTED TO THE NUCLEAR ENGINEERING DEPARTMENT IN PARTIAL
FULFILLMENT OF THE REQUIREMENTS FOR THE DEGREE OF

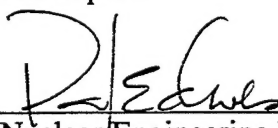
MASTER OF SCIENCE IN NUCLEAR ENGINEERING
AT THE
MASSACHUSETTS INSTITUTE OF TECHNOLOGY

JUNE 1999

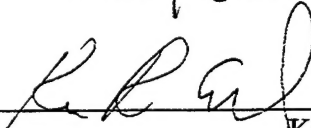
© 1999 Paul E. Owen. All rights reserved.

The author hereby grants to MIT permission to reproduce
and to distribute publicly paper and electronic
copies of this thesis document in whole or in part.


Signature of Author _____


Nuclear Engineering Department
May 7, 1999

Certified by _____


Ken Czerwinski
Associate Professor of Nuclear Engineering
Thesis Supervisor

Certified by _____


Ronald Ballinger
Professor of Nuclear Engineering
Thesis Reader

Accepted by _____

Sow-Hsin Chen
Chairman, Department Committee on Graduate Students

19990722 027

DTIC QUALITY INSPECTED 4

DISTRIBUTION STATEMENT A
Approved for Public Release
Distribution Unlimited

Waste Characteristics of Spent Nuclear Fuel from a Pebble Bed Reactor

by

Paul E. Owen

Submitted to the Nuclear Engineering Department
on May 7, 1999 in partial fulfillment of the
requirements for the Degree of Master of Science in
Nuclear Engineering

ABSTRACT

A preliminary comparative assessment is made of the spent fuel characteristics and disposal aspects between a high-temperature, gas cooled, reactor with a pebble bed core (PBR) and a pressurized water reactor (PWR). There are three significant differences which impact the disposal characteristics of PBR spent pebble fuel from PWR spent fuel assemblies. Pebble bed fuel has burn-up as high as 100,000 MWD(t)/MTHM and thus, there is significantly less activity and decay heat in the fuel when it is disposed. The large amount of graphite in the waste form leads to a low power density and more waste per unit volume than a typical PWR. Pebble Fuel contains a protective layer of Silicon Carbide. The theoretical spacing of waste packages of spent pebble fuel given its unique characteristics as applied to the conditions of Yucca Mountain is of major concern when determining the cost of disposing of the larger volumes of spent pebble fuel. Graphite is a unique waste form and atypical of waste designated for Yucca Mountain. The interactions of silicon carbide with uranium oxide fuel and its implications to long term storage at the repository are examined.

There are three primary conclusions to this thesis. First, the area required to store pebble fuel is less than the area required to store light water reactor spent fuel. Second, graphite has excellent characteristics as a waste form. The waste form of the spent pebble fuel is more robust and will perform better than light water reactor fuel at the United States repository at Yucca Mountain. Third, a secondary phase forms between the layers of silicon carbide and the uranium oxide fuel. The secondary phase retards the release of radionuclides to the environment.

Thesis Supervisor: Ken Czerwinski
Title: Associate Professor of Nuclear Engineering

Acknowledgments

The support and the guidance of various people in the Nuclear Engineering Department at MIT made this report possible. I wish to thank Dr. Andrew C. Kadak for the vision of aggressively pursuing the development of an experimental pebble bed reactor and thus creating an interesting and unique opportunity for me to be a part of an emerging technology. Throughout this project, Dr. Kadak has provided numerous opportunities for me to grow intellectually as well as various forums to present my work.

Secondly, I wish to thank Professor Ken Czerwinski for providing a superior learning environment. His enthusiasm, guidance, and vision kept me on track through what proved to be a steep learning curve. In addition to Professor Czerwinski's help, Gary Cerefice proved to be an invaluable source of information and instruction. Gary's patience and commitment to helping fellow students is something without which I could not have completed this report.

I would like to thank the United States Army for the opportunity to pursue this degree and funding this tremendous educational opportunity. Hopefully their investment will reap dividends.

Finally and most importantly, I wish to acknowledge my wife, Wendy, for all the support during our geographical separation for the past two years. Her understanding and encouragement were essential to my motivation and the completion of this work.

Table of Contents

	<u>Page</u>
Title Page	1
Abstract	2
Acknowledgements	3
Table of Contents	4
List of Figures	6
List of Tables	7
 Chapter 1: Introduction	 8
1.1. Pebble Bed Reactor Background	9
1.2. Organization	11
1.3. References	14
 Chapter 2: Fundamentals of the Pebble Bed Reactor	 15
2.1. Basis for Comparison: The AVR Program	15
2.2. The Fuel Sphere	16
2.3. Natural Safety	20
2.4. Pebble Bed Design Characteristics	21
2.4.1. TRISO Fuel Element Performance	28
2.4.2. Fission Product Behavior	31
2.5. Conclusions	33
2.6. References	34
 Chapter 3: Disposal of Pebble Bed Spent Nuclear Fuel	 37
3.1. Yucca Mountain Standards	37
3.2. Empirically Determined Characteristics	43
3.3. Derived Characteristics	47
3.4. Fuel Elements per Waste Package	52
3.5. Storage Area Requirements	54
3.6. Decay Heat of Waste Package	57
3.7. Implications of Results	61
3.8. References	62

Chapter 4: Graphite as a Waste Form	64
4.1. Durability	66
4.1.1. Corrosion Resistance	66
4.1.2. Thermal Conductivity and Thermal Expansion	67
4.2 Chemical Stability	68
4.2.1. Combustibility	69
4.2.2. Leach Rates	72
4.3. Quantity of Waste Contained in the Primary Barrier	73
4.4. Conclusions	74
4.5. References	76
Chapter 5: Silicon Carbide and Uranium	77
5.1. Experimental Overview and Procedure	78
5.2. Characterization of Samples	79
5.3. Uranium Speciation	87
5.4. Interpretation of Results	90
5.5. Conclusions	93
5.6. References	94
Chapter 6: Conclusions and Recommendations	95
6.1. Conclusions	95
6.1.1. Storage Requirements	96
6.1.2. Graphite as a Waste Form	97
6.1.3. Silicon Carbide and Uranium	98
6.2. Recommendations	98
Appendix A – Supporting Calculations of Waste Volume Data	101
Appendix B – Decay Heat Supporting Calculations	105
Appendix C-1 -- UV Spectroscopy Data and Graphs	108
Appendix C-2 -- Speciation Data	131
Appendix C-3 -- Speciation Data Cell Formulas	134

List of Figures

	<u>Page</u>
2-1. Pebble Fuel Microsphere	16
2-2. Pebble Fuel	17
2-3. Fractional Release of Radionuclides	19
2-4. PBR Fuel Handling System	23
2-5. Top View of PBR Core	26
2-6. Side View of PBR Core	27
 3-1. PWR 21 Waste Canister	 39
 5-1. UV-Spectroscopy Output	 81
5-2. UV Standardization Graph	83
5-3. Comparison of Uranium Concentrations	86
5-4. Uranium Concentration Trend Lines	91
5-5. Uranium Speciation with First and Second Hydroxide Species	92

List of Tables

	<u>Page</u>
1-1. United States Nuclear Power Reactors – 1998	13
1-2. World Nuclear Power Reactors – 1998	13
2-1. Pebble Bed Design Specifications	21
2-2. Important Fission Products	32
3-1. PWR 21 Waste Canister Dimensions	40
3-2. Waste Acceptance Design Parameters	42
3-3. Empirically Determined Factors	43
3-4. Operating Characteristics of the PBR	46
3-5. Operating Characteristics of the PWR	46
3-6. Derived Factors	47
3-7. Fuel Elements per PWR 21 Waste Package	53
3-8. Waste Package Design Choice	53
3-9. Storage Area Requirements	55
3-10. Decay Heat of a PBR Waste Package	60
3-11. Decay Heat of a PWR Waste Package	60
4-1. Thermal Conductivity of Waste Matrix Materials	68
4-2. Thermodynamic Properties at 25 °C	70
4-3. Leach Rates of Waste Matrix Materials	73
5-1. UV Standardization Reference Data	82
5-2. Uranium Concentration with SiC	85
5-3. Uranium Concentration without SiC	85
6-1. Storage Area Requirements	97

Chapter 1: Introduction

Nuclear power must overcome significant problems if it is to remain a viable energy alternative in the future. Public perception, cost and effects of disposal, proliferation concerns, safety and high capital costs are issues that must be overcome. This thesis addresses the issue of nuclear waste disposal by comparing disposal characteristics of the current nuclear power plants with a fresh look at the Pebble Bed Reactor (PBR). With its significantly different design, the PBR has the potential to address many of the problems which currently plague the nuclear power industry.

There are three distinct differences between the light water reactor technology and its associated waste when compared with the PBR. First, because of a lower power density, the PBR has a larger volume of waste. However, the activity and the decay heat associated with the PBR waste are much lower per unit volume than the LWR reactor waste. Second, the primary moderator and dominant material in the spent pebble waste form is graphite. The graphite is shaped in the form of billiard ball size spheres. This waste form differs significantly from the Zircaloy clad fuel assemblies of the LWR. Finally, the pebble fuel kernel is encapsulated in a layer of silicon carbide that acts as a fission product barrier which is not present in LWR fuel.

These significant differences are issues that must be understood before establishing any final disposal plans for spent pebble fuel. This work addresses how these differences affect waste disposal characteristics of spent pebble fuel. It will be demonstrated that the spent fuel from a PBR will 1) occupy less space in the repository

for a given reactor power, 2) be more stable with respect to release of fission products during disposal than LWR spent fuel, and 3) prevent migration of radionuclides during storage better than LWR spent fuel.

1.1. Pebble Bed Reactor Background

The PBR has been intensely studied and investigated in the past [1-1]. However, the power industry choice has always been the light water reactor (LWR). The LWR has dominated the nuclear power industry and there has been little deviation from its basic concept in the evolution of the nuclear power plant. A fundamental problem with the current light water reactor designs is that the core cannot cool itself naturally. While LWR technology has been under constant honing and refining throughout the nuclear power age, one can argue that the light water reactor technology has evolved at the expense of advanced reactor designs. Current LWR designs are not competitive with respect to other forms of energy such as combined cycle natural gas.

This report examines a different type of reactor: The high-temperature gas-cooled reactor (HTGR) with a pebble bed core and gas turbine. The Pebble Bed Reactor is “naturally” safe. Conduction and convection of residual heat to the surrounding environmental conditions are sufficient to cool the core during all emergency conditions. Because the PBR is “naturally safe” it does not require the complex safety systems that increase construction, operations, and maintenance costs for the light water reactor. The LWR also suffers from a negative public perception. Images of the accident at Three Mile Island will always be associated with the light water reactor technology.

For the above reasons, a modular HTGR with a pebble bed core and a gas turbine generator provides a compelling alternative to light water reactors. The PBR achieves the design goal of natural safety under any accident scenario. Chapter 2 provides a more detailed discussion of how this is accomplished.

PBR development has been extensive in Germany until recently [1-1]. From 1966-1988, an experimental, 40MW(t) reactor operated for a total of 21 years. This small reactor was the prototype for several larger German designs including the Thorium High Temperature Reactor (THTR-300), the High Temperature Reactor (HTR-100), and the HTR-Modul reactor. With varying power outputs, these reactor designs were intended to be the next generation of nuclear power for Germany. However, because of political decisions and the economic constraints of unifying Germany, the technology was not further developed. The German engineers were extremely confident that they had developed the future of nuclear energy. One scientist lamented the cancellation of the project by expressing that his largest fear was that some other country would take the next steps in the commercial production of power from this source [1-1]. German scientists saw a home market and a large export market for these small reactors that could be tailored to fit the electricity grid constraints of developing nations.

Recently, the South Africa electric utility, ESKOM, has determined that the German PBR design will economically meet their country's future needs for power. In addition to development for internal use, they also plan to export their finished product to developing nations. Still in the experimental phase of development, the South Africans have taken the basic design of the German AVR and modified it to meet their specific conditions and needs. They plan on having an operational test plant by 2003.

Because of the extensive development and testing done as part of the German AVR program, this thesis uses the operating characteristics of the AVR as the basis for comparison to light water reactors.

1.2. Organization

This report is organized into four sections. Chapter 2 is a detailed description of the high-temperature, gas reactor with a pebble bed core. Chapter 3 presents an analysis of the waste generation and storage area requirement for a pebble bed reactor compared with a representative light water reactor. Chapter 4 presents an analysis of the suitability of graphite as a waste form. Chapter 5 takes a brief look at the interaction of the silicon carbide layer of the fuel particle with the uranium oxide core.

The report focuses initially on the larger waste disposal issues in dealing with the millions of spent fuel pebbles that must be disposed of for each reactor. Next, the individual spent fuel pebble is more closely analyzed for its suitability for long term storage based on the dominant component, graphite. Finally, on a smaller scale, an analysis of the individual microsphere is conducted to develop an initial understanding of how the silicon carbide layer affects the migration of radionuclides. This section will show that a secondary phase forms between the silicon carbide layer and the fuel kernel of the microsphere. The secondary phase is a result of the interaction of silicon carbide and the uranium in the fuel. Experimental results will show that this, yet to be characterized, phase will retard the migration of the most soluble form of Uranium, U(VI).

Each section contributes information to the larger questions associated with the PBR design:

- 1) How do we store the waste?
- 2) What are the long-term storage considerations?

Under current regulations, pebble fuel is not specifically taken into consideration for final disposal in the planned United States repository at Yucca Mountain [1-3]. Pebble fuel falls into the "other" category that the Department of Energy has not addressed for final disposition. There is, however, other spent fuel similar to the graphite waste form of the spent pebble fuel. Spent fuel from the United States experimental high-temperature gas reactor at Fort St. Vrain, Colorado is graphite based. Therefore, the Department of Energy is familiar with this waste form, but to date has not addressed its disposal at Yucca Mountain.

For final disposal characterization, this report assumes that the PBR will be widely used as a source of power thus contributing a significant volume of waste that must be considered specifically for final disposal. This report will not completely answer the long-term behavior of spent pebble fuel. Specifically as applied to the United States, the unique dry and oxidizing conditions of Yucca Mountain need to be analyzed.

Throughout this introduction, references have been made to "light water reactors." In order to gain a more direct and relevant comparison, the PBR will be compared specifically to the pressurized water reactor version of the light water reactor. This simplification is made because of the larger prevalence of the PWR in the United States. Table 1-1 summarizes the types and numbers of light water reactors operating in the United States at the end of the year 1998. When the global situation is considered, the

results are similar. Table 1-2 lists the numbers and types of reactors in operation throughout the world. Based on the dominance of the PWR, its characteristics will be analyzed against the characteristics of the Pebble Bed Reactor.

Table 1-1. United States Nuclear Power Plants --1998 [1-2]

Pressurized Water Reactors	72
Boiling Water Reactors	35
Totals	107

Table 1-2. World Nuclear Power Reactors – 1998 [1-2]

Pressurized Water Reactors	251
Boiling Water Reactors	92
Gas-Cooled Reactors, all types	34
Heavy-water Reactors, all types	38
Graphite Moderated Light Water Reactors	15
Liquid Metal Fast Breeder Reactors	3
Totals	433

1.3. References

1-1. Baumer, R., et al, AVR – Experimental High-Temperature Reactor: 21 Years of Successful Operation for a Future Energy Technology, Association of German Engineers (VDI) – The Society for Energy Technologies, Dusseldorf, 1990.

1-2. “World List of Nuclear Power Plants.” Nuclear News, March 1999, pages 33-56.

1-3. United States Department of Energy, Site Characterization Progress Report: Yucca Mountain, Nevada, Number 16, Office of Civilian Radioactive Waste Management, October 1997, DOE/RW-0501.

Chapter 2: Fundamentals of Pebble Bed Reactors

The Pebble Bed Reactor is not a new idea. The German government developed this technology in the 1960's [2-18]. They operated the small, 40 MW(t) AVR from 1968 to 1988, continuously improving every aspect of the basic principles of safety as the main design parameter. From the AVR, the Germans developed and licensed larger plants with the same design goal of making the reactor naturally safe. Although the AVR program was halted in 1988, it proved a successful testing ground for a new type of reactor that cooled itself naturally with on-line refueling. The simple design implied quick construction and lower operating and maintenance costs. This chapter closely examines the German experience with the AVR and establishes the fundamental characteristics of a representative pebble bed reactor that will be used throughout the rest of this report as the reference PBR.

2.1. Basis for Comparison: The AVR Program

The PBR has the potential to solve some the problems that are plaguing the nuclear power industry today. It can compete economically for several reasons. First, the naturally safe design of the reactor eliminates the need for complex safety systems. The silicon carbide barriers constitute literally millions of small safety systems built into each core because of the design of the fuel. Each silicon carbide layer acts as a tiny pressure vessel for a small amount of fuel. This TRISO fuel design is the basis of the pebble bed reactor (TRISO design and concepts are discussed further in Section 2.2). Second, small, modular

reactors can be constructed in an assembly line fashion and then shipped for fast on site construction. With factory construction, this reactor design attempts to address the financial problems through economies of production instead of the light water reactor theory of economies of scale.

2.2. The Fuel Sphere

The Pebble Bed Reactor incorporates the primary design consideration of keeping coated fuel particles intact for any possible operation or accident scenario. This is the fundamental design criterion. If this criterion is achieved, the reactor will be naturally safe. The TRISO pebble fuel kernel design is the primary barrier to fission product release and the most significant design parameter of natural safety. Figure 2-1 illustrates the various layers and the configuration of the TRISO fuel particle, also referred to as the microsphere. In a deviation from the LWR, graphite in the fuel and the reflectors of the core acts as the moderator.

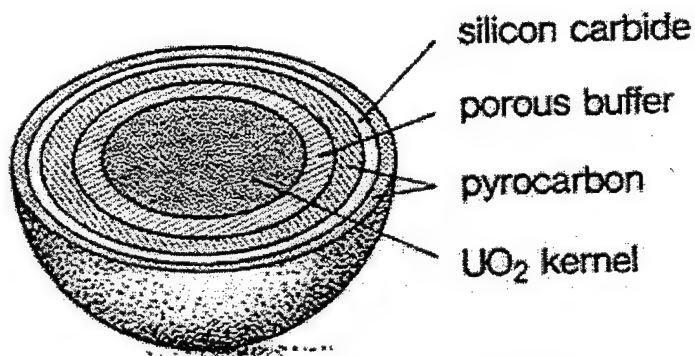


Figure 2-1. Pebble Fuel Microsphere.

Figure 2-2 demonstrates the loading and the various layers of pebble fuel. The silicon carbide layer of the microsphere is situated between protective layers of pyrolytic graphite. The buffer inside the inner pyrolytic graphite layer allows for the expansion of gases generated in the fuel kernel. The innermost region of the microsphere consists of the fuel.

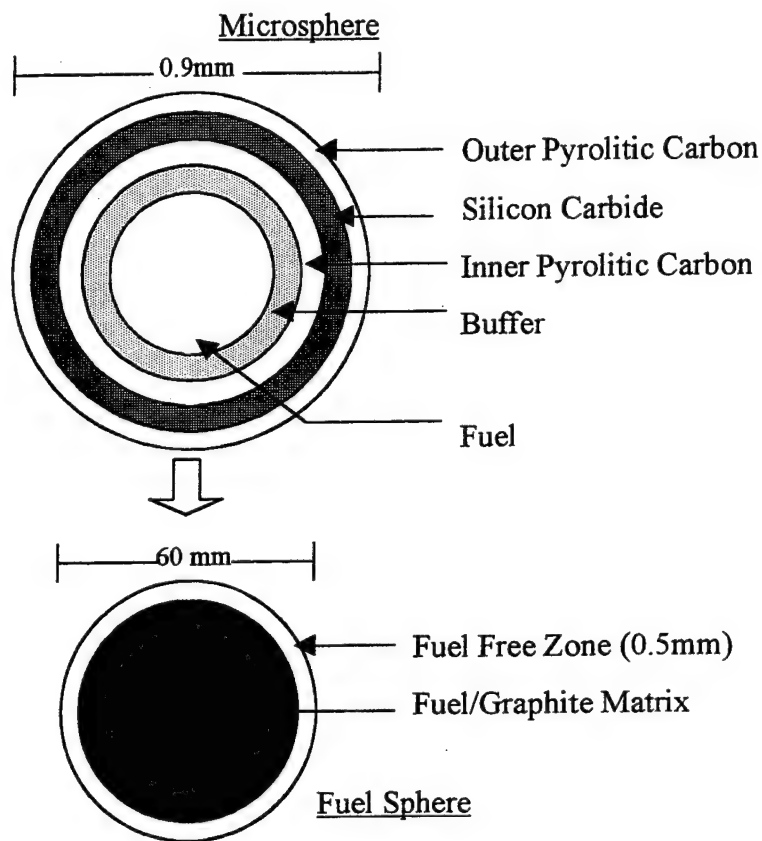


Figure 2.2 Pebble Fuel

The second part of Figure 2-2 is the fuel sphere. For the AVR fuel sphere, there is approximately 11,000 microspheres imbedded in a graphite matrix material. The ESKOM design differs in the fact that there are 23,000 microspheres imbedded in the fuel sphere of the same radius. The higher number of microspheres per fuel sphere in the ESKOM design

allows for fewer fuel spheres in a core with the same power rating as a reactor based on the AVR design. The final layer of the fuel sphere is a protective, fuel free graphite shell. The purpose of this layer is to provide durability and structural strength during operation and disposal.

The limits of the natural safety of the PBR are based on the heat limits of the silicon carbide layer within the microsphere. After being continuously exposed to temperatures of 1600°C or higher for more than 200 hours of operation, the silicon carbide layer begins to breakdown. As a result, fission products begin to escape the pebble fuel. The solution to this problem is to design the reactor so that temperatures never exceed 1600°C in any imaginable operating or accident scenario. Couple this criteria with another simple idea that the reactor will cool itself down naturally, using the natural laws of heat conduction, heat convection, and radiation. The result is a naturally safe reactor that will allow for simple operation and safe, clean, power that can be operated in any part of the world.

The maximum temperature and natural cooling of the reactor lead to one driving design constraint. The 1600°C maximum temperature is more restrictive than the natural cooling. If natural cooling were the only goal, core temperatures could go much higher. However, because the microspheres begin to fail after 200 hours of operation above 1600°C, this becomes the constraining design parameter. Figure 2-3 represents results of annealing tests conducted on microspheres used in the AVR [2-2]. This figure indicates that after 200 hours of exposure to 1600°C temperatures, the microspheres begin to fail and there is an associated increase in fractional release of the indicated fission products. It is interesting to note that the fractional release of ^{110m}Ag remains constant throughout the annealing process.

This is true for this isotope at all temperatures. This isotope is primarily an operational concern. The short half-life (250 days) will not make it radiologically significant after disposal. The significance of fission products is further discussed in Section 2.3.

A direct consequence of the maximum temperature is a relatively low mean core power density of 3.5 MW/m^3 . Higher power densities result in fuel temperatures greater than 1600°C . The low power density and the natural cooling design parameters limit the thermal power of the Pebble Bed Reactor to a maximum of 250 MW. The resulting core shape is tall and thin. The control rods are located outside of the core. They are built into the

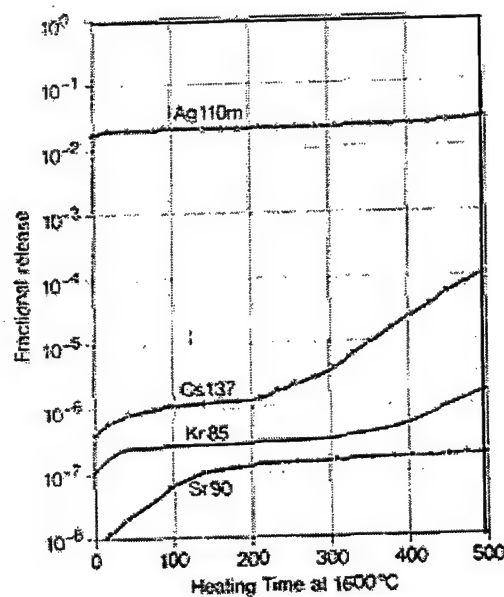


Figure 2.3. Fission Product Fractional Release.

inner graphite reflector. The control rods must be close enough to the fuel to allow them to have a neutronic affect on the core. From the AVR experience, German engineers determined that the core diameter could be no greater than three meters. Control rods,

located outside of the flowing pebble bed core, could not be used to control reactivity in core diameters larger than this.

2.3. Natural Safety

Primary safety concerns for any nuclear reactor are core meltdown and release of fission products to the environment. The conclusions of extensive studies of the German AVR were that the probability of a core heat-up accident occurring are zero because of its ability to dissipate heat at greater rates than it is generated [2-11]. Release of radionuclides through primary system depressurization combined with either water or air ingress plays a more significant role in evaluating the safety. However, with the silicon carbide coated microspheres, fission products are largely retained inside the silicon carbide layer of intact microspheres. One exception to this is the behavior of ^{110m}Ag . The low fractional release and short half-life (250 days) of this isotope and additional fission product barriers within the confinement building ensure there are no environmental or health impacts. Because of the stability of the silicon carbide layer, the dominant source term for fission product release will be the small number of microspheres that are defective by means of manufacturing flaws [2-3].

The reactor's negative temperature coefficient ensures that any increase in temperature results in a decrease in reactivity. The Doppler broadening effect increases the number of absorbed neutrons and as a result, less fissions occur and less heat is generated.

The Pebble Bed Reactor is much easier to operate than current light water reactors. In the PBR, the complex safety systems associated with light water reactors are not

necessary. The complex testing, maintenance, and operating procedures working in conjunction with the safety systems are also not needed. The possibility of human operator error instigating an accident is significantly reduced because operator action is not required to make this reactor safe.

2.4. Pebble Bed Design Characteristics

The primary system of a pebble bed reactor is contained within the pressure vessel. A summary of the design specifications is included in Table 2-1. The core is comprised of approximately 360,000 spherical fuel pebbles. Each spherical fuel pebble contains approximately 11,000 individual microspheres embedded in a graphite matrix. Each

Table 2-1. Pebble Bed Reactor Design Specifications.

Thermal Power	250 MW
Core Height	10.0 m
Core Diameter	3.0 m
Pressure Vessel Height	16.0 m
Pressure Vessel Diameter	5.6 m
Number of Fuel Elements	360,000
Microspheres/Fuel Element	11,000
Fuel	UO ₂
Fuel Element Diameter	60 mm
Fuel Element Enrichment	8%
Uranium mass/Fuel Pebble	7 g
Coolant	Helium
Helium Mass Flow Rate	120 kg/sec (100% power)
Helium Pressure	80 bar
Mean Power Density	3.5 MW/m ³
Number of Control Rods	6
Number of Absorber Ball Systems	18

microsphere is 0.9mm in diameter. No microspheres are allowed in the outer 5mm of the sphere. The outer layer is a protective matrix of solid graphite. The spherical fuel pebble is 60mm in diameter. The South African design has slightly different specifications with essentially the same performance parameters. For example, the South African core will consist of 216,000 fuel spheres. Each fuel sphere will contain approximately 23,000 microspheres. However, both cores will have a similar power density to meet the conditions of natural safety.

Continuous improvement in fuel design eventually led to the TRISO coated fuel particles. These particles are the primary deterrent to fission product release. Each microsphere contains approximately 0.6 mg of low enriched uranium (LEU). The enrichment level is typically 8%.

Figure 2-4 represents the fuel handling system of the PBR. The spherical fuel pebbles funnel through the core, providing heat through fission. Helium gas is the coolant. Cold helium from the top of the pressure vessel passes through the core, efficiently removing the heat and transporting it to the intermediate heat exchanger. It is forced down through the core by means of blowers just outside of the pressure vessel on the upper surface. Once a spherical fuel pebble passes through the core, it is funneled through a fuel handling system. The fuel handling system controls the flow and dissipation of fuel spheres throughout plant operation. It continuously sorts the fuel spheres, discarding the spent and damaged fuel, and returning the remaining fuel spheres to a properly distributed position in the core.

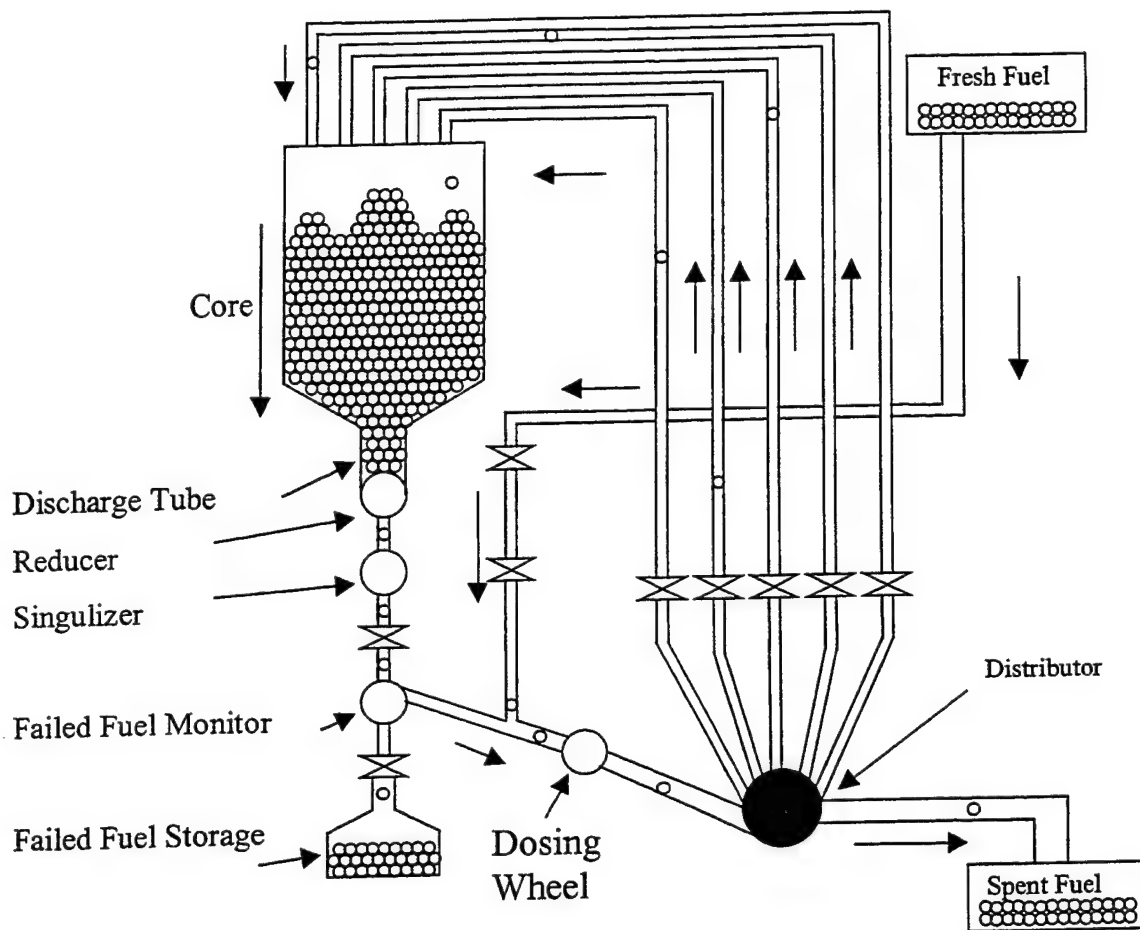


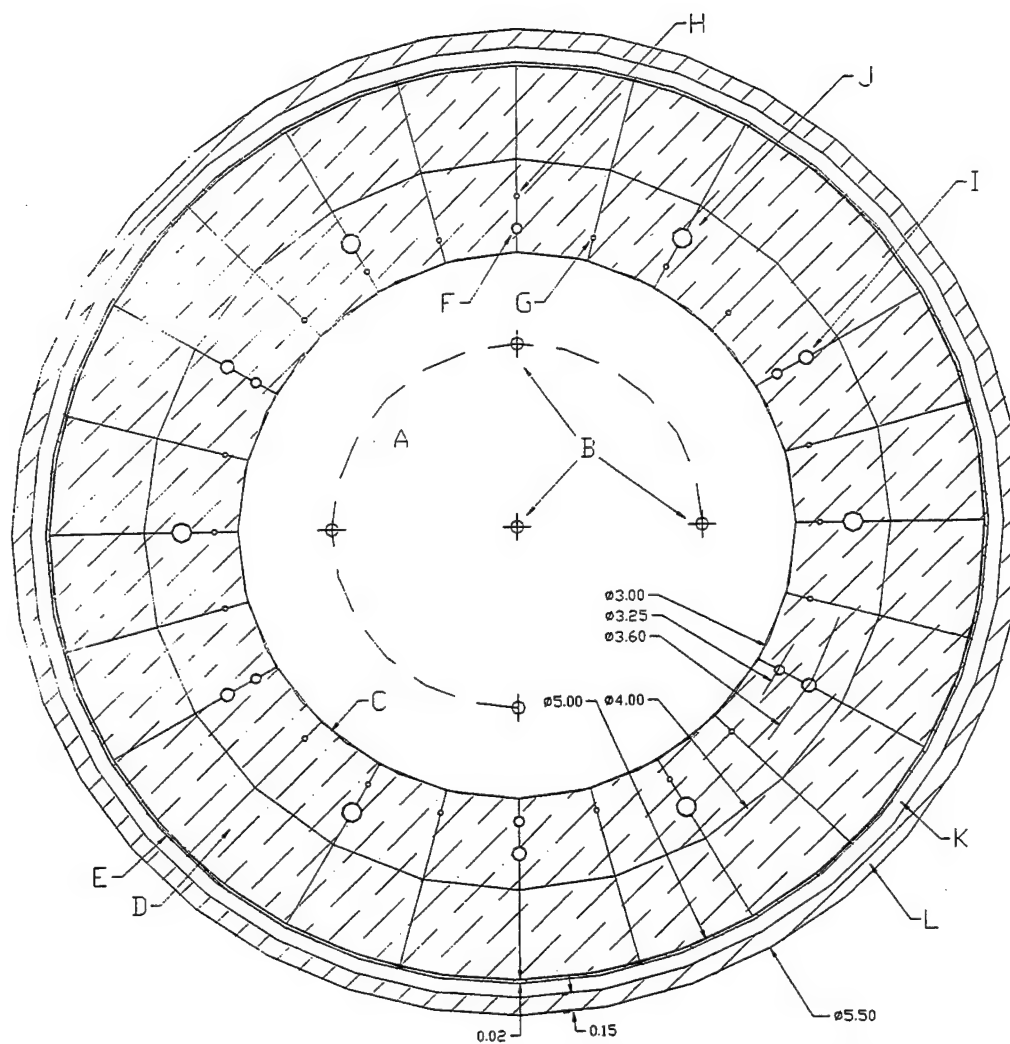
Figure 2-4. PBR Fuel handling System.

The first stage of the fuel handling system is the fuel sphere discharge tube. This tube is 500 mm wide to allow the fuel to flow freely without worry of bridging effects during passage of the fuel spheres. The reducer is at the bottom of this tube. This is a disc with a hole slightly larger than the fuel. It spins to collect the fuel, one ball at a time, at regular intervals. Here the fuel spheres enter the fuel bunker, where the singulizer transfers them individually to the failed fuel separator [2-1]. This device identifies the defective spheres

and scrap fragments and sends them to the scrap container. The rest proceed to the elevator, where the burn-up is measured. The extent of burn-up in each pebble is measured by the amount of the gamma radiation from ^{137}Cs . If a sphere has exceeded its burn-up limit, it will be discarded and sent to a spent fuel pebble storage facility. A full fuel pebble from a reservoir of fresh fuel pebbles will replace the spent fuel pebble. The spheres are differentiated by the amount of remaining fuel and returned pneumatically to the top of the core. There are five positions for the balls to enter the top of the core. The outer regions are for low burn-up fuel and one central region is for the high burn-up fuel. During steady state operation, approximately 3,000 fuel pebbles circulate through this system daily. Approximately 350 fuel pebbles each day will be discarded and replaced by a fresh fuel pebble. Fuel pebbles will pass through the core an average of 15 times before reaching their final burn up of approximately 100,000 MWD(t)/MTHM [2-4].

The vessel design consists of several layers of materials. Figure 2-5 is a horizontal cross-section of the pressure vessel. Figure 2-6 represents two side views of the PBR core. Two layers of graphite reflectors structurally support the fuel pebbles in the core. The inner graphite reflector contains numerous cylindrical tubes for reactivity control, helium gas flow, and the fuel sphere circulation system. Reactivity is primarily controlled by the mass flow rate of the helium. This system automatically equilibrates mass flow rate changes, reactivity and core temperatures. However, as a back up safety system and added reactivity control, six boronated control rods are situated in the inner reflector. Unlike light water reactors, these control rods are not in the core. The control rods are placed in the reflector in order to simplify the core and prevent damage to fuel pebbles during rod movement.

There are 18 channels for an absorber ball control system. A second back up safety system is based on boronated control spheres. These spheres are a graphite boron mix with a diameter of 10mm. They are stored in containers located above the top reflector and drop freely into the reflector channels on demand [2-1]. Surrounding the outer reflector is a core barrel. This provides additional structural stability for the core. The pressure vessel is the outermost surface of the primary side of the reactor.



- | | |
|---|----------------------------------|
| A | Pebble Bed Core |
| B | Fuel Drop Points (5) |
| C | Inner Reflector |
| D | Outer Reflector |
| E | Core Barrel |
| F | Control Rod Channels (6) |
| G | Absorber Ball Drop Channels (18) |
| H | Absorber Ball Lift Channel (1) |
| I | Pebble Fuel Lift Channels (5) |
| J | Coolant Flow Channels (6) |
| K | Stagnant Helium Gap |
| L | Pressure Vessel |

Figure 2-5. Horizontal Cross Section of PBR Core.

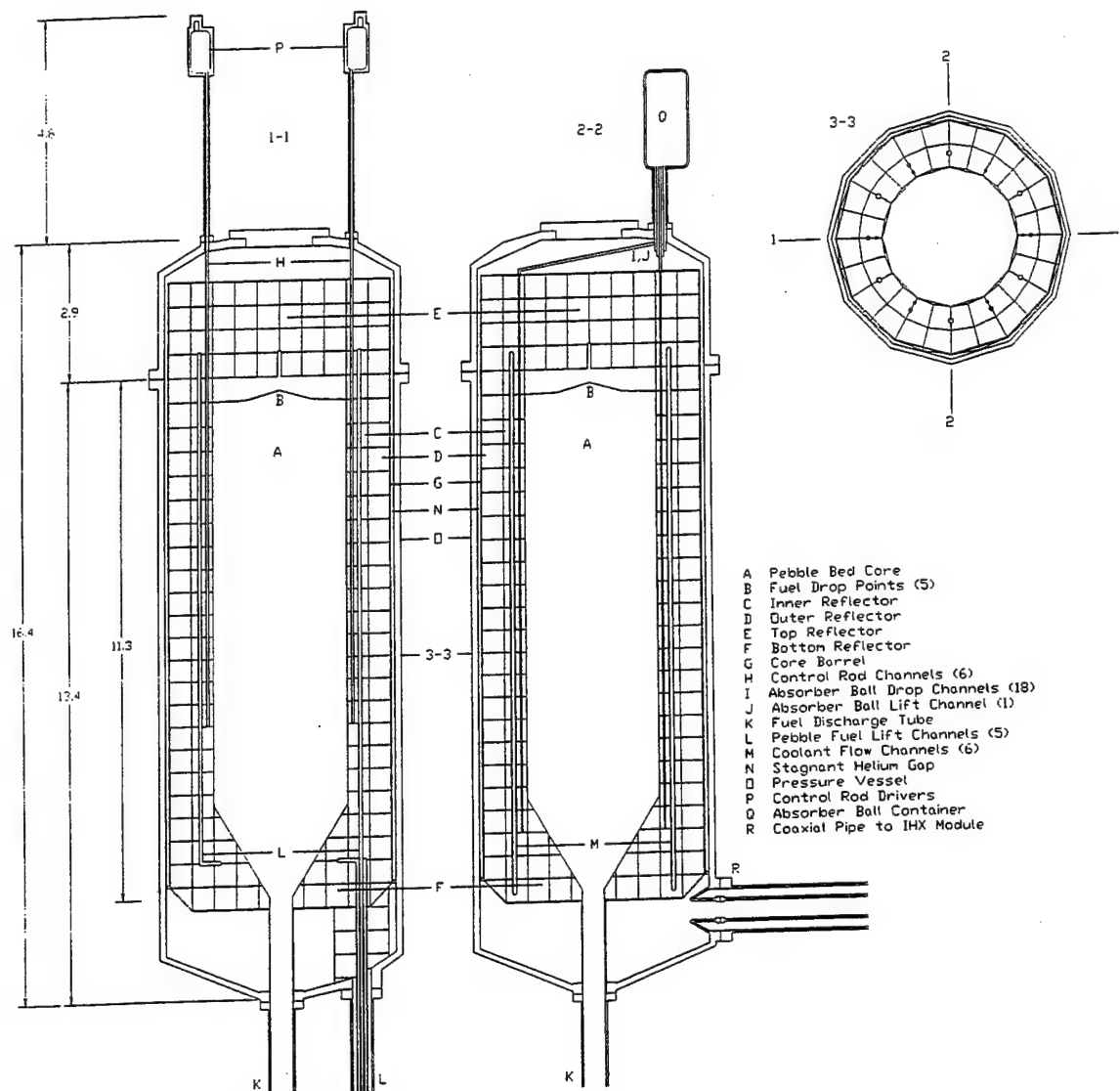


Figure 2-6. Side View of PBR Core.

2.4.1. TRISO Fuel Performance

The TRISO fuel pebbles provide fission product containment while withstanding the pressure from fission gases and the high temperatures and thermal gradients. Each fuel pebble has a diameter of 60mm and contains approximately 11,000 coated microspheres within a graphite matrix. Each 0.9mm microsphere has an inner 0.5mm diameter UO_2 fuel kernel that is coated with layers of pyrocarbon (PyC) and silicon carbide (SiC) to prevent fission product release. These microspheres compose the inner matrix, while the outermost 5mm layer consists of graphite without fuel particles as the final barrier from the coolant. The durability characteristics of this graphite, fuel-free, shell provide protection for the microspheres and prevent the coatings from being damaged by mechanical or chemical impacts that exist in the fuel circulation process within the reactor [2-1].

During normal operating conditions, the maximum steady state temperature of the microsphere is approximately 850°C. However, the silicon carbide layer effectively contains fission products for approximately 200 hours of exposure at 1600°C. Therefore, the PBR is designed in such a way that the maximum fuel pebble temperatures are limited, by natural means, to values of less than 1600°C in all accident conditions. HOEG, the fuel manufacturing company in Hanau, Germany, has manufactured over a million fuel spheres with $(\text{Th,U})\text{O}_2$ microspheres and over 500,000 UO_2 fuel spheres for the AVR and THTR experimental reactors. This experience has shown that there are very few defective coated particles ($3-4 \times 10^{-5}$ failure fraction). Therefore, a low coolant activity is maintained [2-5].

As has been pointed out earlier, the PBR fuel concept relies on the effectiveness of individual, kernel silicon carbide and pyrocarbon layers to act as barriers to fission product release. This is in contrast to the "defense in depth" concept used by the LWR design. For this reason, it is critical that manufacturing defects as well as failure during operation be minimized. The German experience with the fuel sphere manufacturing process has led to one defective microsphere for every 15,000 microspheres manufactured [2-5]. This corresponds to less than one defective microsphere per fuel sphere. The fractional release of fission products from a fuel sphere with one defective microsphere is 6.5×10^{-5} in a worst case core heat up scenario [2-6]. Steady state operating temperatures are lower. The activity released from the fuel of defective particles is too small to result in significant accident consequences [2-6]. Even if fission products are released from the fuel pebble, they are still contained within the core by sorption with the colder graphite materials or by plating out on reactor surfaces.

Because the PBR is designed such that, under the worst accident scenarios, the maximum core temperature will never exceed 1600°C, it is impossible for fuel spheres in a small modular HTGR to fail from being exposed to excessive temperatures. It follows that the main accident scenario for the PBR is depressurization combined with water or air ingress. In this scenario, the small fractions of radionuclides that have plated out on reactor surfaces are re-mobilized. This presents the potential for fission product release to the environment.

Because the maximum core temperature is limited, there is a corresponding limit to the mean power density of the core. Residual heat is completely removed from the low

power density core by the natural dynamics of conduction, convection, and radiation.

Under depressurization accident conditions, the core will heat up to approximately 1500°C 60 hours after the accident is initiated. At this point, the negative temperature coefficient decreases the reactivity of the core. The core gradually cools to an equilibrium temperature of 1100°C 600 hours after the accident begins with no dependence on control rods or absorber ball systems [2-1]. This depressurization accident also assumes helium blowers have ceased to function. This theory has been proven in tests conducted with the AVR [2-1].

The principal safety feature of this reactor is that, even in the case of failure of all active cooling systems and complete loss of coolant, the fuel pebble temperatures remain within failure limits and there is virtually no release of radioactive fission products from the fuel spheres.

The dominant source term for fission product release will be the small number of particles with defective coatings due to undetected flaws in the manufacturing process [2-9]. There are two potential manufacturing defects. First, there is potential that one or more layers of the microsphere will not form properly during the manufacturing steps. The second defect is heavy metal contamination of the outer pyrolytic carbon layer. In this case, fission products are initially outside of the silicon carbide layer. The graphite matrix of the fuel pebble is the only layer that inhibits the transport of these fission products. However, coated particle defects during the microsphere manufacturing process are rare, random events [2-21].

The most convincing aspect of the natural safety of the PBR is the experimental evidence given by AVR operation experience and tests. Safety problems never occurred in the AVR although operational disturbances with prolonged shutdowns were frequent [2-10].

2.4.2. Fission Product Behavior

The fuel particle retains virtually all fission products except for those listed in Table 2-2. The increase in Cs, Sr, and Kr release after a long maximum temperature exposure represents the failure of the silicon carbide layer. The relatively constant fractional release of ^{110m}Ag indicates that the silicon carbide layer's retention capability of this radionuclide is not time dependent at a temperature of 1600°C . Under normal operating conditions, approximately 82% of ^{110m}Ag is retained within the microsphere while 18% escapes [2-8]. Silver eventually plates out on the interior surfaces of the primary system. The cesium release is four orders of magnitude lower than silver. However, cesium's longer half-life makes it the most radiologically relevant isotope [2-8]. Plate out of radionuclides does not inhibit plant operation. It does however, play a role in a depressurization, air ingress, or water ingress accident. Any of these scenarios can mobilize the radionuclides that have been deposited on system surfaces, potentially releasing them to the environment. The largest amount of radionuclide deposition within the primary system of any one isotope is only 18% (^{110m}Ag) during normal operation. Even in the case of a depressurization accident, fission products will be contained within the fuel sphere because accident scenarios do not produce temperatures higher than the fuel particle failure criteria. From these experiments, German

scientists concluded that any hazardous radiation dose to the environment could be excluded [2-5].

Table 2-2. Important Fission Products [2-7]

<u>Solid Fission Products</u>	<u>Half Life</u>	
^{134}Cs	2 years	- quickest release from fuel - highest sorption in buffer
^{137}Cs	30 years	- quick release from fuel - high sorption in buffer
^{90}Sr	28 years	- good retention in fuel
^{131}I	8 days	- released only from defective particles
$^{110\text{m}}\text{Ag}$	250 days	- significant during normal operations - quick transport through coatings - highest release from fuel element
<u>Fission Gases</u>	<u>Half Life</u>	
^{85}Kr	11 years	- indicator of particle defects
^{133}Xe	5 days	- indicator of particle defects

2.5. Conclusions

Discussion of the characteristics of the pebble bed reactor is necessary to understand the qualities and the implications of the waste that is produced as a result of operation. This section described the fundamental operating characteristics of the pebble bed reactor. From these characteristics, performance criteria that are relevant to the production and storage of waste will be developed in the following chapters.

2.6. References

- 2-1. Lohnert, G.H., "Technical Design Feature and Essential Safety Related Properties of the HTR-Module," Nuclear Engineering and Design, Volume 121, July 1990, pages 259-275.
- 2-2. Rehm, W., W. Jahn, and K. Verfondern, "Present Results and Further Developments on Safety Analysis of Small and Medium Sized HTRs for Core Heat-Up Accidents," Nuclear Engineering and Design, Volume 109, September/October 1988, pages 281-287.
- 2-3. Nabielek, H., W. Kuhnlein, and W. Schenk, "Development of Advanced HTR Fuel Elements," Nuclear Engineering and Design, Volume 121, July 1990, pages 199-210.
- 2-4. "Pebble Bed Modular Reactor – Executive Summary," ESKOM Document Number PB-000000-79/1, Issue C.
- 2-5. Lohnert, G.H., H. Nabielek, and W. Schenk, "The Fuel Element of the HTR-Module, A Prerequisite of an Inherently Safe Reactor," Nuclear Engineering and Design, Volume 109, September/October 1988, pages 257-263.
- 2-6. Rehm, W., W. Jahn, and K. Verfondern, "Present Results and Further Developments on Safety Analysis of Small and Medium-Sized HTRs for Core Heat Up Accidents," Nuclear Engineering and Design, Volume 109, September/October 1988, pages 281-287.
- 2-7. Izenson, M.G., Effects of Fuel Particle and Reactor Core Design on Modular HTGR Source Terms, Ph.D. Thesis submitted to the Nuclear Engineering Department at The Massachusetts Institute of Technology, February 1987.
- 2-8. Iniotakis, N., and C.B. von der Decken, "Radiological Consequences of a Depressurization Accident Combined with Water Ingress in and HTR Module-200," Nuclear Engineering and Design, Volume 109, September/October 1988, pages 299-305.
- 2-9. Arndt, E., et al, "Design Status of the HTR 500 Power Plant," Nuclear Engineering and Design, Volume 109, September/October 1988, pages 263-268.
- 2-10. Kroger, W., H. Nickel, and R. Shulten, "Safety Characteristics of Modular High Temperature Reactors," Nuclear Safety, April-May-June 1987.
- 2-11. Katscher, W., R. Moormann, K. Verfondern, C.B. von der Decken, N. Iniotakis, and K. Hilpert, "Fission Product Behaviour and Graphite Corrosion Under Accident Conditions in HTR" Nuclear Engineering and Design, Volume 121, July 1990, pages 219-225.

- 2-12. Kruger, K., G. Ivens, and N. Kirch, "Operational Experience and Safety Experiments with the AVR Power Station," Nuclear Engineering and Design, Volume 109, September/October 1988, pages 233-238.
- 2-13. Wolters, J., R. Bongartz, W. Jahn, and R. Moormann, "The Significance of Water Ingress Accidents in Small HTRs," Nuclear Engineering and Design, Volume 109, September/October 1988, pages 289-294.
- 2-14. Sanchez, Rene, Passive Afterheat Removal: Sensitivity Study of Modular Pebble Bed Reactors, Masters Thesis, submitted to The Massachusetts Institute of Technology Nuclear Engineering Department, January 1986.
- 2-15. Nabielek, H., W. Kuhnlein, and W. Schenk, "Development of Advanced HTR Fuel Elements," Nuclear Engineering and Design, Volume 121, July 1990, pages 199-210.
- 2-16. Nabielek, H., K. Verfondern, and D.T. Goodin, "HTR Fuel: Prediction of Fission Product Release in Accidents," paper presented at IAEA Specialists' Meeting on Fission Product Release and Transport in Gas-Cooled Reactors, Gloucester, UK, October 22-25, 1985.
- 2-17. Schenk, W., and H. Nabielek, "Recent Results on F.P. Release and Postheating F.P. Distributions After Conduction Cooldown Simulation Tests," presentation given during ORNL Experts Meeting on MHTGR/HTR Fuel Performance Under Accident Conditions, June 8-9, 1989.
- 2-18. Baumer, R., et al, AVR—Experimental High-Temperature Reactor: 21 Years of Successful Operation for a Future Energy Technology, Association of German Engineers (VDI) – The Society for Energy Technologies, Dusseldorf, 1990.
- 2-19. Gottaut, H. and K. Kruger, "Results of Experiments at the AVR Reactor," Nuclear Engineering and Design, Volume 121, July 1990, pages 143-153.
- 2-20. Hosegood, S.B., "An Independent Engineer's View of the Modular HTGR," Nuclear Engineering and Design, Volume 109, September/October 1988, pages 221-226.
- 2-21. Hrovat, M., H. Huschka, A.W. Mehner, and W. Warzawa, "Spherical Fuel Elements for Small and Medium Sized HTR" Nuclear Engineering and Design, Volume 109, September/October 1988, pages 253-256.
- 2-22. Ziermann, E., "Review of 21 Years of Power Operations at the AVR Experimental Nuclear Power Station in Julich," Nuclear Engineering and Design, Volume 121, July 1990, pages 135-142.

2-23. Kirch, N., E.D. Grosser, and K.H. Herzberger, "Status and Aims of the Research and Development Program for High-Temperature Reactors," Nuclear Engineering and Design, Volume 121, July 1990, pages 167-171.

2-24. Nickel, H., F. Schubert, H. Breitling, and E. Bodmann, "Development and Qualification of materials for Structural Components for the High-Temperature Gas-Cooled Reactor," Nuclear Engineering and Design, Volume 121, July 1990, pages 183-192.

Chapter 3: Disposal of Pebble Bed Spent Nuclear Fuel

Spent fuel spheres from a Pebble Bed Reactor will need to be placed in a repository for long term storage. The most significant aspect of pebble bed spent fuel is its high volume. The high volume combined with relatively low decay heat represent the primary differences of Pebble Bed Reactor spent fuel when compared with standard light water reactor spent fuel. Typical light water reactor waste is stored on site in a spent fuel pool. Eventually, it will go into on-site dry cast storage, or it will be transferred to a long-term storage facility when the Yucca Mountain facility opens. The purpose of this chapter is to compare the space needed to store pebble bed fuel with the space needed to store light water reactor fuel. The primary assumption of this work is that repository loading emplacement techniques at Yucca Mountain, Nevada are flexible, such that spent pebble fuel in waste packages can be placed closer in proximity than light water reactor waste packages.

This chapter will identify and compare specific characteristics of spent pebble fuel and spent light water reactor fuel. This comparison is made using representative PWR and PBR values to determine the space needed to store spent nuclear fuel at the proposed repository at Yucca Mountain.

3.1. Yucca Mountain Standards

This report examines a situation in which Pebble Bed Reactors have become a prevalent source of energy in our near future. The only way to make an equitable

comparison with the PWR is to make this assumption. It allows a comparison of nuclear waste generation on a similar scale and thus creates a situation where the waste from a Pebble Bed Reactor must be treated as something other than "other" type fuel. This is currently the case in accordance with Yucca Mountain standards. The spent fuel of the United States is dominated by light water reactor spent fuel. All design and acceptance criteria are based on the packaging and characteristics of light water reactor spent fuel. There is a small fraction of fuel from the Fort St. Vrain experimental reactor that is of a graphite waste form. However, this fuel did not achieve the burn-up and other characteristics that truly represent spent pebble fuel.

Yucca Mountain waste acceptance criteria has not been fully determined yet. However, Progress Report #16 outlines what the current thinking on what the waste acceptance criteria will be [3-2]. The engineers of the Yucca Mountain Project realize that there are many different forms of spent nuclear fuel. For this reason, they have adopted a broad outline for the design of the waste canister that will contain the spent fuel. The report states "Because of the large variability in spent nuclear fuel characteristics, several waste package designs will be required to accommodate all the spent fuel earmarked for the disposal in the first repository" [3-2]. For simplicity of comparison and to reduce the number of unknowns, this report assumes that a spent fuel from a pebble bed reactor will be placed in the proposed repository at Yucca Mountain.

In dealing with the individuality of the spent fuel characteristics, the Yucca Mountain engineers also have decided that "a family of waste package designs is required, and each individual design must have a specifically designated design basis fuel" [3-2]. This is an

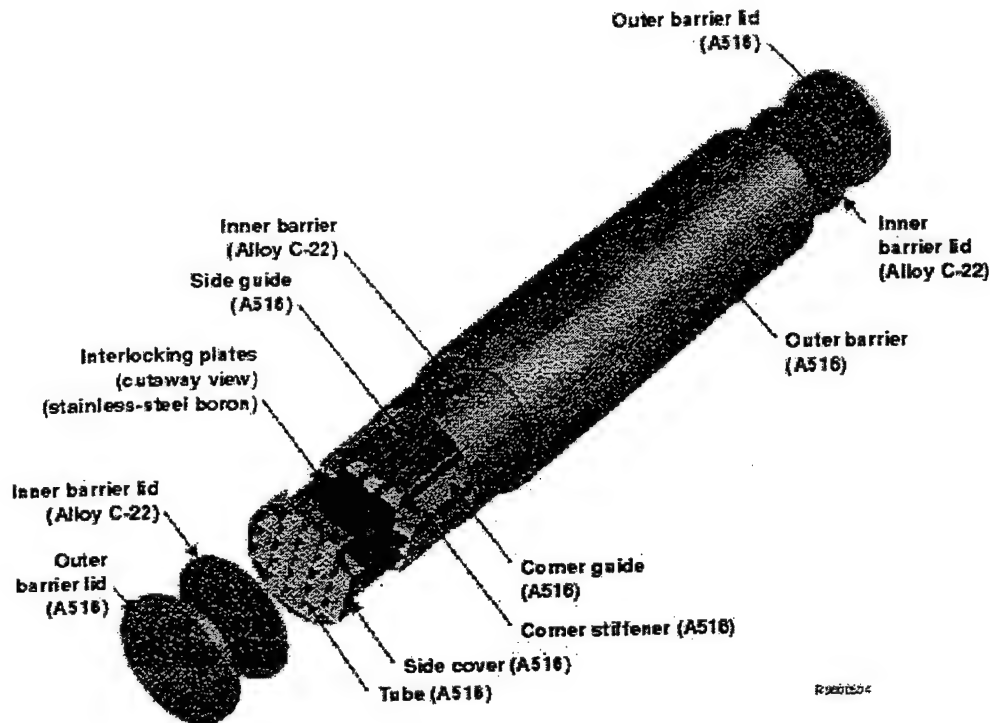


Figure 3-1. PWR 21 Spent Fuel Canister.

important aspect for the spent pebble fuel. Because the PBR fuel characteristics are so different from PWR spent fuel, using the exact same canister to store pebble fuel would create large, unneeded expense. However, for the purposes of this report, both fuel types will be placed in the same canister as a tool for comparison.

The waste package used for comparison in this report is the PWR 21. This waste package is currently being analyzed for suitability at the repository. It is designed to hold 21 pressurized water reactor assemblies. Figure 3-1 illustrates the design features of the PWR 21 spent nuclear fuel canister. The German design for spent pebble fuel includes none of the inner structure of the PWR 21 spent fuel canister [3-3].

The dimensions of the PWR 21 waste canister are summarized in Table 3-1 [3-1].

The inner dimensions of the waste package are derived from the waste acceptance criteria for Department of Energy high level waste. The Viability Assessment for Yucca Mountain specifies a 10 cm thickness for the side outer barrier and a 2 cm thickness for the inner barrier [3-24]. This thickness will strongly attenuate the gamma radiation that is capable of penetrating the container. The lids of the canisters are designed to be slightly thicker. The

Table 3-1. PWR Waste Canister Dimensions

Outer Length:	5.335 meters
Outer Diameter:	1.650 meters
Side Thickness:	12.0 cm
Lid Thickness:	13.5 cm
Inner Length	5.065 meters
Inner Diameter:	1.410 meters

total thickness of the inner barrier lid and the outer barrier lid is 13.5 cm. The thick outer layer provides structural stability while the thin inner layer is a corrosion resistant material designed to increase the design life of the waste package.

This report assumes that spent pebble fuel will use containers with the exact outer and inner dimensions of the PWR 21 waste canister. Because the graphite waste form is much more durable than the long, thin fuel assemblies of the PWR, the inner structure of the PWR 21 is not necessary. Thus, the inner structure of the PWR 21 will be removed for the purposes of storing spent pebble fuel. This concept is in conjunction with the German spent pebble fuel disposal concept [3-3]. The inner structure of the PWR 21 is designed to provide structural stability, cooling, and criticality control for the spent fuel assemblies. Because of

the much lower decay heat output and lower power densities, this structure is not necessary to control these characteristics of spent pebble fuel [3-23]. Specific design parameters are discussed in greater detail in the rest of this chapter.

The thermal loading criteria of Yucca Mountain will provide the fundamental basis for the comparison of the spent fuel types. Based on Progress Report #16, the thermal loading criteria can be summarized in two parameters. The first parameter is the heat output from a fully loaded spent fuel canister must not exceed 18 kilowatts. The heat will decrease as time passes in the repository. Therefore, the maximum heat loading occurs the time of emplacement. Heat generation within the waste package at the time of emplacement is the single strongest determining parameter for peak waste package temperature [3-1]. This important design parameter is constrained by the need to avoid cladding creep and mineral phase transformations at the emplacement drift wall [3-1]. Based on this thermal loading criteria, the second important parameter is determined. Results from Progress Report #16 determine that "preliminary analyses have indicated that initial individual waste package heat loads of around 18 kW can be tolerated assuming a reference repository thermal loading range of 80 to 100 metric tons of uranium per acre" [3-2]. Based on this statement, a mid-range value of 90 MTU/acre will be used throughout this report for the thermal loading criteria for Yucca Mountain. This parameter is determined through modeling and experimentation done by the Yucca Mountain Project. There is a direct relationship between heat output per canister and the amount of heavy metal that can be placed within an acre. Experimental results from the Yucca Mountain Project indicate that lower heat output waste packages could allow for an increased amount of heavy metal allowed per acre [3-2]. The

much lower decay heat characteristics of the spent pebble fuel would allow for greater than 100 MTHM/acre currently allowed. However, this relationship is not fully understood and any conclusions would have to be supported through extensive evaluation of the waste form. This analysis is currently not available for spent pebble fuel. For these reasons, the 90 MTHM/acre standard is applied for both PWR waste and spent pebble fuel. Table 3-2 summarizes the Yucca Mountain standards.

Waste handling for pebble fuel is simple and straightforward. Spent fuel pebbles arrive at the repository site already packaged in a sealed fitted container that is lifted out of

Table 3-2. Waste Acceptance Design Parameters.

Canister Design:	PWR 21
Canister Thermal Loading:	18 kW/canister
Yucca Mountain Heavy Metal Loading:	90 MTU/acre

the storage/transportation cask and slipped into the waste canister in a one step operation. The ruggedness of the graphite spheres allows a simple "pouring" of spent fuel spheres from one container to another. The complex machinery and containers used to transfer and store light water reactor spent fuel are not needed. Light water reactor spent fuel arrives at repositories in the form of spent fuel assemblies. It requires many separate lifting and lowering operations to fill a single waste container [3-4]. Light water reactor spent fuel assemblies are extremely fragile and have the potential to break or shatter during any of these operations if accidentally dropped.

3.2 Empirically Determined Characteristics

The first step in the comparison process is to determine the fundamental operating characteristics for each type of reactor. Table 3-3 summarizes the empirically determined parameters for a pressurized water reactor and a pebble bed reactor. This section is dedicated to explaining the empirically determined characteristics outlined in Table 3-3. These characteristics are determined for one unit of each type of plant. One PBR produces 112 MW(e). One PWR produces 1000 MW(e). It is important to note throughout this report that nine PBR units would have approximately the same electrical output as one PWR unit.

The thermodynamic efficiency of the PBR was determined from two independent sources. The German engineers claim an efficiency of 45% possible with the HTR-Module [3-5] and the South Africa Utility ESKOM claims their design will achieve 45% efficiency [3-6]. The PWR efficiency of 33% is a common and accepted efficiency for a pressurized

Table 3-3. Empirically Determined Factors.

<u>symbol</u>	<u>definition</u>	<u>PBR</u>	<u>PWR</u>	
h	thermodynamic efficiency	0.45	0.33	
L	capacity factor	0.90	0.82	
th	thermal power	250	3030	MW(t)
g	grams of uranium/MWD(t)	1	1	g/MWD(t)
R	refueling rate	0.895	30	MTHM/yr
t	post irradiation cooling time	15	15	hrs
fel(m)	fuel element loading (max)	7	450,000	gU/FE
fel(av)	fuel element loading (average)	3.47	450,000	gU/FE
V	core volume (fuel only)	40.715	30	m ³
I	core inventory of heavy metals	1.25	90	MTHM

water reactor [3-7]. An HTGR is inherently more efficient because of the larger temperature differential that is achieved in the core of the PBR. Also, the gas turbine of the pebble bed is more efficient than the steam generator of the PWR.

The capacity factor of the PBR is determined from experiences of the AVR. Capacity factors as high as 92% were achieved in this experimental reactor [3-8]. Most years the AVR worked at lower capacities, however, the design assumption of the PBR in broad use infers that the experimental stage of the design is complete. Therefore, the system will be configured and engineered well and knowledgeably maintained and operated. For this reason, a capacity factor of 90% is assigned to the PBR. Due to the complexity and off-line refueling of the PWR, there is a lower capacity factor. Although some PWR power stations achieve capacity factors as high as 90%, a more representative value is 82% [3-9, 3-10].

Thermal power characteristics of the PBR were discussed in Chapter 2. As determined in that section, the thermal power of the PBR is limited to approximately 250 MW. At larger power, the PBR will lose the natural safety advantage. Therefore, 250 MW is determined as the operating power of the PBR. PWR power stations operate at a large range of thermal outputs. For the simplicity of comparison and as a representative value, the thermal output of the PWR is set at 3030 MW. This value combined with the 33% efficiency yields the convenient comparison number of 1000 MW(e).

Uranium based fission reactors produce approximately 1 gram of fission products per megawatt-day, and for each gram of uranium, approximately one gram of fission products is produced [3-13]. Since both reactor designs have uranium fuel, these values are equal.

Refueling the PBR is accomplished on-line by replacing spent fuel spheres with fresh fuel spheres. Approximately 350 fuel spheres are discarded daily [3-5]. Using this number, combined with the fuel sphere loading of a fresh fuel sphere, the PBR will need to refuel with approximately 0.895 MTU/year. The PWR will require approximately 30 MTU/year to refuel the core [3-10]. As previously stated, it is important to note the larger difference in thermal output of each reactor type when comparing these numbers.

The post irradiation cooling time for the spent fuel is assumed to be the same for both reactor types. Although on site storage at nuclear power stations across the country is indefinite based on the failure of Yucca Mountain to accept waste, a representative value of 15 years is assumed for both types of reactors [3-10].

Fuel spheres for the PBR are fully fueled when they contain 7g of 8% enriched uranium oxide. However, not every fuel sphere in the core is fully fueled. The ESKOM PBR design predicts that only half of the fuel spheres will be fully fueled throughout the core. The AVR/HTR-Module design suggests that a variable fuel sphere loading design is necessary throughout the core. The full fuel sphere power was found to be 1.4 kW [3-10]. To determine the characteristics of a representative spent fuel sphere, it is necessary to normalize the power associated with fuel spheres that contain no fuel and ones that are fully fueled. Average uranium fuel sphere power is determined by dividing the thermal power of the reactor by the number of fuel elements in the core. This process yields an average fuel element power of 0.694 kW. The average power represents an average fuel loading of 3.47 grams of uranium per fuel sphere. A representative value for the PWR is accepted as 450,000 grams of uranium per fuel assembly, or 0.45 MTHM/fuel assembly [3-9, 3-10].

The volume of space occupied by the fuel spheres in the core of the PBR is determined by multiplying the volume of one fuel sphere with the number of fuel spheres. The volume of the core itself is much larger because void space (approximately 40%) is a necessary condition in the closest packing arrangement. Within the core of a PWR, fuel assemblies occupy essentially all of the volume.

Based on the above numbers and the characteristics of the PBR and the PWR, the core inventory of heavy metal is determined by multiplying the fuel sphere/assembly loading by the number of fuel spheres/assemblies in the core. This calculation yields a result of 1.25

Table 3-4. Operating Characteristics of the PBR - 112 MW(e).

# of fuel spheres discarded per day	350
Fuel Spheres in the Core	360,000
Fuel Sphere Diameter	60 mm
Fuel Sphere Volume	113 cm ³
Fuel Spheres Circulated per day	3,000
Fuel Sphere Volume in Core	40.7 m ³
Core Height	10 m
Core Radius	1.5 m
Core Volume	70.7 m ³
Full Fuel Sphere Power	1.4 kW
Average Fuel Sphere Power	0.694 kW

Table 3-5. Operating Characteristics of the PWR - 1000 MW(e).

# of Fuel Assemblies	200
Fuel Assembly Volume	0.15 m ³
Refueling Rate	0.30 core/yr
Fuel Assemblies Discarded per year	60

MTHM for the PBR and 90 MTHM for the PWR. Table 3-4 summarizes the operating characteristics of the PBR used to determine the above factors. These factors will also be used to determine important derived factors from the assumptions made above. Table 3-5 lists the operating characteristics assumed for a typical PWR.

3.3. Derived Characteristics

There are three derived characteristics that will govern the placement of waste in a repository. These characteristics are waste package heat loading, waste volume generation rate and waste package fission product loading. To determine these important parameters, the above empirically determined characteristics and the specific characteristics of the reactor type are combined. Table 3-6 lists all derived characteristics. The remaining part of this section describes the derivation of these characteristics.

Table 3-6. Derived Factors

<u>symbol</u>		<u>PBR</u>	<u>LWR</u>	<u>units</u>
T	residence time of fuel in core	5.0	4.5	yr
Q"	core power density	3.54	101.01	MW/m ³
B	fuel discharge burnup	93,921	45,380	MWD(t)/MTHM
P	rated power	112.5	1000	MW(e)
f	fraction of core refueled each year	0.20	0.22	
d	fuel assembly density	0.062	3.000	MTU/m ³
	MWD(t)	117,402	4,084,159	MWD(t)
p	specific decay power	3.131	1.513	kW/MTU
q"	waste package loading	0.194	4.538	kW/m ³
F	waste volume generation rate	29.148	10.000	m ³ /yr
h	waste loading	5.813	136.14	(kg of fp)/m ³

The residence time of the fuel within the core is determined from available data.

Results from the HTR-Module design indicated that a full pebble will pass through the core approximately 15 times before reaching a burn-up level that warrants its removal from the reactor [3-5]. Based on AVR fuel handling experience, approximately 3,000 fuel spheres are cycled through the core each day.

With 360,000 fuel spheres in the core, it takes approximately 120 days for a fuel sphere to progress from the very top of the core to the fuel handling system. Therefore, a fuel sphere will cycle through the core three times in one year. Since a fuel sphere will pass through 15 times before reaching its burn-up limit, each fuel sphere will spent approximately five years in the core. Pressurized water reactors have improved fuel core residence time to the point where an assembly can be efficiently used in the core for 4.5 years [3-9].

Core power density is determined by dividing the rated thermal power of the plant by the volume of the core. The much lower core power density of the PBR is the major factor in the ability of the core to cool itself naturally. However, because of this small core power density, the dimensions of the 112 MW(e) PBR core are similar to the 1000 MW(e) PWR core.

Fuel discharge burn-up is determined for the PBR through the design criteria and evaluation of the HTR-Module and the design experiences of ESKOM. A realistic value for the burn-up of the spent pebble fuel is 100,000 MWD(t)/MTHM [3-6]. This value can also be calculated using the following relationship:

where:

$$\text{Burnup} = \frac{365 * L * T * Q''' }{d} \quad (3-1)$$

L = capacity factor,

T = fuel in core residence time (years),

Q''' = core power density (MW/m³)

d = fuel assembly density (MTU/m³).

This equation yields a discharge burn-up of approximately 94,000 MWD(t)/MTHM for the PBR and 45,000 MWD(t)/MTHM for the PWR. Both of these values accurately represent their respective reactor types.

The fraction of the core refueled each year is determined by taking the inverse value of the fuel in core residence time. As with the in core residence time, these values are similar for both reactor types.

Fuel assembly density is determined by dividing the core inventory of heavy metals by the volume of the fuel within the core. This number is significantly less for the PBR than the PWR because of the larger core space. The graphite within each fuel sphere occupies the majority of the fuel sphere volume within the PBR core. Hence, the PBR has a much lower fuel assembly density than the PWR.

Specific decay power is determined by using the following approximation [3-10]:

$$p = \frac{B}{2000 * t} \quad (3-2)$$

where,

p = specific decay power (kW/MTU)

B = fuel discharge burn-up (MWD(t)/MTHM)

t = post irradiation cooling time (years).

Based on this calculation, the PBR achieves approximately twice as much power per metric ton of uranium than a PWR.

The waste package loading parameter (q''') is paramount to the determination of the heat in the waste package. This parameter is determined by multiplying the specific decay power and the fuel assembly density to yield an answer in the units of kW/m³ [3-10]. This is an important determination because the amount of heat in a waste package (a Yucca Mountain loading criterion) is directly related to the volume of the waste canister. Section 3.6 contains a more robust determination of the thermal power of the waste form, and a supporting analysis for the decay heat and temperature of spent pebble fuel. The decay heat of a waste package containing spent pebble fuel aged 15 years after removal from the core is calculated to be 1.91 kW. This is similar to the 1.53 kW value determined from the above approximation. This difference is trivial. As long as the decay heat of the waste package is less than 18kW, it meets Yucca Mountain acceptance criteria.

Waste volume generation rate is determined using the following formula [3-10]:

$$F = \frac{R * V}{I} \quad (3-3)$$

where:

F = waste volume generation rate (m³/yr)

R = refueling rate (MTHM/yr)

V = core fuel volume (m^3)

I = core inventory of heavy metals (MTHM).

This parameter is a key aspect to understanding the large amount of waste that is connected with the use of the Pebble Bed Reactor. The value is significantly higher for the pebble bed because most of the volume within the waste is composed of the graphite matrix that surrounds the fuel. From the values given in Table 3-6, the 112 MW(e) PBR generates 2.91 times more waste than the 1000 MW(e) PWR. However, even though the amount of waste is greater, it has much less activity and heat. Therefore, spacing needed in a repository could theoretically be less.

The final derived parameter that must be evaluated is waste loading of fission products. This is calculated using the following formula [3-10]:

$$h = g * d * B \quad (3-4)$$

where:

h = waste loading (kg of fission products/ m^3)

g = grams of fission products/MWD(t),

d = fuel assembly density (MTHM/ m^3)

B = fuel discharge burn-up (MWD(t)/MTHM).

This value will be a governing factor in determining how many canisters can be placed in an acre at Yucca Mountain. Once again, this value is much lower for the PBR because most of the volume of waste consists of the graphite matrix of the fuel sphere.

3.4. Fuel Spheres per Waste Package

Now that the important parameters for each reactor type have been determined, the next step is to determine how many of each type of fuel elements can fit in the PWR 21 spent fuel storage canister. The answer for the PWR is simple. The canister is designed solely for this purpose and can fit 21 fuel assemblies from a pressurized water reactor. As stated previously, the control devices within the PWR 21 canister are not necessary for spent pebble fuel. The entire volume of the canister can be filled with spent fuel spheres. The number of fuel spheres that can fit in a canister can be determined by dividing the volume of one canister by the volume of one fuel sphere. Based on this calculation, 69,929 fuel spheres can fit in one PWR 21 canister. However, the closest packing of the spheres must account for void space. Typical void space within the core of the HTR-Module and AVR has been determined to be 39% [3-12]. A conservative value of 40% is adopted to allow for any coating defects or departure from spherical symmetry. The use of this factor reduces the number of fuel spheres that can geometrically fit into a PWR 21 canister with the inside structure removed to 41,957 fuel spheres. If the number of fuel spheres were unconstrained by the geometry of the canister, then over 800,000 fuel spheres could be fit into a canister and still meet the heat output constraints of Yucca Mountain. This is the equivalent volume of more than two pebble bed reactor cores. Table 3-7 summarizes the number of fuel spheres capable of fitting in one PWR 21 spent fuel storage canister. In order to place 821,000 spent fuel spheres in a single spent fuel storage canister, it would take a volume 13.5 times greater than the PWR 21. If pebble bed reactors become prevalent in the future, this waste canister

Table 3-7. Fuel Spheres per PWR 21 Waste Package.

	<u>PBR</u>	<u>PWR</u>
Heat Constrained	821,355	26
Geometry Constrained	41,957	21

design would still be impractical because of the difficulties of handling a waste package of that size and weight.

From the above discussion, it is clear the 41,957 spent fuel spheres will meet the Yucca Mountain guidelines of 18 kW/waste package. The total heat of the waste package is determined by multiplying the number of fuel spheres in waste package by the waste package loading factor (q''') and the fuel sphere volume. Based on these criteria, the heat output from a PWR 21 filled with 41,957 spent fuel spheres will be 1.53 kW. A similar calculation is done for the PWR spent fuel assemblies. Results from this analysis are indicated in Table 3-8.

Table 3-8. Waste Loading Design Choice.

	<u>PBR</u>	<u>PWR</u>
Fuel Spheres per waste package	41,957	21
Waste Package Heat	1.53 kW	15.53 kW

The weight of the waste package with the above loading criteria is of concern. The majority of volume of the PBR spent fuel is the relatively light weight graphite. Based on design weight given by the Reference Design Decision, the loaded weight of a PWR 21 waste canister with PWR spent fuel is 50,423 kg. The empty weight of a PWR 21 waste canister is 34,039 kg. The difference is the weight of the fuel assemblies from a PWR:

16,384 kg. As mentioned earlier, much of the weight of the internal structure of the PWR 21 is not needed for storage of spent pebble fuel. Therefore, the empty PWR 21 canister modified for storage of spent pebble fuel will weigh much less than the PWR 21 canister for PWR spent fuel. The weight of the spent pebble fuel is 99.99% graphite. Multiplying the number of spent fuel spheres in a waste canister by the volume of one spent fuel sphere and the density of graphite ($2,210 \text{ kg/m}^3$) [3-20] yields a spent pebble fuel weight of 10,487 kg. This is 5,897 kg less than the weight of the spent fuel from a PWR in a PWR 21 spent fuel canister. It would take approximately 65,600 spent fuel spheres to equal the weight of 21 spent fuel assemblies from a PWR. The bottom line is that graphite weighs much less than Zircaloy. (The density of Zirconium is $6,570 \text{ kg/m}^3$ [3-20]). Also, there is a higher heavy metal density in the form of uranium within the spent fuel assemblies than exists in spent fuel spheres. This weight difference takes no credit for the removal of internal structure of the PWR 21 modified for PBR spent fuel.

3.5. Storage Area Requirements

Now that a fuel sphere and assembly loading configuration has been determined, it is possible to take the next step to determine how many waste packages can be placed over one acre of land. In order to make an equitable comparison, nine PBRs producing 1008 MW(e) are compared with one PWR producing 1000 MW(e). Table 3-9 includes the results of this analysis. The remaining parts of this section explain how the values in this table were determined.

Table 3-9. Storage Area Requirements		1000 MW(e)	1000MW(e)	
	PBR	PWR		<u>units</u>
Fuel elements/waste package	41,957	21		
Fuel elements discarded/year	1,150,538	60		
Years of operation	30	30	yrs	
Fuel element storage requirement	34,516,125	1,800		
waste packages needed	823	86		
MTHM/fuel element	3.47E-06	0.45	MTHM	
MTHM/waste package	0.1456	9.45	MTHM	
MTHM/acre	90	90	MTHM/acre	
kW/waste package	1.53	15.53	kW/canister	
waste packages/acre	617	9	cansiters/acre	
Acres needed for storage	1.33	10.06	acres	
Storage Requirement	5.33	40.70	m²/MW(e)	

The number of fuel spheres per waste package was determined in the previous section. Both reactor types are constrained geometrically and not by heat for the loading of the spent fuel.

The number of fuel spheres discarded each year is based on the refueling rate. For the PBR, approximately 350 fuel spheres are discarded daily. Multiplying this number by 365 days in one year and nine PBR reactors yield a result of approximately 1.1 million fuel spheres that must be disposed of on an annual basis. A similar calculation for the spent fuel assemblies of the PWR concludes that 60 fuel assemblies must be disposed of annually. Assuming a thirty year operating life for each reactor type, the total amount of fuel that must be disposed is approximately 34 million fuel spheres for the PBR and 1,800 fuel assemblies for the PWR.

Dividing this result by the number of fuel spheres that can geometrically fit in the PWR 21 spent fuel storage canister will determine the number of canisters required for

disposal. This analysis determines that 823 modified PWR 21 canisters are needed to store thirty years worth of spent fuel from nine Pebble Bed Reactors. Eighty-six PWR 21 canisters are needed to store the spent fuel from one PWR reactor. A PBR of equal electrical output will require 9.6 times more waste canisters than a PWR.

To determine spacing requirements at Yucca Mountain, it is necessary to determine the amount of heavy metal in the spent fuel. Multiplying the amount of heavy metal per fuel sphere/assembly (as determined in Section 3.2) with the number of fuel spheres/assemblies in the waste package will yield the amount of heavy metal per waste package. Because of the higher burn-up achieved by the PBR, there is much less heavy metal in the PBR spent fuel canister than the PWR spent fuel. For this reason, spacing at Yucca Mountain can be closer for the PBR and more waste packages can be allowed in an acre.

The heat loading of the waste packages was previously determined to be 1.53 kW for the PBR waste canister and 15.53 kW for the PWR waste canister. Both of these values are below the maximum heat loading of 18 kW per waste canister dictated by waste acceptance criteria of Yucca Mountain. Because each waste package meets this criterion, 90 MTHM can be placed in one acre. This value is a median value of the 80-100 MTHM given as guidelines for the Yucca Mountain waste acceptance criteria [3-2].

The number of waste packages that will be allowed in one acre is determined by dividing the allowed value of 90 MTHM by the heavy metal loading of the waste canister. The PBR will require spacing equal to 617 canisters/acre. Nine PBRs with a 1008 MW(e) output will require a total space requirement of 1.334 acres of storage for spent fuel spheres for the 30-year operating life of the facility. The PWR will require spacing equal to 9

canisters/acre. The 30-year life of the PWR producing 1000 MW(e) will require 10.056 acres for storage of spent fuel assemblies. The PBR will require 7.54 times less space than the PWR for storage of spent nuclear fuel.

Equations used to determine the key parameters of storage area requirements and waste package heat loading are located in Appendix A. Appendix A also contains a flow sheet for these parameters outlining their dependency on operating and design characteristics.

3.6. Decay Heat of Waste Packages

The design of the repository at Yucca Mountain is controlled by radioactive decay heat [3-18]. The question is whether the spent fuel can be disposed of in its current form or if it must be processed in such a way to reduce the heat load of the waste canister to meet repository acceptance requirements. If waste decay heat levels are too high, damage to the waste package may occur. Stress in the geologic media may cause tunneling and could cause damage to the structural integrity of the repository. For these reasons, Yucca Mountain sets conservative limits on the heat load of the waste packages. As seen in the above section, this value is 18 kilowatts per waste package. Both the PBR and the PWR spent fuel are in compliance with this criterion when packaged in the PWR 21 spent fuel waste package.

The heat load of one waste package of spent pebble fuel based on the above design is determined using the following equation:

$$P(t) = P_0 * 0.066 * (t^{-0.2} - (t + t_0)^{-0.2}) \quad (3-5)$$

where:

$P(t)$ = decay power at time t , Watts

P_0 = steady state operating power of reactor, Watts

t = time after fuel was removed from reactor, years

t_0 = time of steady state power the fuel was exposed to, years [3-19].

Using this equation to predict the decay heat of one waste package requires that the parameters defined for the PBR be applied. The decay heat of the PBR waste package meets regulatory decay heat guidelines 2.5 years after the fuel has been removed from the reactor. The supporting calculations for this data are included in Appendix C. Also included in the table is the temperature of the waste package. This temperature is calculated using a simplified model consisting of a two-dimensional plane wall with a uniform heat generation rate and symmetrical boundary conditions. The decay heat from the waste package is the uniform heat generation rate. The plane wall is a cross-section of the waste package. The equation used to determine the temperature of the waste package simplifies to:

$$T_{MAX} = \frac{\dot{q} * L^2}{2k} + T_s \quad (3-6)$$

where:

T_{MAX} = the maximum temperature in the waste package, °C.

\dot{q} = uniform heat generation rate, W/m³.

L = the radius of the waste package.

k = effective thermal conductivity of interior of the waste package W/(m-K).

T_s = ambient temperature of the repository medium, °C [3-20].

The most difficult part of the above calculation is the determination of the effective thermal conductivity of the matrix of spent pebble fuel combined with the convective

properties of the void space within the waste package. This number was determined by W. Stewart et al, [3-12] in analysis associated with the cooling ability of the pebble bed core. Stewart's analysis can be directly applied to this calculation because the cylindrical geometry of the core and the waste package are proportionally similar. The materials of the fuel spheres are also the same.

The calculation uses a conservative repository temperature of 110 °C. This value is based on design criteria of Yucca Mountain. Emplacement design attempts to utilize this slightly higher than boiling temperature to keep water from reaching the waste package during the earlier (higher heat output) years of waste package emplacement. The temperature of the ambient ground around the waste package is dependent on many factors with the most significant being how close the waste packages are placed to each other. A major assumption with the placement of spent pebble fuel in the repository is that it will be placed much closer together than light water reactor spent fuel. The Yucca Mountain Project has done extensive experimentation to determine the temperature limits of the repository. This experiment is still ongoing in the form of the "Single Heater Test" and the "Drift Scale Test" [3-2]. Results of these tests will further define the thermal loading criteria of the repository.

Because of the close proximity of the PBR waste packages, this higher temperature allows for the consideration of heat from the surrounding waste packages to increase the ambient temperature of the geologic media of the repository. Table 3-10 summarizes the decay heat of one waste package for various time values.

Table 3-10. Decay Heat of a PBR Waste Package.

<u>Time after Removal</u>	<u>Decay Heat</u>	<u>Temperature (°C)</u>	<u>Repository Limit</u>
5 years	5.52 kW	178	18 kW
10 years	2.89 kW	146	18 kW
15 years	1.91 kW	134	18 kW
20 years	1.41 kW	127	18 kW

Because this report assumes that spent fuel will be stored on-site for 15 years after removal of the reactor, the temperature of the waste package at the time of emplacement at Yucca Mountain will be 134°C. The temperature calculation is important in gauging the heat associated with the waste package. However, it is important to note that temperature does not guide repository waste acceptance criteria. Decay heat is the governing criteria [3-1].

Table 3-11. Decay Heat of a PWR Waste Package.

<u>Time after Removal</u>	<u>Decay Heat</u>	<u>Temperature (°C)</u>	<u>Repository Limit</u>
5 years	47.69 kW	1239	18 kW
10 years	24.68 kW	694	18 kW
15 years	16.24 kW	494	18 kW
20 years	11.93 kW	392	18 kW

Table 3-11 represents the waste package heat and temperatures at various times after removal from a PWR core using a similar method of calculation. It is clear that residual heat and temperatures of spent fuel assemblies from a PWR are much higher than spent pebble

fuel from a PBR. Supporting calculations and assumptions used to calculate this data are in Appendix B.

3.7. Implications of Results

This analysis makes it clear that PBR spent fuel will require more waste canisters but less space for final disposal of its spent fuel. This conclusion has clear economic impacts. The cost of manufacturing and transporting the approximately 9.6 times more waste packages needed for spent pebble fuel is daunting. However, the design specifications of the waste package for spent pebble fuel provides for easier manufacturing and could potentially require thinner engineered barriers. Should a specifically designed PBR spent fuel canister be licensed, its cost has the potential to be significantly less expensive than the canister designed for PWR spent fuel. Cost savings can also be gained by the factor of 7.5 in land requirements for final disposal. Assuming a large number of operating PBR plants, the specific requirements pertaining to spent pebble fuel can be utilized. The spent pebble fuel form offers cost savings advantages only if emplacement in a repository can be designed for advantageous characteristics of high burn-up and low heavy metal content characteristic of this type of fuel. Emplacement of spent pebble fuel in a system that mirrors the current design of Yucca Mountain will not allow for space savings. Vertical bore-holes, which the Germans have used for the spent fuel of the AVR and the THTR, are the key to space savings in a repository for spent fuel with the unique characteristics of PBR fuel.

3.8. References

- 3-1. "World List of Nuclear Power Plants." Nuclear News, March 1999, pages 33-56.
- 3-2. United States Department of Energy, Site Characterization Progress Report: Yucca Mountain, Nevada, Number 16, Office of Civilian Radioactive Waste Management, October 1997, DOE/RW-0501.
- 3-3. Kirsch, N., H.U. Brinkmann, and P.H. Brucher, "Storage and Final Disposal of Spent HTR Fuel in the Federal Republic of Germany," Nuclear Engineering and Design, Volume 121, July 1990, pp. 241-248.
- 3-4. Holloway, R., An Assessment of High Level Radioactive Waste Disposal for Advanced Reactor Fuel Cycles, Thesis for masters of science in the Nuclear Engineering Department, Massachusetts Institute of Technology, May 1989.
- 3-5. Lohnert, G. H., "Technical Design Features and Essential Safety Related Properties of the HTR-Module," Nuclear Engineering and Design, Volume 121, July 1990, pages 259-275.
- 3-6. ESKOM, Pebble Bed Modular Reactor: Executive Summary, Issue C, Document Number PB-000000-79/1.
- 3-7. Todreas, N.E., and M.S. Kazimi, Nuclear Systems I: Thermal Hydraulic Fundamentals. Taylor and Francis Publishers, 1990.
- 3-8. Ziermann, E., "Review of 21 Years of Power Operation at the AVR Experimental Nuclear Power Station in Julich," Nuclear Engineering and Design, Volume 121, July 1990, pages 135-142.
- 3-9. Conversation with Professor M. Driscoll, MIT, April 7, 1999.
- 3-10. Holloway, W. R., An Assessment of High-Level Radioactive Waste Disposal For Advanced Reactor Fuel Cycles, Masters of Science Thesis submitted to The Massachusetts Institute of Technology Nuclear Engineering Department, May 1989.
- 3-11. Clack, R.W. and N. Dean Eckhoff, "On Estimating Fission-Product Radiation and Thermal-Power Source Strength," Nuclear Safety, Vol. 13, No. 1, January-February 1972.
- 3-12. Stewart, R., W. Rehm, and W. Jahn, A Contribution to the Sensitivity and Study of the Effective Thermal Conductivity in a Depressurized Pebble Bed Gas Cooled High Temperature Reactor in Connection with Temperature Calculations, Kernforschungsanlage, Julich, GmbH, Institut fur Nukleare Sicherheitsforschung, November, 1988.

- 3-13. Glasstone, S., Principles of Nuclear Reactor Engineering, 1st Edition, D. Van Nostrand Company, New York, 1955.
- 3-14. DOE/RW, Viability Assessment of a Repository at Yucca Mountain, United States Department of Energy, Office of Civilian Radioactive Waste Management, December 1998.
- 3-15. DOE/RW, Reference Design Description for a Geologic Repository, Revision 02, United States Department of Energy, Office of Civilian Radioactive Waste Management, January, 1999.
- 3-16. DOE/RW, Engineered Materials Characterization Report, Volume 3, Revision 1.1, United States Department of Energy, Office of Civilian Radioactive Waste Management, March 1998.
- 3-17. DOE/RW, Waste Acceptance System Requirements Document, Revision 03C, United States Department of Energy, Office of Civilian Radioactive Waste Management, March 19, 1999.
- 3-18. Lotts, A.L., et al, Options for Treating High-Temperature Gas-Cooled Reactor Fuel for Repository Disposal, Oak Ridge National Laboratory, Oak Ridge, Tennessee; Managed by Martin Marietta for the United States Department of Energy, February, 1992.
- 3-19. Henry, Allan F., Nuclear Reactor Analysis, Massachusetts Institute of Technology, Cambridge, MA, 1975.
- 3-20. Incropera, F.P. and D.P. De Witt, Introduction to Heat Transfer, John Wiley and Sons, New York, 1985.
- 3-21. Lotts, A.L., et al, Options for Treating High-Temperature Gas-Cooled Reactor Fuel for Repository Disposal, Oak Ridge National Laboratory, Oak Ridge, Tennessee; Managed by Martin Marietta for the United States Department of Energy, February, 1992.
- 3-22. DOE/OCRWM/YMP, Reference Design Decision, <http://www.ymp.gov/toc/rdd>.
- 3-23. Richards, M.B., D.A. Alberstein, and A.J. Neylan, "PC-MHR Spent Fuel - An Ideal Waste Form for Permanent Disposal," International Conference on Nuclear Engineering, Volume 5, American Society of Mechanical Engineers, 1996, pages 1-4.
- 3-24. DOE/OCRWM/YMP, Viability Assessment, <http://www.ymp.gov/toc/va>.

Chapter 4: Graphite as a Waste Form

The dominant characteristic of spent fuel from a PBR is the proportionally large volume of graphite. If the sum total of the volume of the microspheres is compared to the total volume of the fuel element, it is clear that graphite occupies the majority of the volume. The graphite matrix and the outer graphite protective coating comprise 99.99% of the volume of the fuel element. Thus the characteristics of graphite are of significant concern when considering spent pebble fuel for final disposal.

For the purposes of this analysis, the only protective engineered barrier considered in this section is the 5mm, fuel-free, graphite layer of the fuel sphere. No credit is taken for the engineered barrier provided by the PWR 21 waste canister. Yucca Mountain performance criteria require that the waste canister last for 1000 years. As will be seen in the following sections, this time frame is orders of magnitude less than the time required for the corrosion of the protective graphite layer of the fuel sphere. Studies by W.J. Gray conclude that graphite is at least three orders of magnitude more durable than the next best material [4-5].

The requirements for the best qualities of a waste form are varied and numerous. Each source consulted for this report has a slightly different manner for determining what the most favorable characteristics are. However, there are three characteristics that transcend all referenced reports on this topic.

These characteristics are:

- 1) Durability,
- 2) Chemical stability,
- 3) Quantity of waste contained by the primary barrier.

These qualities are not comprehensive. There are other concerns such as proliferation resistance and the short and long term safeguard requirements for final disposal. For these characteristics, all consulted studies have concluded that graphite is a better waste form than the metal alloys [4-1, 4-4, 4-5, 4-6, 4-9]. The following statements are summaries of the analysis of graphite as a waste form. "HTGR spent fuel is a superior waste form to LWR spent fuel," Oak Ridge National Laboratory [4-1]. "HTR Spent fuel elements achieve these qualities [durability and stability] to a much greater degree than other waste forms including Zircaloy-clad fuel rods irradiated in a LWR," General Atomics [4-4]. "The results confirm the expected low rates and therefore demonstrate that graphite has the potential for use in the isolation of radioactive wastes," Pacific Northwest National Laboratory [4-5]. Finally, in another Pacific Northwest National Laboratory report, "A matrix formed by cold compaction of graphite powders offers several advantages over metallic matrix materials. These advantages include exceptional corrosion resistance, high thermal conductivity, advantageous anisotropy in both thermal conductivity and thermal expansion, almost unlimited availability and very low cost" [4-9].

The Oak Ridge study looked at the possibility of removing the graphite from the microspheres within the fuel element. This procedure would greatly reduce the volume of the waste form. However, it would also remove the favorable characteristics of the graphite.

Oak Ridge concludes that this procedure could be accomplished economically and that the graphite removed from the fuel elements would be classified as low level waste [4-1].

However, the advantages of having the spent microspheres immobilized in a material with the advantageous characteristics of graphite makes retention of the graphite of the spent fuel elements favorable, even at the cost of larger volumes.

4.1. Durability

Durability is defined in terms of three characteristics: corrosion resistance, thermal conductivity, and thermal expansion. Each characteristic has a significant contribution to the overall suitability of the waste form. This section describes how graphite compares with other waste forms in terms of corrosion resistance, thermal conductivity and thermal expansion.

4.1.1. Corrosion Resistance

In the United States, graphite has been considered as an advanced material of construction for waste packages in the repository based on its extremely low corrosion rate under repository conditions [4-1]. The expected corrosion mechanism for graphite is slow oxidation. For an average temperature of 150°C within the waste package, it is estimated to take 7 billion years to oxidize one centimeter of graphite [4-1]. The temperature of the waste package is an average over the entire life of the waste in the repository. Temperatures within the waste package after being stored at the reactor site fifteen years are estimated to be approximately 134°C (See section 3.6 of this report).

These are the conditions of the waste package when placed in the repository. Since temperatures within the waste package will continue to decrease as the decay heat of the waste package decreases with time, this corrosion estimation is conservative. The outer protective graphite layer of the fuel element is 0.5 cm thick. Without considering the engineered barriers of the PWR 21, the spent fuel element of the PBR would last on the order of one billion years. It would take this long to expose the outer layer of the outermost microspheres within the fuel matrix of the fuel sphere. The engineered barriers of the waste canister have current design requirements to last for 1000 years [4-10]. Based on the Performance Assessment of Yucca Mountain, a large fraction of LWR spent fuel would become exposed within several hundred to several thousand years because of the failing of the Zircaloy cladding and corrosion of metallic canisters [4-11]. After this occurs, only the geologic media of Yucca Mountain acts as a barrier to radionuclide transport and release to the biosphere. From this information, it is clear that graphite will greatly out perform the waste package design criteria established by the Yucca Mountain Program.

4.1.2. Thermal Conductivity and Thermal Expansion

Graphite is highly heat conductive. This reduces the probability of a hot spot forming in the fuel element or in the waste package. The thermal conductivity of graphite does not vary with increasing temperatures. Table 4-1 compares the thermal conductivity value of various materials.

The high, stable thermal conductivity characteristics of graphite are a benefit in a waste form because the decay heat will be distributed about the waste package more evenly.

Also, heat will be more quickly passed from the canister to the heat sink constituting the biosphere.

<u>Table 4-1. Thermal Conductivity of Waste Matrix Materials.</u>		
<u>Material</u>	<u>Density</u>	<u>Thermal Conductivity*</u>
Pyrolytic Graphite	2.25 Mg/m ³	1840 W/(m-K)
Copper (pure)	8.93 Mg/m ³	401 W/(m-K)
Al (12%)-Si	2.70 Mg/m ³	120 W/(m-K)
Cu-Be	8.10 Mg/m ³	95 W/(m-K)
Titanium	4.50 Mg/m ³	17 W/(m-K)
Borosilicate Glass	2.20 Mg/m ³	1.2 W/(m-K)

* At room temperature [4-9].

The thermal expansion characteristics of the graphite will not vary with temperature. The low value of thermal expansion for graphite will benefit the waste form [4-9]. The graphite will tend to maintain good mechanical contact with the microspheres within the fuel element. This strong bond will prevent gaps and non-uniform stresses and will ensure the structural integrity of the fuel element.

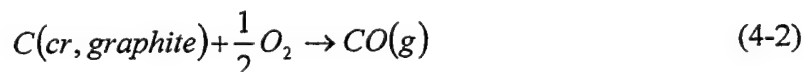
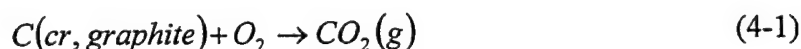
4.2. Chemical Stability

Graphite is one of the most inert elements [4-9]. Thus far, it has been established that graphite corrosion is negligible and thermal conductivity and thermal expansion do not vary with temperature. The two major issues with chemical stability are graphite reactions with oxygen (combustibility) and water (leaching). The following sections describe the conditions required for graphite to burn and the conditions required for water to penetrate the graphite layer of the fuel sphere.

4.2.1. Combustibility

There are two parts in the determination of chemical reactions: thermodynamics and kinetics. This section explores the issue of graphite combustibility in terms of these parameters and a logical analysis of the characteristics of graphite.

Thermodynamic data indicates that the reaction of graphite with oxygen to combust and produce both carbon monoxide and carbon dioxide is energetically favored. The two possible reactions of graphite with oxygen are:



Each of these equations has a negative value for Gibbs free energy, ΔG_f^0 , at standard temperature, and pressure. For reaction 4-1, $\Delta G_f^0 = -394.36$ kJ/mol. For reaction 4-2, $\Delta G_f^0 = -137.15$ kJ/mol. These negative values indicate that the reactions will occur spontaneously and will release energy under natural conditions. Reaction 4-1 will release more energy than reaction 4-2 because of its higher negative value.

Gibbs free energy is dependent on the enthalpy and the entropy of the system and can be calculated using the following formula:

$$\Delta G_f^0 = \Delta H_f^0 - T\Delta S^0 \quad (4-3)$$

where:

ΔG_f^0 = Gibbs' free energy at standard temperature and pressure, J/mol

ΔH_f^0 = standard enthalpy of formation, J/mol

T = temperature, K

ΔS° = standard entropy, J/K-mol.

Enthalpy, H , is a measure of the heat that is withdrawn from the surroundings in a constant pressure process. The change in enthalpy in both reactions is negative. Therefore, these reactions add heat to the surroundings. Such reactions are classified as exothermic, or heat producing. No energy is required to make this reaction occur. Entropy, S , is a property of a reaction that measures the natural changes in a system. Positive values for entropy indicate that a reaction will occur naturally. It is clear that a negative value for enthalpy and a positive value for entropy will make Gibbs free energy highly negative. The more negative the value of Gibbs free energy, the more spontaneous the reaction.

The complete thermodynamic data for these reactions is included in Table 4-2 [4-12]. Also included in the data is a comparison of the graphite form of carbon with the diamond form of carbon. The specific heat, C_p° , is included for each molecule as a reference to complete the thermodynamic data but is not used in the determination of Gibbs free energy.

Table 4-2. Thermodynamic Properties at 25 °C				
	ΔH_f°	ΔG_f°	S°	C_p°
	(kJ/mol)	(kJ/mol)	(J/K-mol)	(J/K-mol)
C(c,graphite)	0	0	5.74	8.53
O ₂ (g)	0	0	205.037	29.35
CO(g)	-110.53	-137.15	197.556	29.12
CO ₂ (g)	-393.51	-394.36	213.677	37.11
C (c,diamond)	1.897	2.9	2.38	6.12

To summarize the work above, the highly negative values of Gibbs free energy for the reaction of graphite with oxygen indicate that this process is energetically favorable according to thermodynamic considerations. Graphite will spontaneously react with oxygen to form carbon dioxide. However, as determined through experimentation and referenced in the previous section, graphite is extremely stable and corrodes at rates far slower than almost all materials. Graphite is tremendously abundant. The reason why oxidation of graphite does not occur is because the kinetic properties of the reaction are highly unfavorable. Also, the conditions for the thermodynamic reaction do not often occur. This determination can only be done through experiment. The rest of this section describes why the kinetic properties of graphite reacting with oxygen are unfavorable and ultimately why graphite will not oxidize or combust under repository conditions.

There are three primary reasons why graphite matrix of the spent fuel elements will not burn. First, The surface area to volume ratio is very low. The rate at which oxygen can reach graphite will not support a sustained heat source [4-1]. If the graphite were ground to an extremely fine powder to dramatically increase the surface area to volume ratio, it can be pyrophoric on initial exposure to air [4-9]. However, for the application of spent pebble fuel, the waste form is in spheres with surface area to volume ratio that is orders of magnitude lower than is required to make combustion kinetically possible. General Atomics adds to the consensus that graphite will not combust in a repository by concluding that the high-purity, nuclear grade graphite fuel elements are non-combustible by conventional standards [4-4].

The second reason graphite will not burn is that most organics (including coal) burn by decomposition of the fuel as it is heated which release combustible gases and breaks up

the surface. Graphite does not contain hydrogen or water. Therefore, no mechanisms can breakup the surface and release the combustible gases. The higher the carbon content of the density of the fuel elements, the lower the combustibility [4-1]. This was the essential problem with the Chernobyl nuclear reactor. Chernobyl used a graphite block moderator. However, the carbon content of this particular graphite was low , and higher content of impurities including hydrogen, making the moderator more vulnerable to the hot gases of the core. It is important to note that the temperatures experienced in the Chernobyl core were many times higher than the most extreme conditions expected in a repository under a worse-case accident scenario [4-1].

The third reason why graphite will not combust in the repository is the high thermal conductivity of the material. As stated above, this high thermal conductivity will prevent the formation of any hot spots within the waste package. Because of this characteristic, the temperature of the waste package will be uniform throughout.

4.2.2. Leach Rates

Another concern with the inertness of a material is the ability to resist an attack by water. "Graphite is known to resist attack by conventional aqueous reagents. In the chemical industry, graphite heat exchangers are used for very highly corrosive conditions when most metals fail. Graphite is generally considered 'completely' inert to all but the most oxidizing conditions" [4-1]. Gray compiled a list of leach rates of various materials [4-5]. These values are summarized in Table 4-3.

Table 4-3. Leach Rates of Waste Matrix Materials [4-5].

<u>Material</u>	<u>Leach Rate (g/cm²-day)</u>	
	<u>250°C</u>	<u>99°C</u>
Synroc	4×10^{-5}	6×10^{-6}
Waste Glass	8×10^{-3}	4×10^{-4}
Al ₂ O ₃	4×10^{-5}	2×10^{-6}
ZrO ₂	6×10^{-5}	6×10^{-5}
Graphite	1×10^{-8}	3×10^{-10}

The values in Table 4-3 demonstrate that graphite leach resistance is four orders of magnitude better than other waste matrix materials. Waste packages in Yucca Mountain are located in the unsaturated zone, therefore, no significant water ingress is expected. However, future climatic changes could possibly bring water to the environment. Should this occur, the leach rate values indicate that graphite is the most resistant. The water will not be able to penetrate the microsphere to carry away the radionuclides locked tightly inside three more protective layers.

4.3. Quantity of Waste Contained in the Primary Barrier

The fission products of the spent fuel sphere of the PBR are distributed within 11,000 separate, tiny pressure vessels with in the fuel element. Furthermore, there are approximately 42,000 fuel sphere is a waste package. This implies that the fission products in spent pebble fuel are distributed among 462 million separate pressure vessels. If any of these pressure vessels should fail, only a relatively small amount of radioactivity will be released to the graphite matrix. This is much different for the spent fuel assemblies of the PWR. The fission products within the waste package of PWR spent fuel are separated into 21 pressure

vessels. Should one of these Zircaloy clad pressure vessels fail, a much larger amount of radioactivity would be released. The PWR spent fuel does not have the extra buffer of graphite should this happen.

This analysis makes it clear that the quantity of spent fuel contained within an individual pressure vessel is of concern. When this quantity is low, the release of radioactivity due to accident or fuel failure of an individual primary barrier will be less.

4.4. Conclusions

The discussion in this chapter focused on the attributes of graphite. In fact, graphite is the final barrier to fission product release from the spent fuel element of the Pebble Bed Reactor. The primary barrier against fission product retention is the silicon carbide layer of the microsphere. Within the microsphere, the fission products must negotiate a number of layers to reach the graphite matrix. The most formidable of these layers is the silicon carbide layer, which possesses many of the favorable characteristics of graphite.

Also not mentioned above is the ease of handling of the spent fuel elements. Spent fuel assemblies from a PWR are extremely long and thin. Thus making them fragile and difficult to manipulate when trying to load into a waste canister. The small spherical shape of the spent fuel element of the PBR is much easier to handle. The durable graphite protective layer assures that the fuel can be handled roughly. The fuel elements can be essentially "poured" into the waste canister with no fear of damage.

This chapter has demonstrated the superior qualities of graphite as a waste form. Using the above criteria, it is clear that graphite outperforms the metal alloys used today.

The evidence is overwhelmingly in favor of graphite. Fears of a Chernobyl type accident are unjustified and should not slow the development and research of this waste form. The clearest reason why graphite has not been used thus far because metal alloys are much easier to machine. This machining is not necessary for spent pebble fuel because the graphite is placed on the fuel during the fuel manufacturing process. The construction techniques of cold compacted graphite as developed by General Atomics and described by W.C. Morgan indicate that the benefits of graphite construction outweigh potential costs [4-4, 4-9].

The conclusions of this chapter mirror those of Pacific Northwest National Laboratories: "The chemical and physical properties of graphite are in many instances superior to those of metals; thus, it is logical to consider graphite as an alternative to metals for use as a matrix material" [4-9]. "It is recommended that increased emphasis be placed on further development of the low-temperature compacted graphite matrix concept" [4-9].

4.5. References

- 4-1. Lotts, A.L., et al, Options for Treating High-Temperature Gas-Cooled Reactor Fuel for Repository Disposal, Oak Ridge National Laboratory, Oak Ridge, Tennessee; Managed by Martin Marietta for the United States Department of Energy, February, 1992.
- 4-2. Lutze, W., and R. Ewing, Radioactive Waste Forms for the Future, North Holland Physics Publishing, The Netherlands, 1988.
- 4-3. Incropera, F., and D. Dewitt, Introduction to Heat Transfer, John Wiley and Sons, New York, 1985.
- 4-4. Richards, M.B., D.A. Alberstein, and A.J. Neylan, "PC-MHR Spent Fuel - An Ideal Waste Form for Permanent Disposal," International Conference on Nuclear Engineering, Volume 5, American Society of Mechanical Engineers, 1996, pages 1-4.
- 4-5. Gray W.J., "A Study of the Oxidation of Graphite in Liquid Waster for Radioactive Storage Applications," Radioactive Waste Management and the Nuclear Fuel Cycle, Volume 3, Number 2, pages 137-149, 1982.
- 4-6. Kirch, N., Brinkmann, H.U., and Brucher, P.H., "Storage and Final Disposition of Spent HTR Fuel in the Federal Republic of Germany," Nuclear Engineering and Design, Volume 121, pages 241-248.
- 4-7. Richards, M.B., "Combustibility of High-Purity, Nuclear-Grade Graphite," Proceedings of the 22nd Biennial Conference on Carbon, American Carbon Society, pages 598-599, 1995.
- 4-8. Stinton, D.P., P. Angelini, A.J. Caputo, and W.J. Lackey, "Coating of Crystalline Nuclear Waste Forms to Improve Inertness," Journal of the American Ceramic Society, Volume 65, Number 8, pages 394-398.
- 4-9. Morgan, W.C., "Graphite-Matrix Materials for Nuclear Waste Isolation," United States Department of Energy, Pacific Northwest Laboratories, Report # PNL-3556, June, 1981.
- 4-10. DOE/OCRWM/YMP, Viability Assessment, <http://www.ymp.gov/toc/va>.
- 4-11. Wilson, M.L., "Total Performance Assessment for Yucca Mountain - SNL Second Iteration (TSPA-1993)," SAND93-2675, Sandia National Laboratories, Albuquerque, NM, 1994.
- 4-12. Castellan, G.W., Physical Chemistry, Third Edition, The Benjamin/Cummings Publishing Company, Inc., Menlo Park, California, 1983.

Chapter 5: Interactions of Silicon Carbide and Uranium

The silicon carbide layer of the microsphere is a unique characteristic of pebble fuel. Under repository conditions, the silicon carbide layer will interact with the fuel kernel within the microsphere. This chapter analyzes the interaction of two main components within the microsphere, silicon carbide and uranium, to determine if there is an effect on the migration rate of radionuclides. The experimental work, reported in this chapter, attempts to determine if a secondary phase forms as a result of interactions between silicon carbide and uranium. Should it be determined that a secondary phase does form, the next step is to determine whether this phase will deter or enhance radionuclide migration. To determine this, the concentrations of UO_2^{2+} , representing the most soluble form of uranium, U(VI), was measured at various pH levels after it was conditioned with and without the presence of silicon carbide. Any decrease in concentration of UO_2^{2+} in the presence of silicon carbide indicates that the migration of soluble uranium is being retarded by the formation of a secondary phase within the microsphere.

To fully understand the value of silicon carbide as a deterrent to radionuclide migration, it is necessary to conduct an experiment which will mirror the conditions the spent fuel will likely experience at Yucca Mountain. This experiment was designed to determine if the presence of silicon carbide would inhibit or enhance the migration of radionuclides from the repository to the biosphere. The radionuclide inventory of the spent fuel after final disposal is of significant concern. There are three primary radiologically significant isotopes:

Iodine-129, Cesium-137, and Neptunium-237. No experiments were conducted with these isotopes. In this study, an experiment was conducted using U(VI). Although U(VI) is not a radiologically significant isotope after final disposal, it provides a baseline evaluation for the performance of silicon carbide in the deterrence of radionuclide migration.

The silicon carbide layer and the effects of its interactions with uranium are only one step in the process of radionuclide migration to the biosphere. The time at which this interaction becomes significant is after the waste canister has eroded and after each of the protective layers within the microspheres of the fuel element has failed, including the silicon carbide layer. At this point, perhaps the interaction of silicon carbide with uranium has produced a secondary phase that will add yet another barrier to the migration of radionuclides to the biosphere.

5.1. Experimental Overview and Procedure

The fuel element of the Pebble Bed Reactor is composed of a buffer, an inner pyrolytic carbon layer, a layer of silicon carbide and an outer layer of pyrolytic carbon. These various layers surround a core of uranium oxide fuel. Under long term storage conditions, uranium and other fission products will generally migrate from these confining layers. The amount of uranium dioxide left in the fuel element is small due to the high burn-up associated with pebble bed reactors. However, there will be fission products and isotopes within the microsphere. This experiment is concerned solely with the behavior of U(VI) under repository conditions. Because the U(VI) phase of uranium is the most soluble in

water, it will migrate fastest to the biosphere and serves as the baseline for this experiment. Additionally, U(IV) is expected to oxidize to U(VI) under the conditions at Yucca Mountain.

In order to understand how U(VI) reacts with silicon carbide under various repository conditions, the pH of the solution was varied from 3 to 7 in half integral steps. The expected pH conditions of the spring water associated with Yucca Mountain is 7.6 [5-6]. A solution of 1.0×10^{-5} M uranyl nitrate $[\text{UO}_2(\text{NO}_3)_2]$ in a 0.1 M sodium perchlorate $[\text{NaClO}_4]$ matrix was used as the analog for the fuel kernel of a microsphere. Each sample contained approximately 0.1 grams of 400-mesh silicon carbide and 5 ml of 1×10^{-5} M uranyl nitrate. Another set of nine samples was prepared with 5 ml of 1×10^{-5} M uranyl nitrate but no silicon carbide.

Once all samples were prepared, they were placed on a shaker table and mixed for four days. When mixing was complete, the samples were centrifuged. At this point, the samples were conditioned and were ready to be analyzed. The following section describes how the samples were characterized after the experimental procedure was completed.

5.2. Characterization of Samples

A change in the uranyl nitrate concentration of the solution will determine if any of the uranium reacted with either the silicon or the carbide in the prepared solution. Should the measured solution concentration of the uranyl nitrate in the samples change after conditioning, then the uranium nitrate reacted with the silicon carbide to form a secondary phase. UV-Spectroscopy was used to characterize the conditioned samples by measuring the uranium concentration. The UV-Spectroscopy system generates a graph of absorption versus

wavelength. This method uses the indicator dye arsenazo III to complex with the uranium present in the sample [5-4]. The solution that the UV-Spectrometer analyzes is a mixture of 3 ml of 1.91×10^{-5} M arsenazo III mixed with 3 ml of the conditioned samples of uranyl nitrate and silicon carbide. Arsenazo III was diluted from 1.91×10^{-3} M solution using pH 2 buffer as the dilute.

Arsenazo III is used specifically as an indicator dye for uranium. The arsenazo will complex with the uranium ions in solution, absorbing at wavelengths from approximately 625 to 670 nanometers. The excess, uncomplexed arsenazo is represented in the absorption wavelengths from approximately 500 to 600 nanometers. This separation in wavelength is the key aspect of determining the uranium concentration of the sample solution. The graphical representation in Figure 5-1 depicts two distinct peaks. Because the arsenazo III concentration is slightly higher (1.91 : 1.00) than the highest expected uranium concentration, all uranium ions present will complex with the arsenazo III. Because of this, the free arsenazo III peak in the graph will be present.

It is important to manipulate the data such that the absorption lines tail off along the zero absorption x-axis. The range of wavelengths for each sample scan was deliberately larger than the expected peaks to accomplish this purpose. The absorption spectrum flattens in the 700-800 nanometer range. The average absorption data obtained from 700-800 nanometers was subtracted from all values of the spectrum to ensure all samples are normalized.

Figure 5-1 is the spectrum obtained from the uranium and silicon carbide sample that was conditioned at pH 3.5. This spectra is collected for each sample. The uranium complex

absorbs with a peak mean absorption of 650 nm, as shown in Figure 5-1. Appendix C-1 includes the UV-Spectroscopy output for all samples.

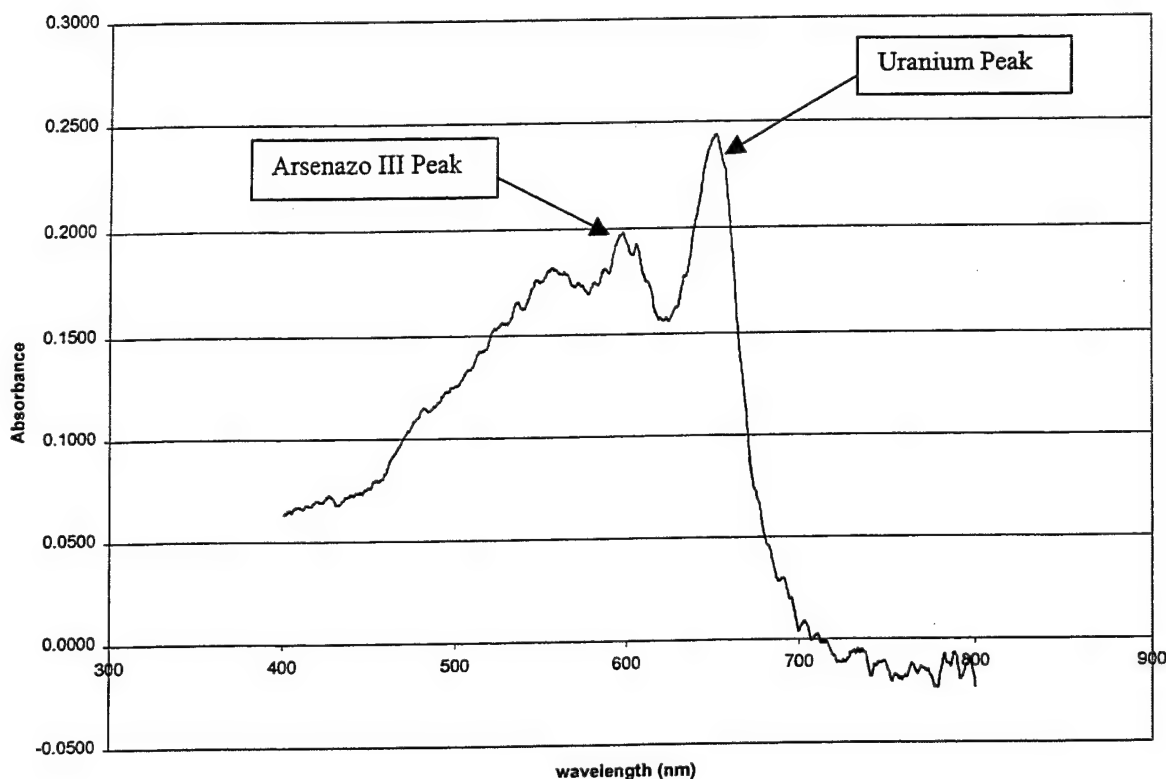


Figure 5-1. UV-Spectroscopy output.

Thus far, all that has been obtained is a measure of UV absorption. The area under the uranium peak represents the absorption of the uranium ions from the wavelengths of approximately 625-670 nanometers. Therefore, the area under this peak is an indication of how much uranium is free in the solution through Beer's Law. The concentration of uranium is determined by measuring the area under the peak of the uranium absorption curve. This area is then converted to a concentration by comparing it to values of known concentrations

of uranium. An absorption spectrum was recorded for four different known concentrations of uranium, which form the calibration curve. These four samples are the standards by which the conditioned samples are compared, as indicated in Figure 5-2.

Area measured under the uranium absorption peak for each standard was recorded. The known concentrations were compared with the absorption spectra to determine a conversion equation for absorption to concentration. A graph of uranium concentration versus cumulative absorption was constructed from these reference points. The equation of the line was determined by calculating the linear regression of these four points. The equation of this standardization line is the conversion factor from cumulative absorption to uranium concentration. The results from four standard samples are summarized in Table 5-1 and graphically depicted in Figure 5-2.

Table 5-1. UV Standardization Reference Data

<u>Concentration</u>	<u>Integration</u>	<u>error</u>
1.00E-06	2.303	0.0153
5.00E-06	12.968	0.0548
7.00E-06	19.984	0.0545
1.00E-05	27.480	0.0799

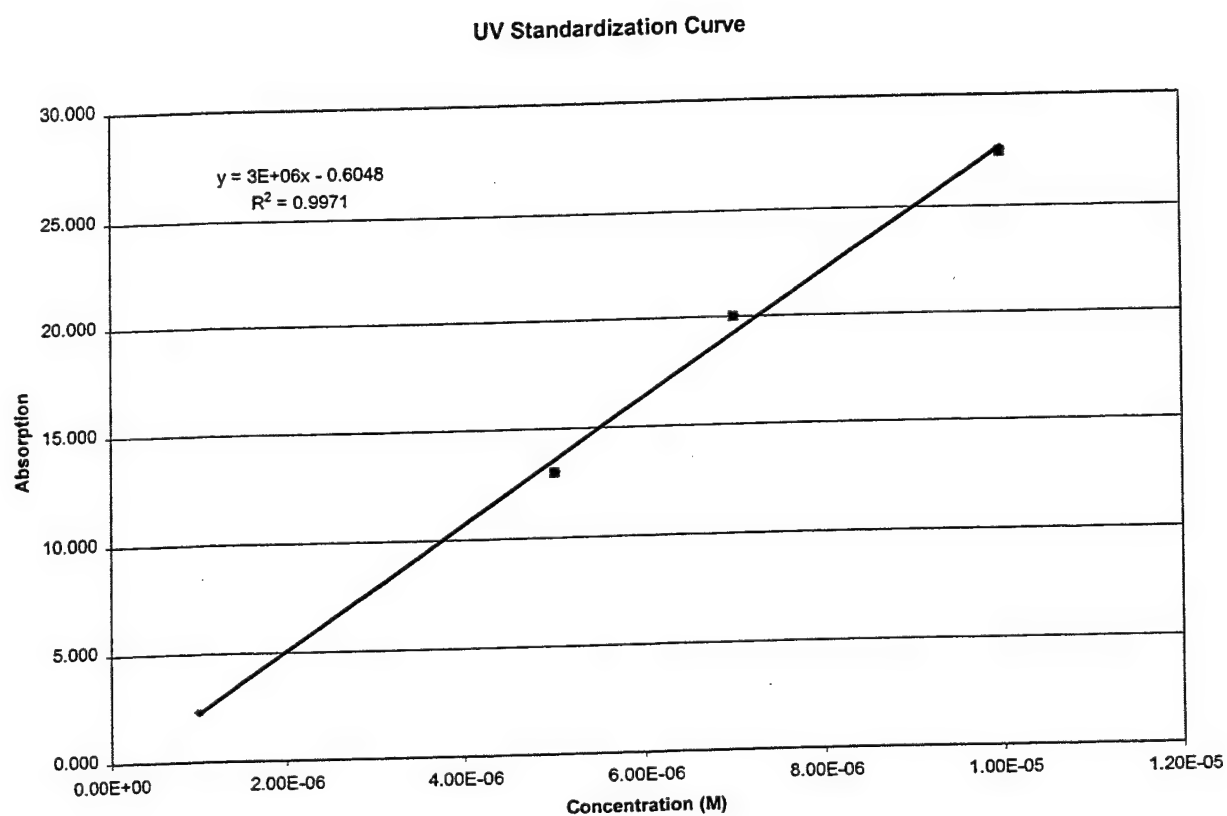


Figure 5-2. UV Standardization Graph.

The conversion factor, as determined through linear regression was found to be:

$$[UO_2^{2+}] = \left(\frac{Absorption + 0.6048}{3 \times 10^6} \right) \quad (5-1)$$

Now that a conversion equation has been obtained, it is possible to convert the uranium absorption to uranium concentration. Table 5-2 represents a summary of the data obtained for samples 1-9 that contained uranyl nitrate and silicon carbide. Table 5-3 represents a summary of the data obtained for samples 10-18 that contained only uranyl nitrate. Figure 5-3 is a graphical representation of this information.

Table 5-2. Uranium Concentration with SiC

<u>U+SiC</u>			
<u>Final</u>			
<u>SiC (g)</u>	<u>pH</u>	<u>concentration</u>	<u>error</u>
0.108	3.37	8.86E-06	1.82E-07
0.108	3.93	7.98E-06	1.82E-07
0.113	4.48	6.00E-06	1.70E-07
0.099	4.95	3.15E-06	1.88E-07
0.105	5.84	9.49E-07	1.75E-07
0.096	6.27	4.41E-07	4.57E-08
0.113	6.63	7.26E-08	1.79E-07
0.095	6.84	7.24E-07	1.91E-07
0.107	7.04	5.40E-07	1.96E-07

Table 5-3. Uranium Concentration without SiC.

<u>U only</u>			
<u>Final</u>			
<u>SiC (g)</u>	<u>pH</u>	<u>concentration</u>	<u>error</u>
0.000	3.06	9.19E-06	7.91E-08
0.000	3.48	8.42E-06	1.56E-08
0.000	3.96	9.13E-06	1.84E-07
0.000	4.80	8.22E-06	1.76E-07
0.000	5.11	9.28E-06	1.85E-07
0.000	5.99	8.11E-06	1.86E-07
0.000	6.22	8.56E-06	1.84E-07
0.000	6.57	8.46E-06	1.79E-07
0.000	7.10	8.24E-06	1.80E-07

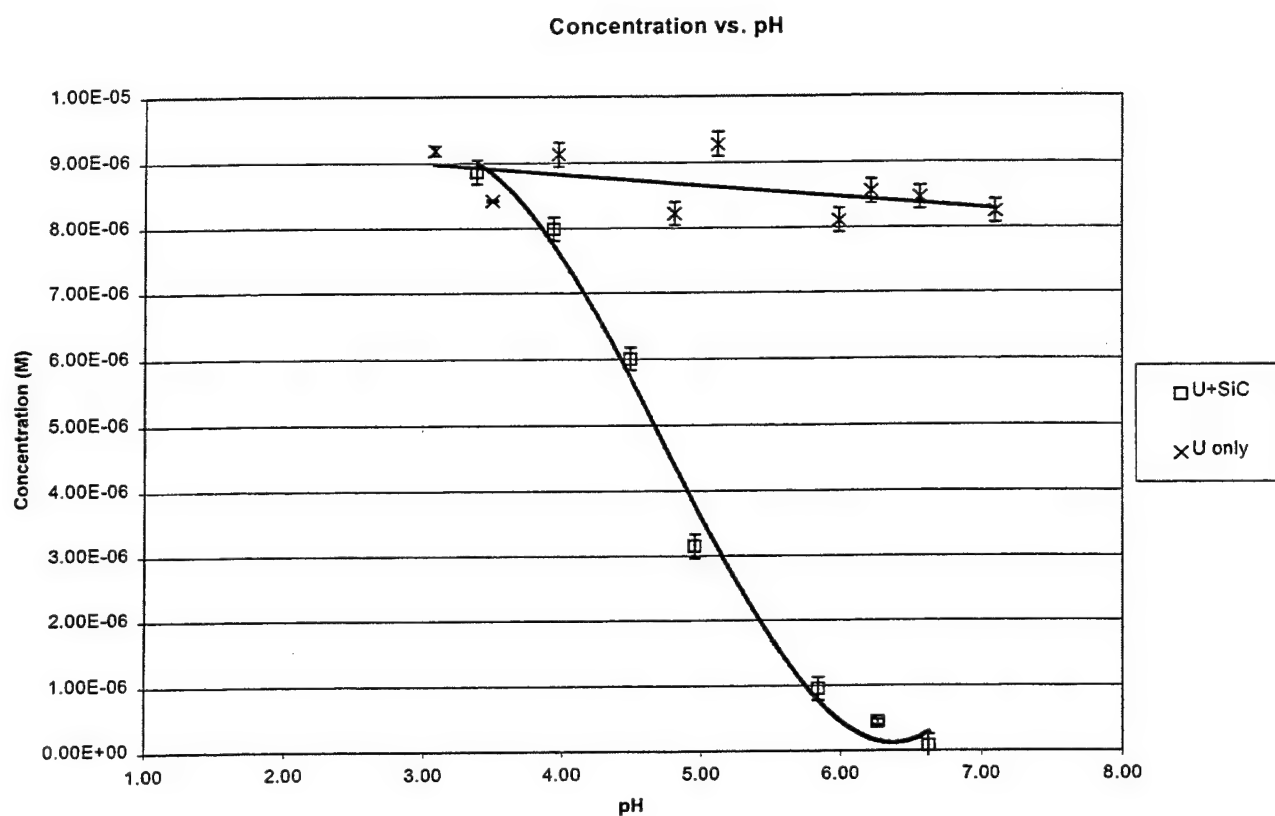


Figure 5-3. Comparison of uranium concentration with and without the presence of silicon carbide.

5.3. Uranium Speciation

To interpret the expected shape of the curves represented in Figure 5-3, it is necessary to construct a speciation curve for uranium. Speciation is the determination of the chemical species possible under the given experimental conditions. The shape of the speciation curve will explain the shapes of the experimental results curves. The uranium species in solution are dependent on the pH of the solution. A theoretical calculation of this speciation will demonstrate the pH range where free ion concentrations vary.

Determination of the speciation curve begins with an evaluation of which species will form. The species of concern are the free uranyl ion, hydroxides, carbonates and nitrates [5-1]. The total U(VI) or $[UO_2]_T$ concentration in the pH range considered is expressed by:

$$[UO_2]_T = [UO_2^{2+}] + \sum_{x=1}^4 [UO_2(OH)_x^{2-x}] + \sum_{y=1}^2 [(UO_2)_2(OH)_y^{4-y}] + \sum_{z=1}^3 [UO_2(CO_3)_z^{2-2z}] + \sum_{w=1}^3 [UO_2(NO_3)_w^{2-w}] \quad (5-2)$$

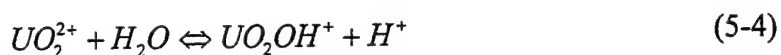
The value of $[UO_2]_T$ was set during the procedure at 1×10^{-5} M. Using stability constants, solving equation 5-2 for $[UO_2^{2+}]$, and plotting these values against a varying pH will produce the speciation curve. Solving for $[UO_2^{2+}]$ is an iterative process. The amount of free metal ions (% M_f) in solution is expressed by:

$$\%M_f = \frac{10^{-pM}}{\left[10^{-pM} + \sum_{x=1}^4 [U(OH)_x] + 2 \sum_{y=1}^2 [U_2(OH)_y] + \sum_{z=1}^3 [U(CO_3)_z] + \sum_{w=1}^3 [U(NO_3)_w] \right]} \quad (5-3)$$

It is first necessary to determine the concentrations of the individual species to evaluate the percentage of free metal ions in solution. For the hydroxide species, this is accomplished

using equilibrium constants. The first hydroxide species, $[UO_2OH]$, is given as an example.

The reaction equation for the first hydroxide species is given below:



The equilibrium constant, K , is determined by dividing the concentrations of the products by the concentrations of the reactants. The symbol K_{10-10} is used to represent the first hydroxide species which contains one uranium ion (10), and one hydroxide ion (10). The subscripts for K vary with each species. The equilibrium constants are known values that have been determined experimentally. All equilibrium and stability constants were obtained from the references at the end of this chapter. The first hydroxide equilibrium constant is represented by the following equation:

$$K_{10-10} = \frac{[UO_2OH^+] * [H^+]}{[UO_2^{2+}]} \quad (5-5)$$

The value of K_{10-10} is known [5-3]. The value of $[H^+]$ is the pH of the solution, and is therefore also known. The value of $[H_2O]$ does not vary in the reaction and may be neglected in the determination of the equilibrium constant. This leaves two unknowns, the first hydroxide species concentration and the free uranium concentration. For now, equation 5-5 is solved for the first hydroxide species:

$$[UO_2OH^+] = \frac{[UO_2^{2+}] * K_{10-10}}{[H^+]} \quad (5-6)$$

This process is continued for all species. The only difference is that stability constants, β , are used instead of equilibrium constants for the carbonate and the nitrate species. The determination of $[UO_2^{2+}]$ is an iterative, circular process. Beginning the process at pH values of 1, the logarithm of the calculated value of the free metal ion (UO_2^{2+}) concentration, pM_c is determined:

$$pM_c = -\log(\%M_f * [UO_2]_T) \quad (5-7)$$

This calculated value replaces the previous estimate of the free metal ion concentration, pM , and the calculation is redone. This process continues until the difference between these two values is zero for all pH ranges. A spreadsheet macro was written to perform this calculation. When the iteration process is done, the value of pM is a known quantity at all pH values considered.

Part of the circular process includes the individual species concentrations. With the pM value estimated, the value of the speciation concentration was estimated by substituting known values in equation 5-6. These simplifications are:

$$-\log[UO_2^{2+}] = pM \quad (5-8)$$

$$-\log[OH^-] = (pK_w - pH) \quad (5-9)$$

$$pOH^- + pH^+ = pK_w \quad (5-10)$$

Making these substitutions, the equation for the determination of the first hydroxide species is:

$$[UO_2OH^+] = 10 \exp(-)[pM + (pK_w - pH) - (\log K_{10-10} + pK_w)] \quad (5-11)$$

After this process was completed for all species, an accurate estimation of pM can be determined. The result of this process is shown in Figure 5-4.

A full list of equations, constants and results are included in this report as Appendix C-2. Cell formulas used for the spreadsheet calculations are included in Appendix C-3.

5.4. Interpretation of Results

The theoretical results of the uranium speciation calculation can be used to identify trends of the experimental data. In the experiment, the concentration of free uranium ions begins to decrease rapidly around pH 4 in the presence of silicon carbide. This phenomenon does not occur when there is no silicon carbide present to react with the dominant soluble species. The concentration of the solution uranium remains constant through all ranges of pH analyzed in this experiment.

With the confirmation of the shape and trend of the experimental data, it is clear that the uranium concentration in the presence of silicon carbide is less than the uranium concentration when no silicon carbide is present under all pH conditions. Figure 5-4 clearly indicates the trends that the experimental results represent. The difference between these curves represents the formation of a secondary phase. Because of this secondary phase formation, there is less free uranium that is capable of migrating to the biosphere. The secondary phase can be attributed to the sorption of uranium hydroxide to silicon carbide.

This occurs because the uranium forms a hydroxide species. Figure 5-5 depicts the formation of the hydroxide species. Increases in the hydroxide species correspond well with the sorption to the silicon carbide.

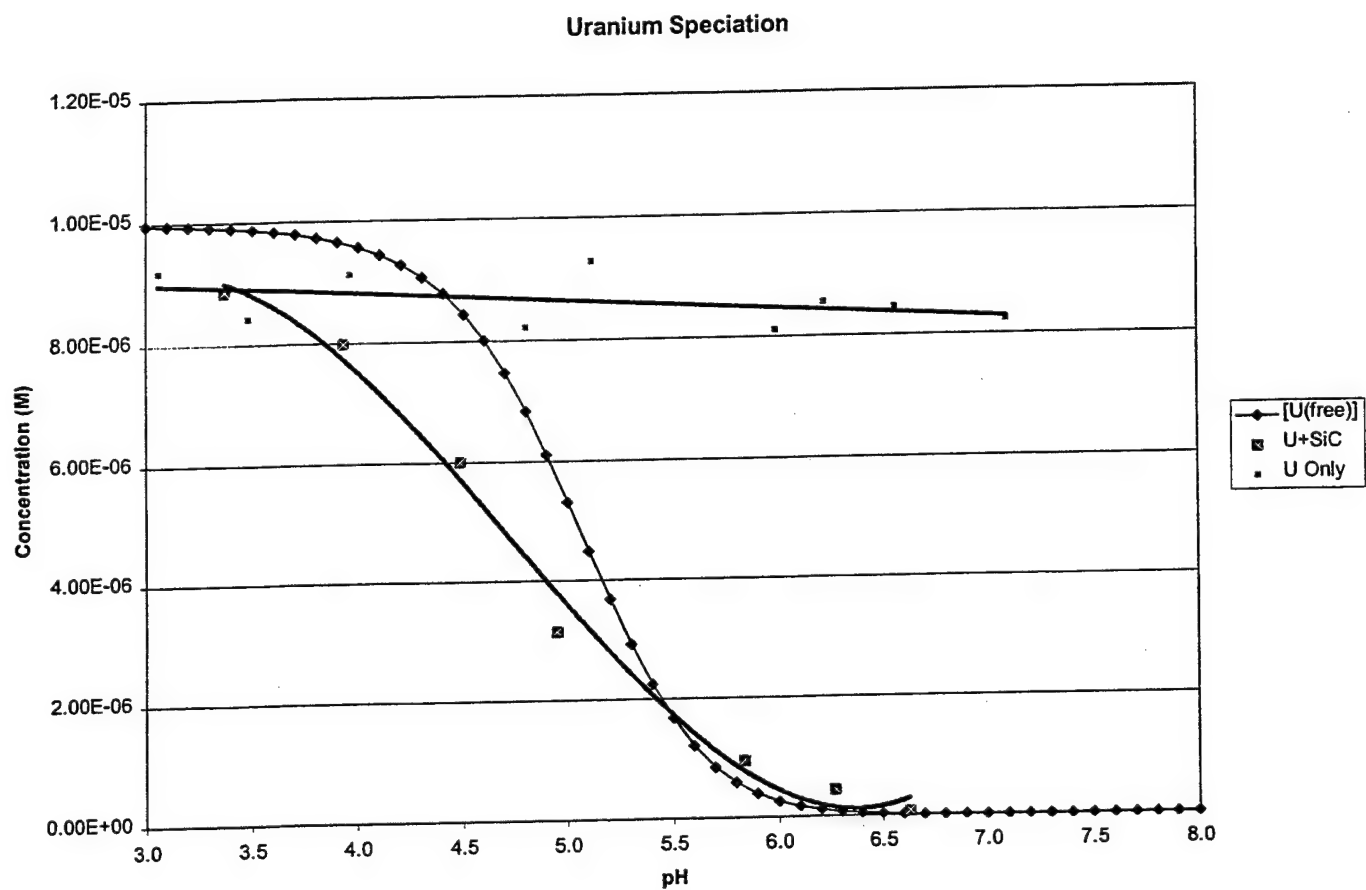


Figure 5-4. Trend lines for uranium concentrations conditioned with and without silicon carbide present in solution.

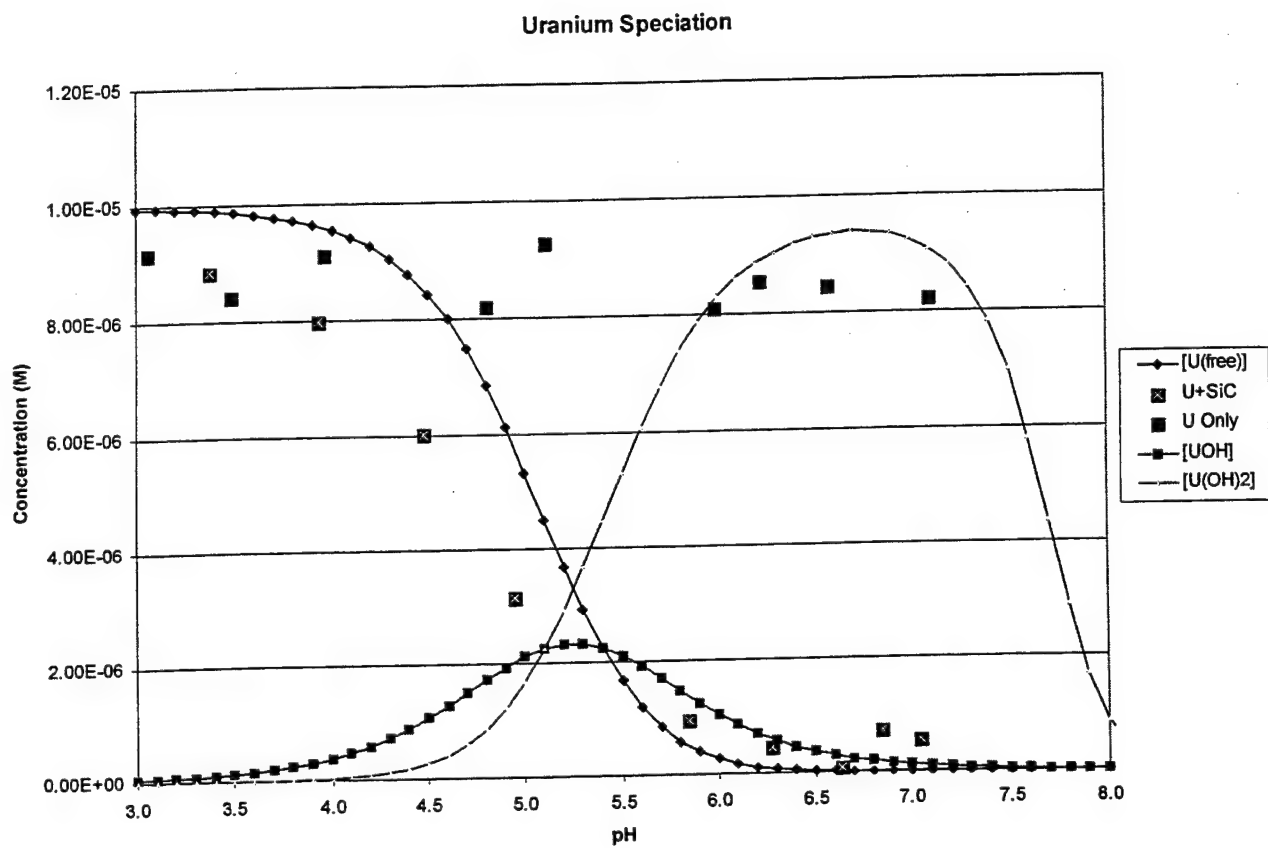


Figure 5-5. Uranium Speciation with first and second hydroxide species.

5.5. Conclusions

This experiment demonstrated that there is less free uranium when silicon carbide is present in solution than when no silicon carbide is present. This result is significant in that this represents the formation of a secondary phase that inhibits the migration of the most soluble form of uranium, U(VI). Now that this scoping experiment proved the retention possibilities of the secondary phase formation, the basis for further experimentation exists. The next step is to determine the secondary phase formation affect on other, more radiologically significant isotopes.

5.6. References

- 5-1. Zeh, P., K.R. Czerwinski, and J.I. Kim, "Speciation of Uranium in Gorleben Groundwaters," Radiochimica Acta 76, 1997, pages 39-44.
- 5-2. Bruton, C.J., and H.F. Shaw, "Geochemical Simulation of Reaction Between Spent Fuel Waste Form and J-13 Water at 25°C and 90°C," Presentation given at Materials Research Society Symposium, Boston, MA, November 30 - December 5, 1987.
- 5-3. Fanghanel, Th., V.Neck, and J.I. Kim, "The Ion Product of H₂O, Dissociation Constants of H₂CO₃, and Pitzer Parameters in the System Na⁺/H⁺/OH⁻/HCO₃⁻/CO₃²⁻/ClO₄⁻/H₂O at 25°C," Journal of Solution Chemistry, Volume 25, Number 4, 1996, pages 327-343.
- 5-4. de Beer, H., and P.P. Coetzee, "Ion Chromatographic Separation and Spectrophotometric Determination of U(IV) and U(VI)," Radiochimica Acta 57, pages 113-117, 1992.
- 5-5. Grenthe, Ingmar, et al, Chemical Thermodynamics, Volume 1: Chemical Thermodynamics of Uranium, Nuclear Energy Agency, Organization for Economic Cooperation and Development, North-Holland, Amsterdam, 1992.
- 5-6. Delany, J.M., Reaction of Topopah Spring Tuff with J-13 Water: A Geochemical Modeling Approach Using the EQ3/6 Reaction Path Code, Lawrence Livermore National Laboratory, November 25, 1985, UCRL-535631.

Chapter 6: Conclusions and Recommendations

This chapter outlines the work done in the previous four chapters and attempts to draw broader conclusions from the results concerning the performance and long-term considerations of wide use of the pebble bed reactor concept. The first section will summarize the findings of the three important questions examined throughout this report. The second section will use the results and conclusions to draw some general trends and make recommendations for future study. Conclusions are reached concerning the advantages and disadvantages of the waste disposal aspects of each reactor system and how this may relate to the future development of the technology.

6.1. Conclusions

This report consists of three primary topics: (1) Storage requirements of spent pebble fuel compared with storage requirements of spent fuel from a pressurized water reactor, (2) An analysis of graphite as a waste form, and (3) Interactions of silicon carbide with uranium. Each of these topics are extremely important to understanding the long-term impact should pebble bed reactors be implemented on a wide scale in the near future. The characteristics examined in this report favor the use of pebble bed reactors over light water reactors. The results and conclusions of each of the three main topics are summarized below.

6.1.1. Storage Requirements

The implication of the results obtained in Chapter 3 are that it will take less space to store spent pebble fuel than it will take to store spent fuel assemblies from a pressurized water reactor. In fact, the space saving potential is almost 7.5 times as great for the pebble bed reactor based on megawatts of electricity available to the consumer. However, this savings in area comes at a price of more canisters needed. This report assumes that spent pebble fuel will be placed in the same size canister with the same protective material as the spent fuel assemblies of the light water reactors. With this as the case, the spent pebble fuel will require 9.60 times more waste packages than light water reactor spent fuel.

There are significant costs associated with the increase in the required number of waste canisters. The materials used in the manufacturing process of the canister are the most significant cost contributors to the overall design. The exotic materials needed for the protection of spent fuel assemblies are not needed for spent pebble fuel. A licensing process is necessary that credits spent pebble fuel for its already superior packaging in the form of the protective outer layer made of graphite. As discussed in Chapter 4, the expensive canister material adds only 1,000 years to the corrosion resistance of the graphite matrix which will last on the order of 1 billion years. Therefore, the most expensive part of the canister provides virtually no added protection for the spent pebble fuel. Perhaps a less expensive material can be used. Because all proposed canister materials will corrode at rates that are orders of magnitude faster than graphite, it is reasonable to attempt to save cost on materials that add no benefit to the corrosion resistance of the graphite waste form. Table 6-1 is a summary of the results presented in Chapter 3.

Table 6-1. Storage Area Requirements	1000 MW(e)	1000MW(e)	
	PBR	PWR	
Fuel elements/waste package	41,957	21	
Fuel elements discarded/year	1,150,538	60	
Years of operation	30	30	yrs
Fuel element storage requirement	34,516,125	1,800	
waste packages needed	823	86	
MTHM/fuel element	3.47E-06	0.45	MTHM
MTHM/waste package	0.1456	9.45	MTHM
MTHM/acre	90	90	MTHM/acre
kW/waste package	1.53	15.53	kW/canister
waste packages/acre	617	9	canisters/acre
Acres needed for storage	1.333	10.056	acres
Storage Requirement	5.33	40.70	m²/MW(e)

6.1.2. Graphite as a Waste Form

Three characteristics of waste forms were examined. These characteristics were determined to be the most relevant and derived from a variety of sources. There is overwhelmingly positive support for graphite as a waste form from all researchers that have specifically looked at this question. No contradictions to these conclusions were found in any of the reports that compared graphite to the metal alloys associated with PWR spent fuel. The exceptional durability, thermal conductivity, thermal expansion, and inertness of graphite make it a superb barrier. The only negative characteristic according to the analysis of these reports was that graphite is difficult to machine. However, these researchers were primarily concerned with the development of a waste canister for spent fuel assemblies. No manufacturing or machining process is necessary for spent pebble fuel. The graphite already

exists on the fuel. The graphite is placed on during the fuel manufacturing process and remains with the fuel throughout the fuel cycle including final disposal. Conveniently, spent pebble fuel already exists in a matrix that is far superior to any that can be reasonably placed around the spent fuel assemblies of light water reactors.

6.1.3. Silicon Carbide and Uranium

The results from Chapter 5 clearly indicate that there is less soluble uranium in a system with silicon carbide than a system without silicon carbide. Therefore, the silicon carbide layer of the spent fuel element of a pebble bed reactor will act as a barrier to migration of radionuclides throughout the fuel cycle. Most significantly, it will act as a retention mechanism for millions of years during final disposal in a repository. Further work should be directed to characterize the ability of the silicon carbide to retain other radiologically significant isotopes.

6.2. Recommendations

Further work needs to be accomplished. However, storage area requirements for spent pebble fuel will always be less than storage area requirements for light water reactor spent fuel. The high burn-up and low power density characteristics of the spent pebble fuel will always relate to less decay heat and thus less space requirements in a repository. The most crucial work is to increase space savings and decrease the added canister cost. A re-examination of the regulations governing spent nuclear fuel specifically from a pebble bed reactor will optimize pebble bed design. The design of a canister that is made specifically for

spent pebble fuel will maximize the advantages. Larger canisters, limited in size only by transportation and handling considerations, that can accommodate more spent fuel pebbles will decrease the amount of costly material needed. Different, less robust (therefore less costly) canister materials should be considered for the spent fuel sphere waste package. Chapter 4 clearly showed that the protective graphite coating of the fuel sphere lasts longer than any material that can be reasonably used as a waste package. Finally, vertical boreholes in the repository will allow utilization of the vertical plane.

Today's regulations are written primarily for light water reactors. Many of the regulations governing redundant safety systems are obsolete when applied to the PBR. A simple plant that relies on natural laws of science for safety does not require many of the systems deemed necessary by United States regulations. A fresh look at how the PBR works by the Nuclear Regulatory Commission will help redefine what is necessary and what can be omitted from the current regulations pertaining to pebble bed reactors.

Experiments with graphite as a waste form have been few. However, a cursory look at the positive characteristics of graphite is convincing that further study is warranted. Most significantly, the scientific community must fully disprove the theory that nuclear-grade graphite will combust in the repository. A precise documentation of experiments to determine the kinetic properties of this system is needed. This analysis will provide the detachment from the unwarranted fears of an accident similar to the one at Chernobyl. This report did not completely refute the idea that this is possible. Only documented experimentation specifically targeted at this subject will fully disprove the theory that graphite could ignite and burn in the repository.

The retention capability of silicon carbide was only examined for the U(VI) radionuclide. This was done to determine approximate radionuclide retention characteristics of silicon carbide. Basically, a scoping experiment was performed. As indicated in the results section, the silicon carbide layer adds another barrier to the transport of the U(VI) ion. The next step is to examine more significant radionuclides such as Neptunium-237, Iodine-129, and Cesium-137. These radionuclides will move more quickly through the gauntlet of retention devices of the spent fuel element than the U(VI) ion. For these reasons, more study is needed of this most significant radionuclides.

Appendix A: Waste Volume Data Supporting Calculations

Spent Pebble Fuel Characteristics
Assume: Steady state operation

** All shaded numbers are set as accepted values. All other numbers are derived from these.

EMPIRICALLY DETERMINED FACTORS				ref
symbol	definition	PBR	PWR	units
η	thermodynamic efficiency	0.45	0.33	ESKOM
L	capacity factor	0.90	0.82	Zeimann, NED 121
th	thermal power	250	3030	HTR-100
g	grams of fission products/MWD(t)	1	1	$g = \text{fel(av)} \cdot \text{FE/day/MWD(t)}$
R	refueling rate	0.895	30.000	$R = \text{FE(dis)} \cdot \text{fel(m)}$
t	post irradiation cooling time	15	15	Brinkman, NED 109
fel(m)	fuel element loading (max)	7	450,000	$? \text{Fep(av)} \cdot (\text{Fel(m)}/\text{fep(m)})$
fel(av)	fuel element loading (average)	3.47	450,000	Halloway
V	core volume (fuel only)	40.715	30	$I = \text{FE} \cdot \text{fel(av)}/10^6$
I	core inventory of heavy metals	1.25	90	MTHM

PBR Characteristics:		PWR Characteristics	
# of FE discarded/day	350 FE/day	Fuel Assemblies	200 Kazimi
FE in core	360,000 FE	Fuel Assembly vol	0.15 m ³
FE diameter	0.06 m	Refuel Rate	0.30
FE volume	0.000113 m ³ /FE	FA discarded/year	60
FE circulated/day	9,000 FE/day	HTR-Module	
fuel assembly volume	40.715 m ³	HTR-Module	
Core Height	10 m	HTR-Module	
Core Radius	1.5 m	HTR-Module	
Core Volume	70.686 m ³	HTR-Module	
full FE power	1.4 kW	halloway	
average FE power	0.694 kW	th/FE in core	

symbol	DERIVED FACTORS	PB reactor	LWR	Parameter Dependency
T	residence time of fuel in core	5.0	4.5	$T = I/R$
Q ^{'''}	core power density	3.54	101.01	$Q''' = P/\eta V$
B	fuel discharge burnup	93,921	45,380	$B = LTQ'''/d$
P	rated power	112.5	1000	$P = \text{th} \cdot \eta$
f	fraction of core refueled each year	0.20	0.22	$f = R/I = 1/T$
d	fuel assembly density	0.062	3.000	$d = I/V$
	MWD(t)	117,402	4,084,159	$\text{MWD(t)} = B \cdot I$
p	specific decay power	3.131	1.513	$p = B/2000t$
q ^{'''}	waste package loading	0.194	4.538	$q''' = pd$
F	waste volume generation rate	29.148	10.000	$F = RV/I \quad 2.91$
h	waste loading	5.813	136.14	$h = gdB \quad \text{more waste}$
			(kg of fp)/m ³	

	fuel elements per waste package	PB reactor	LWR	
hc	heat constrained	821,355	26	$hc = 18 \cdot q''' / \text{FE(vol)}$
gc	geometry constrained	41,957	21	

Design Choice	PB	LWR	
FE per container	41,957	21	
waste package heat	1.532	15.530	kW/waste pkg

percentage of space filled by FE 100% 30%

Yucca Mountain Requirements

(Site Characterization Progress Report #16)

90 MTHM/acre 16 kW/waste package

1 acre 4047 m²Dimensions of Waste package

	diameter	length	Volume	
21 PWR (meters)	1.65	5.335	11.4076	*www.ymp.gov
outer layer thickness	0.12	0.135		YMP VA
inner volume of 21 PWR	1.41	5.065	7.9088	
Tare Weight	34,039 kg		with PWR asbl's	www.ymp.gov
Loaded Weight	50,423 kg		PWR 21 with PWR SF	www.ymp.gov
density of graphite	2,210 kg/m ³		incropera	
weight of graphite in canister	10,487 kg			
with tare weight of canister	44,526 kg		PWR 21 with PBR SF	
PWR weight - PBR weight	5,897 kg			

Dimensions of Fuel Element

meters	0.06	0.06	1.131E-04	0.0028
--------	------	------	-----------	--------

# of spheres by volume	69,929
space of allowed for packing voids	40%
Total fuel elements per waste pkg	41,957 fuel elements/waste package

	1000 MW(e)	1000MW(e)	
Results	PBR	PWR	
fuel element/waste package	41,957	21	
fuel elements discarded/year	1,150,538	60	
years of operation	30	30 yrs	
fuel element storage requirement	34,516,125	1,800	
waste packages needed	823	86	
MTHM/fuel element	3.47E-06	4.50E-01	MTHM
MTHM/waste package	0.1457	9.4500	MTHM
MTHM/acre	90	90	Yucca Mountain
kW/waste package	1.532	15.530	kw/wp
waste packages/acre	617	9	
Acres needed for storage	1.334	10.056	acres
Storage Requirement	5.33	40.70	m ² /MW(e)

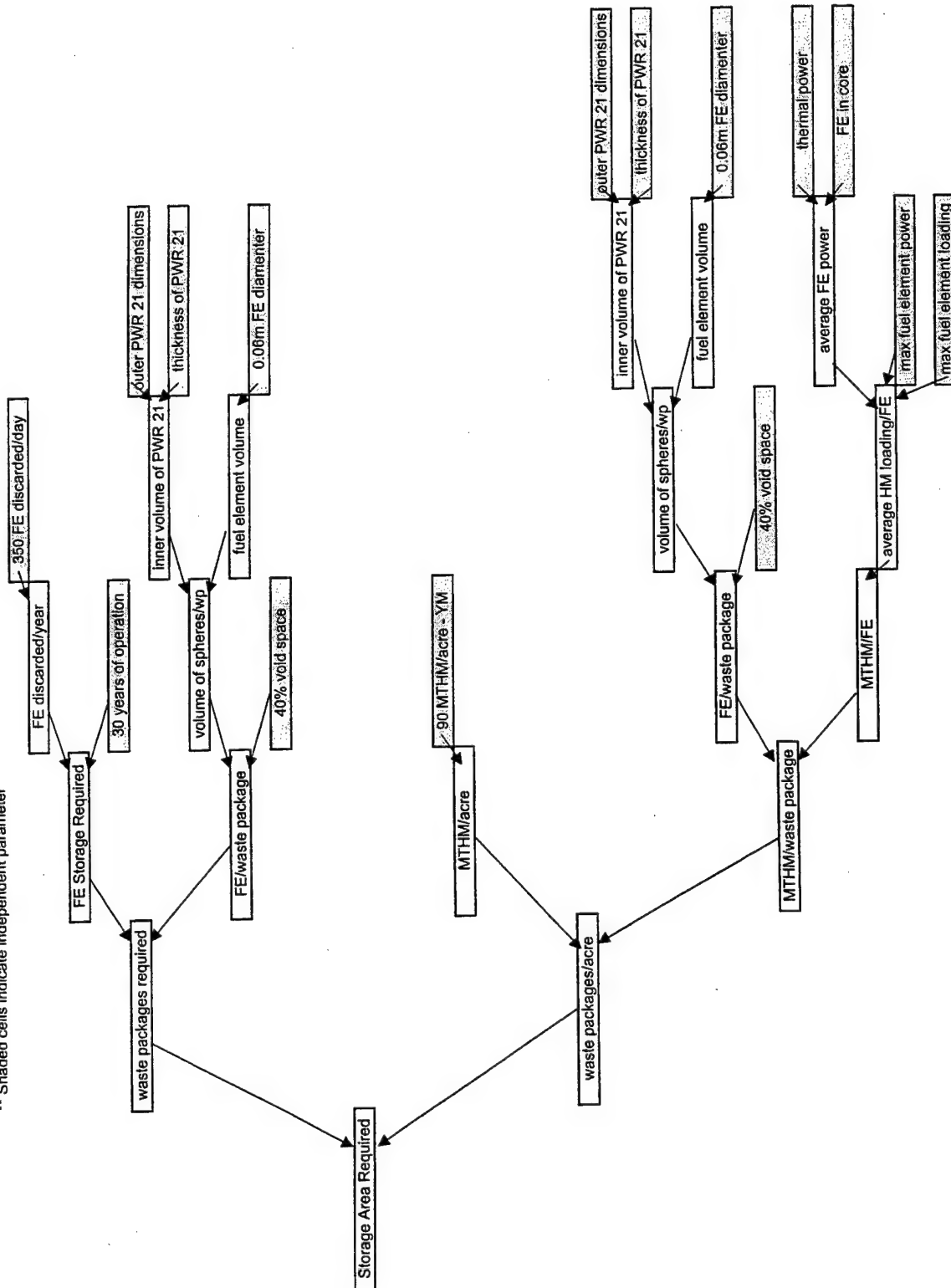
9.60 times more waste pkgs

7.54 times less space

7.63 times less space/MW(e)

Appendix A: Storage Area Calculation Flow Chart

** Shaded cells indicate independent parameter



Appendix B -- Decay Heat Supporting Calculations

Assumptions

Power	250 MWt
# of balls	360000
avg fuel ball	694 W/ball
fully fueled ball	1400 W/ball
F (avg ball)	$2.08\text{E}+13$ fissions/sec
F (full ball)	$4.20\text{E}+13$ fissions/sec
fuel residence time	5 years
balls/waste package	41957

Constants

	$3.00\text{E}+10$ fiss/(W*sec)
	$1.60\text{E}+13$ J/MeV
	$3.16\text{E}+07$ sec/year
	180000 fully fueled balls in core
	50% percentage of fuel balls
$T_p =$	110 °C
wp width =	1.41 m
$k_{eff} =$	20.2 W/mK (1000 °C)

PBR Decay Heat/waste package

time after shutdown years	vg Decay Power MeV/sec	Avg Watts/ball	Avg Decay Power/ Waste Package kW	Max Temp °C
5	$8.22\text{E}+11$	0.13	5.52	177.92
10	$4.31\text{E}+11$	0.07	2.89	145.58
15	$2.85\text{E}+11$	0.05	1.91	133.55
20	$2.10\text{E}+11$	0.03	1.41	127.36
0.0027	$2.22\text{E}+13$	3.55	148.88	1941.62
0.14	$6.73\text{E}+12$	1.08	45.17	665.66
0.68	$3.26\text{E}+12$	0.52	21.91	379.56
1.23	$2.33\text{E}+12$	0.37	15.63	302.27
1.78	$1.83\text{E}+12$	0.29	12.31	261.42
2.33	$1.52\text{E}+12$	0.24	10.19	235.33
2.87	$1.30\text{E}+12$	0.21	8.70	216.98
3.42	$1.13\text{E}+12$	0.18	7.58	203.30
3.97	$1.00\text{E}+12$	0.16	6.72	192.66
4.52	$8.98\text{E}+11$	0.14	6.03	184.14
5.07	$8.13\text{E}+11$	0.13	5.46	177.16
5.61	$7.43\text{E}+11$	0.12	4.99	171.33
6.16	$6.83\text{E}+11$	0.11	4.58	166.39
6.71	$6.31\text{E}+11$	0.10	4.24	162.15
7.26	$5.87\text{E}+11$	0.09	3.94	158.48
7.80	$5.48\text{E}+11$	0.09	3.68	155.26
8.35	$5.14\text{E}+11$	0.08	3.45	152.42
8.90	$4.83\text{E}+11$	0.08	3.24	149.89
9.45	$4.56\text{E}+11$	0.07	3.06	147.63
9.99	$4.31\text{E}+11$	0.07	2.89	145.60
10.54	$4.09\text{E}+11$	0.07	2.74	143.77
11.09	$3.89\text{E}+11$	0.06	2.61	142.10
11.64	$3.70\text{E}+11$	0.06	2.49	140.58
12.18	$3.53\text{E}+11$	0.06	2.37	139.18
12.73	$3.38\text{E}+11$	0.05	2.27	137.90
13.28	$3.24\text{E}+11$	0.05	2.17	136.72
13.83	$3.10\text{E}+11$	0.05	2.08	135.63
14.37	$2.98\text{E}+11$	0.05	2.00	134.62
14.92	$2.87\text{E}+11$	0.05	1.92	133.68
15.47	$2.76\text{E}+11$	0.04	1.85	132.80
16.02	$2.66\text{E}+11$	0.04	1.79	131.99
16.56	$2.57\text{E}+11$	0.04	1.72	131.22
17.11	$2.48\text{E}+11$	0.04	1.67	130.50
17.66	$2.40\text{E}+11$	0.04	1.61	129.83
18.21	$2.32\text{E}+11$	0.04	1.56	129.19
18.75	$2.25\text{E}+11$	0.04	1.51	128.60
19.30	$2.18\text{E}+11$	0.03	1.47	128.03
19.85	$2.12\text{E}+11$	0.03	1.42	127.50
20.40	$2.06\text{E}+11$	0.03	1.38	126.99
20.95	$2.00\text{E}+11$	0.03	1.34	126.51
21.49	$1.94\text{E}+11$	0.03	1.31	126.06
22.04	$1.89\text{E}+11$	0.03	1.27	125.63
22.59	$1.84\text{E}+11$	0.03	1.24	125.21
23.14	$1.79\text{E}+11$	0.03	1.20	124.82
23.68	$1.75\text{E}+11$	0.03	1.17	124.45
24.23	$1.71\text{E}+11$	0.03	1.15	124.09
24.78	$1.67\text{E}+11$	0.03	1.12	123.75
25.33	$1.63\text{E}+11$	0.03	1.09	123.43
25.87	$1.59\text{E}+11$	0.03	1.07	123.11
26.42	$1.55\text{E}+11$	0.02	1.04	122.81
26.97	$1.52\text{E}+11$	0.02	1.02	122.53
27.52	$1.48\text{E}+11$	0.02	1.00	122.25
28.06	$1.45\text{E}+11$	0.02	0.97	121.99
28.61	$1.42\text{E}+11$	0.02	0.95	121.73
29.16	$1.39\text{E}+11$	0.02	0.93	121.49
29.71	$1.36\text{E}+11$	0.02	0.91	121.25
30.25	$1.34\text{E}+11$	0.02	0.90	121.03
30.80	$1.31\text{E}+11$	0.02	0.88	120.81

PWR Decay heat/waste packageAssumptions

Power 3030 MWt
 # of fuel assemblies 200
 avg fuel assembly power 15150000 W/fuel assembly

Constants

$3.00\text{E}+10$ fissions/(W*sec)
 $1.60\text{E}-13$ J/MeV
 $3.16\text{E}+07$ sec/year

F (avg assembly) $4.55\text{E}+17$ fissions/sec

$T_g = 110$ °C

fuel residence time 4.5 years

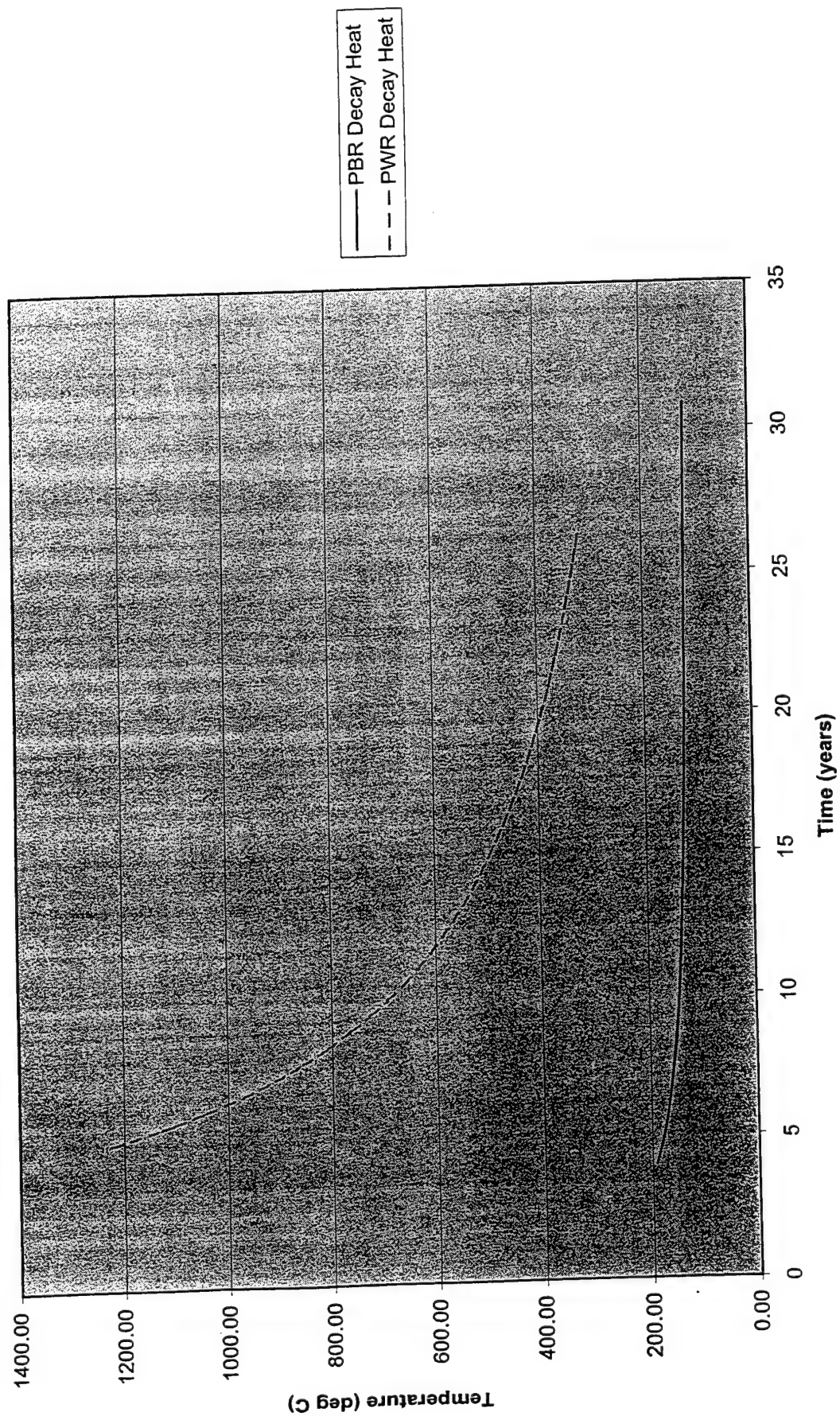
wp width = 1.41 m

assemblies/waste package 21

$k_{eff} = 10.5$ W/mK (at 600 K)

days	time after shutdown years	Decay Power		Avg Decay Power/ Waste Package	Max Temp
		MeV/sec	Watts/assembly	kW	°C
	5	$1.67\text{E}+16$	2671.64	47.69	1238.69
	10	$8.64\text{E}+15$	1382.64	24.68	694.13
	15	$5.69\text{E}+15$	910.03	16.24	494.46
	20	$4.18\text{E}+15$	668.49	11.93	392.42
1	0.0027	$4.81\text{E}+17$	76940.40	1373.39	32615.11
50	0.14	$1.44\text{E}+17$	23028.04	411.05	9838.68
250	0.68	$6.87\text{E}+16$	10991.19	196.19	4753.46
450	1.23	$4.86\text{E}+16$	7768.03	138.66	3391.77
650	1.78	$3.80\text{E}+16$	6077.38	108.48	2677.52
850	2.33	$3.13\text{E}+16$	5004.40	89.33	2224.21
1050	2.87	$2.66\text{E}+16$	4254.10	75.94	1907.24
1250	3.42	$2.31\text{E}+16$	3696.99	65.99	1671.87
1450	3.97	$2.04\text{E}+16$	3265.85	58.30	1489.73
1650	4.52	$1.83\text{E}+16$	2921.89	52.16	1344.41
1850	5.07	$1.65\text{E}+16$	2640.94	47.14	1225.72
2050	5.61	$1.50\text{E}+16$	2407.11	42.97	1126.93
2250	6.16	$1.38\text{E}+16$	2209.48	39.44	1043.44
2450	6.71	$1.28\text{E}+16$	2040.29	36.42	971.96
2650	7.26	$1.18\text{E}+16$	1893.84	33.81	910.09
2850	7.80	$1.10\text{E}+16$	1765.89	31.52	856.04
3050	8.35	$1.03\text{E}+16$	1653.16	29.51	808.41
3250	8.90	$9.71\text{E}+15$	1553.13	27.72	766.15
3450	9.45	$9.15\text{E}+15$	1463.80	26.13	728.41
3650	9.99	$8.65\text{E}+15$	1383.56	24.70	694.51
3850	10.54	$8.19\text{E}+15$	1311.10	23.40	663.90
4050	11.09	$7.78\text{E}+15$	1245.38	22.23	636.14
4250	11.64	$7.41\text{E}+15$	1185.51	21.16	610.84
4450	12.18	$7.07\text{E}+15$	1130.75	20.18	587.71
4650	12.73	$6.75\text{E}+15$	1080.49	19.29	566.47
4850	13.28	$6.46\text{E}+15$	1034.20	18.46	546.92
5050	13.83	$6.20\text{E}+15$	991.45	17.70	528.86
5250	14.37	$5.95\text{E}+15$	951.85	16.99	512.13
5450	14.92	$5.72\text{E}+15$	915.08	16.33	496.59
5650	15.47	$5.51\text{E}+15$	880.84	15.72	482.13
5850	16.02	$5.31\text{E}+15$	848.88	15.15	468.63
6050	16.56	$5.12\text{E}+15$	819.01	14.62	456.01
6250	17.11	$4.94\text{E}+15$	791.01	14.12	444.18
6450	17.66	$4.78\text{E}+15$	764.72	13.65	433.07
6650	18.21	$4.63\text{E}+15$	740.01	13.21	422.63
6850	18.75	$4.48\text{E}+15$	716.72	12.79	412.79
7050	19.30	$4.34\text{E}+15$	694.74	12.40	403.51
7250	19.85	$4.21\text{E}+15$	673.98	12.03	394.74
7450	20.40	$4.09\text{E}+15$	654.33	11.68	386.43
7650	20.95	$3.97\text{E}+15$	635.71	11.35	378.57
7850	21.49	$3.86\text{E}+15$	618.03	11.03	371.10
8050	22.04	$3.76\text{E}+15$	601.25	10.73	364.01
8250	22.59	$3.66\text{E}+15$	585.28	10.45	357.26
8450	23.14	$3.56\text{E}+15$	570.07	10.18	350.84
8650	23.68	$3.47\text{E}+15$	555.58	9.92	344.72
8850	24.23	$3.39\text{E}+15$	541.75	9.67	338.87
9050	24.78	$3.30\text{E}+15$	528.53	9.43	333.29
9250	25.33	$3.22\text{E}+15$	515.90	9.21	327.95
9450	25.87	$3.15\text{E}+15$	503.82	8.99	322.85
9650	26.42	$3.08\text{E}+15$	492.24	8.79	317.96

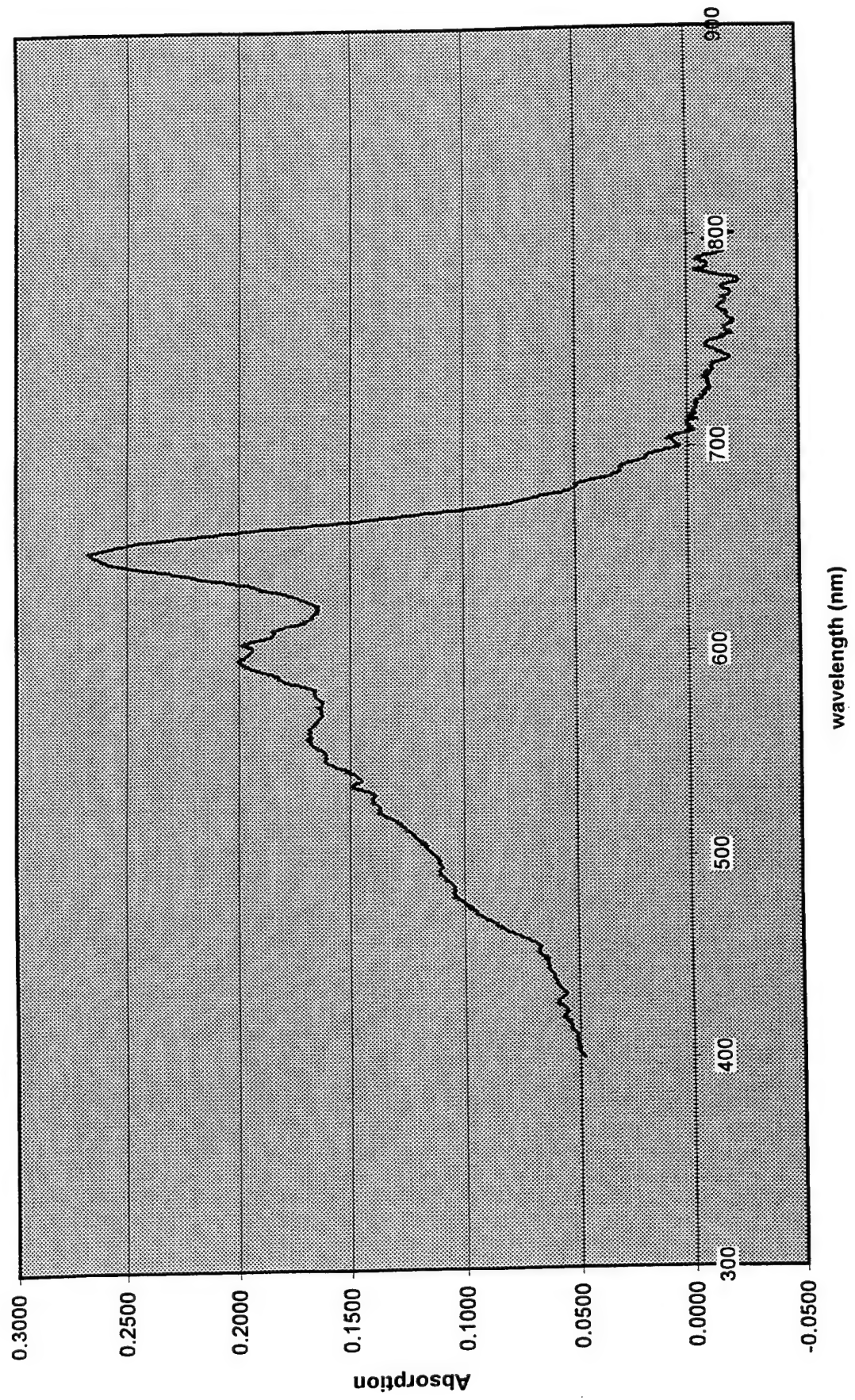
Waste Package Temperatures



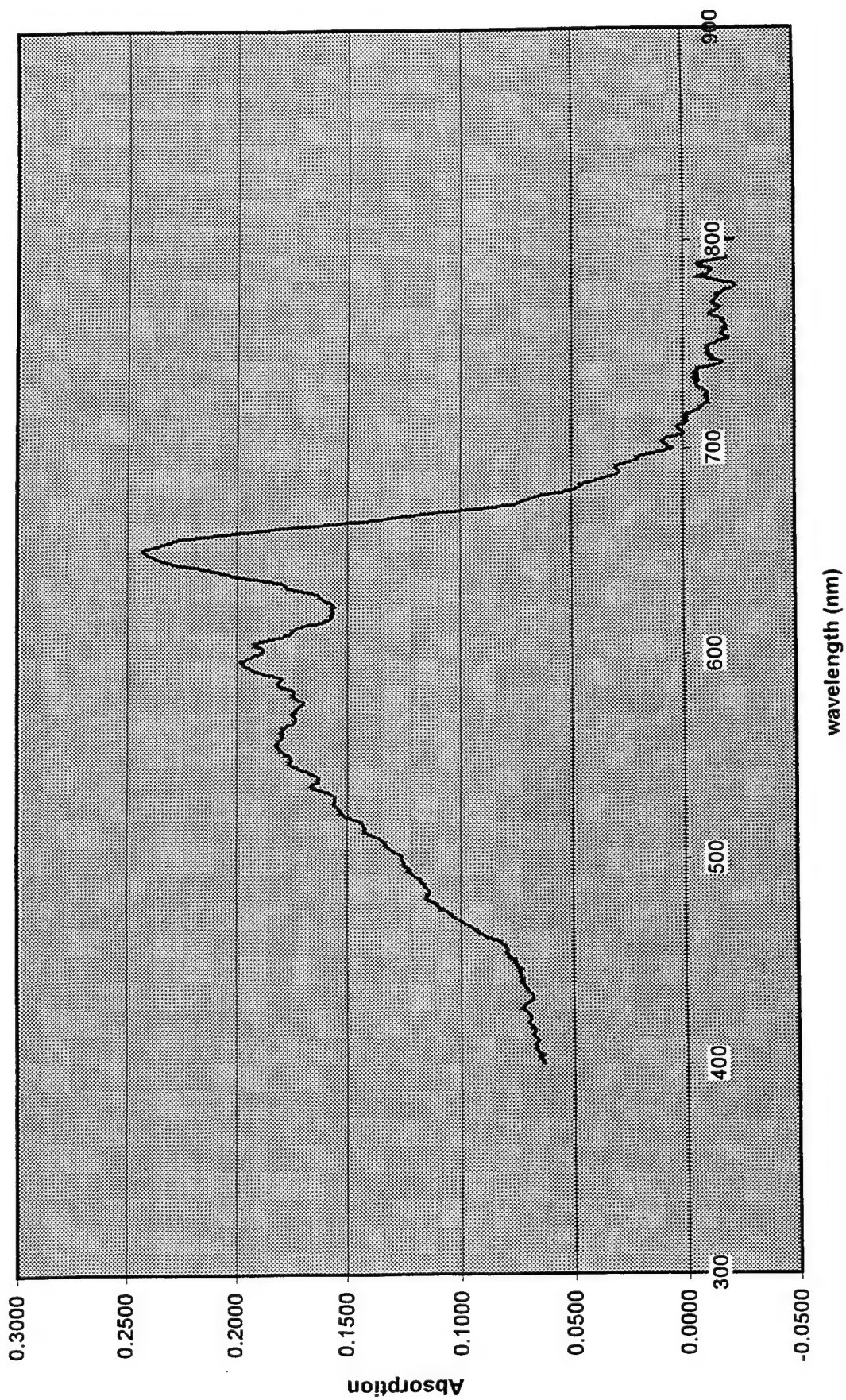
Appendix C-1: UV Spectroscopy and Graphs

<u>Sample</u>	<u>page</u>
Us1	109
Us2	110
Us3	111
Us4	112
Us5	113
Us6	114
Us7	115
Us8	116
Us9	117
Us10	118
Us11	119
Us12	120
Us13	121
Us14	122
Us15	123
Us16	124
Us17	125
Us18	126
S1	127
S2	128
S3	129
S4	130

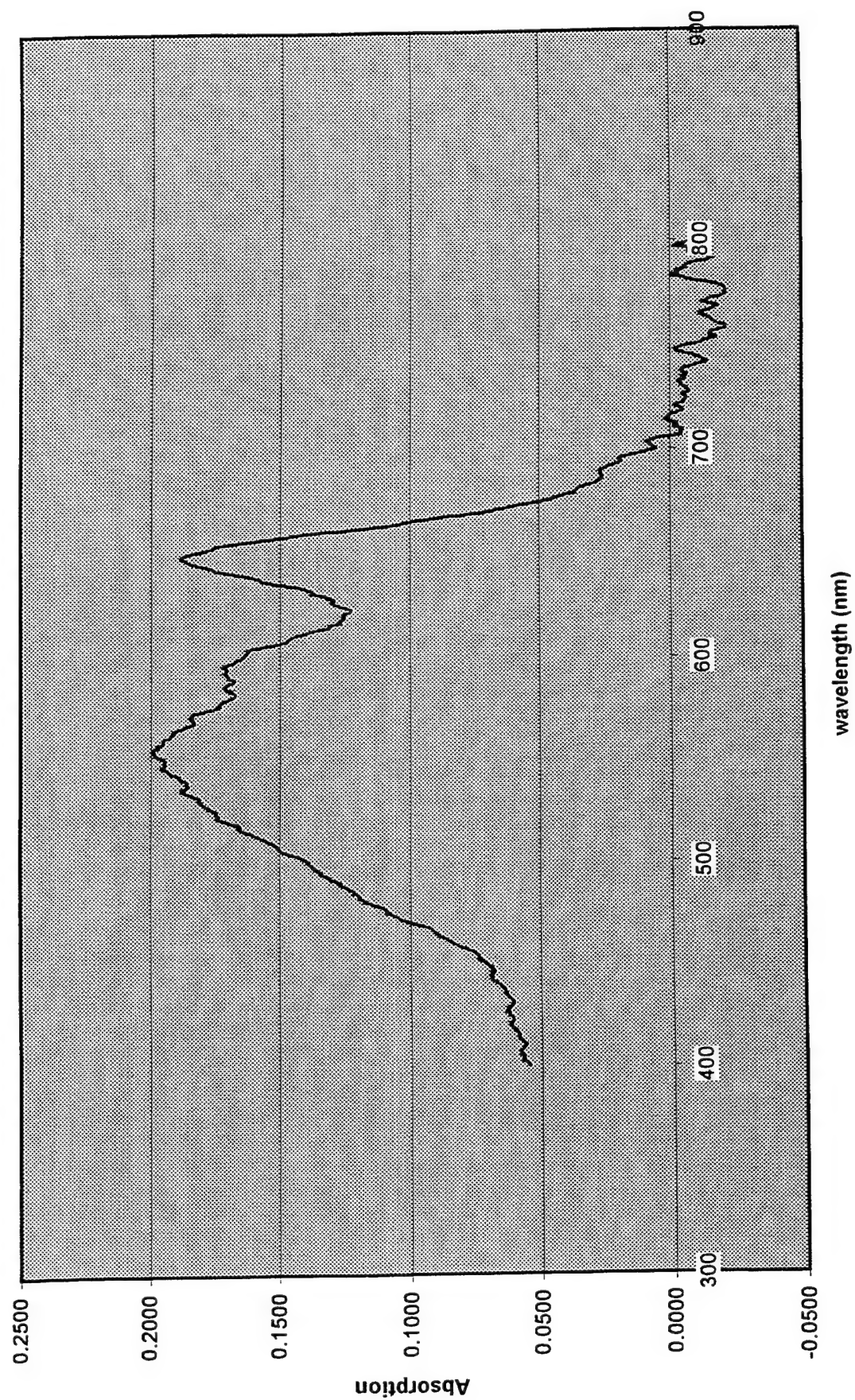
Sample us1



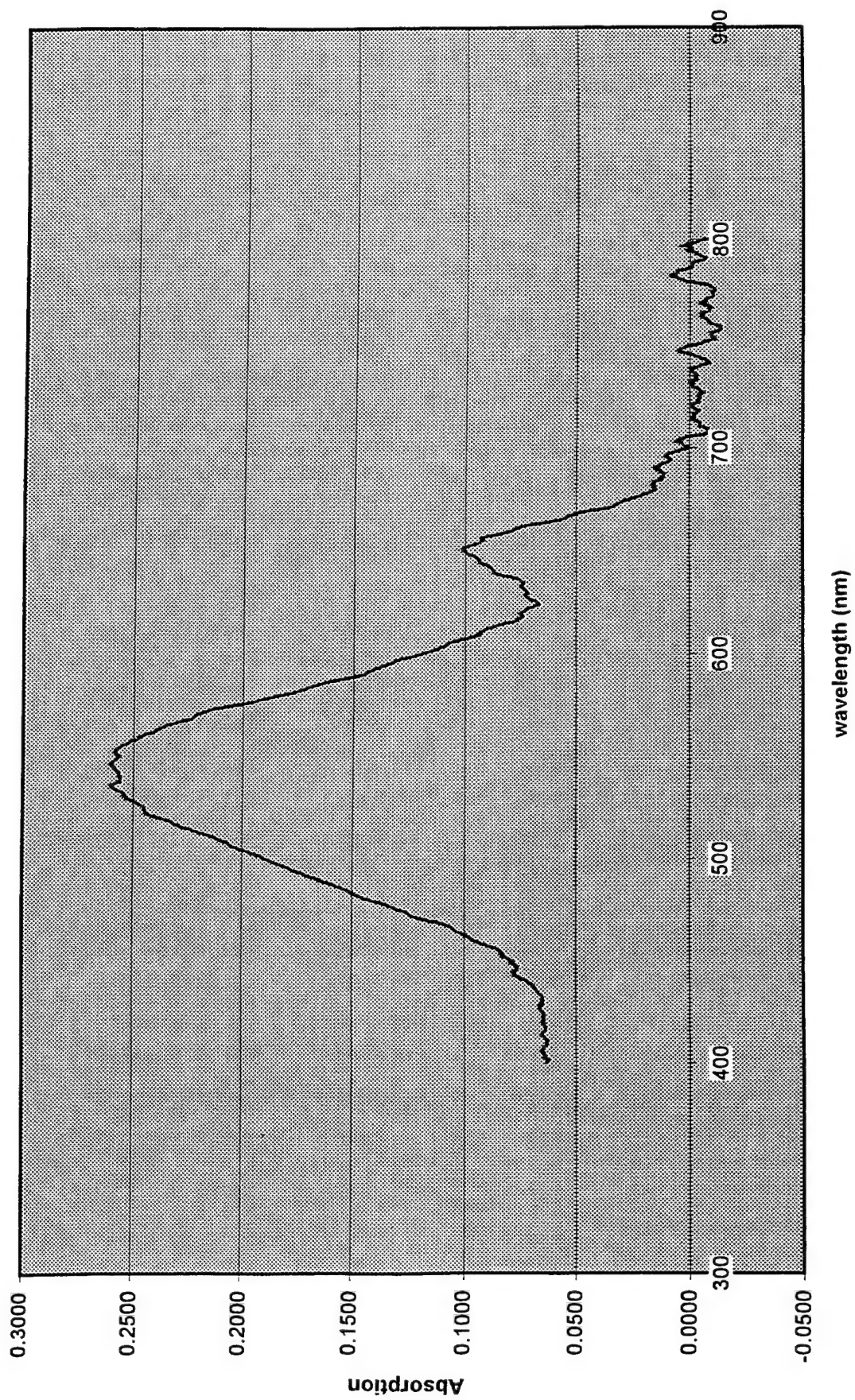
Sample us2



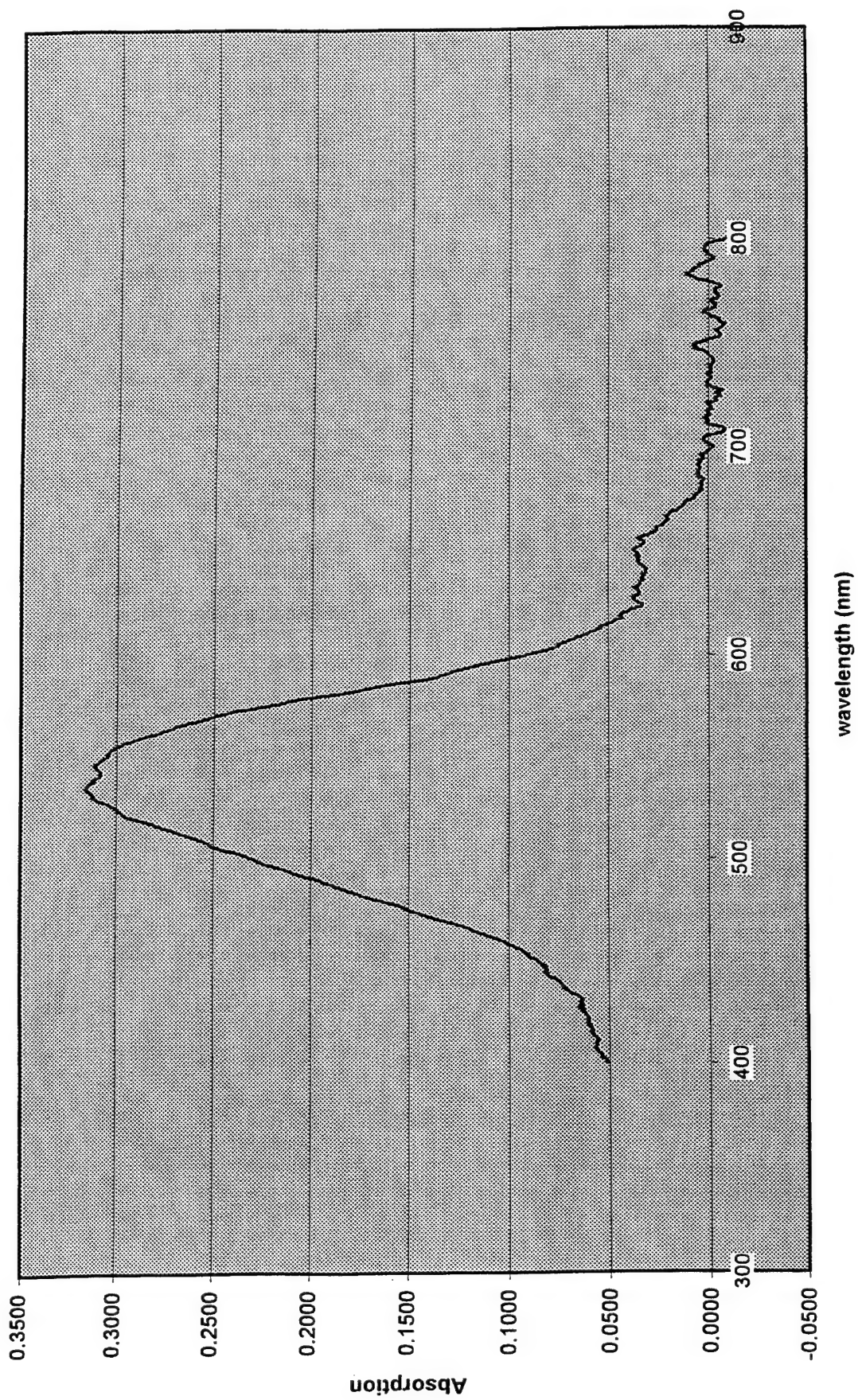
Sample us3



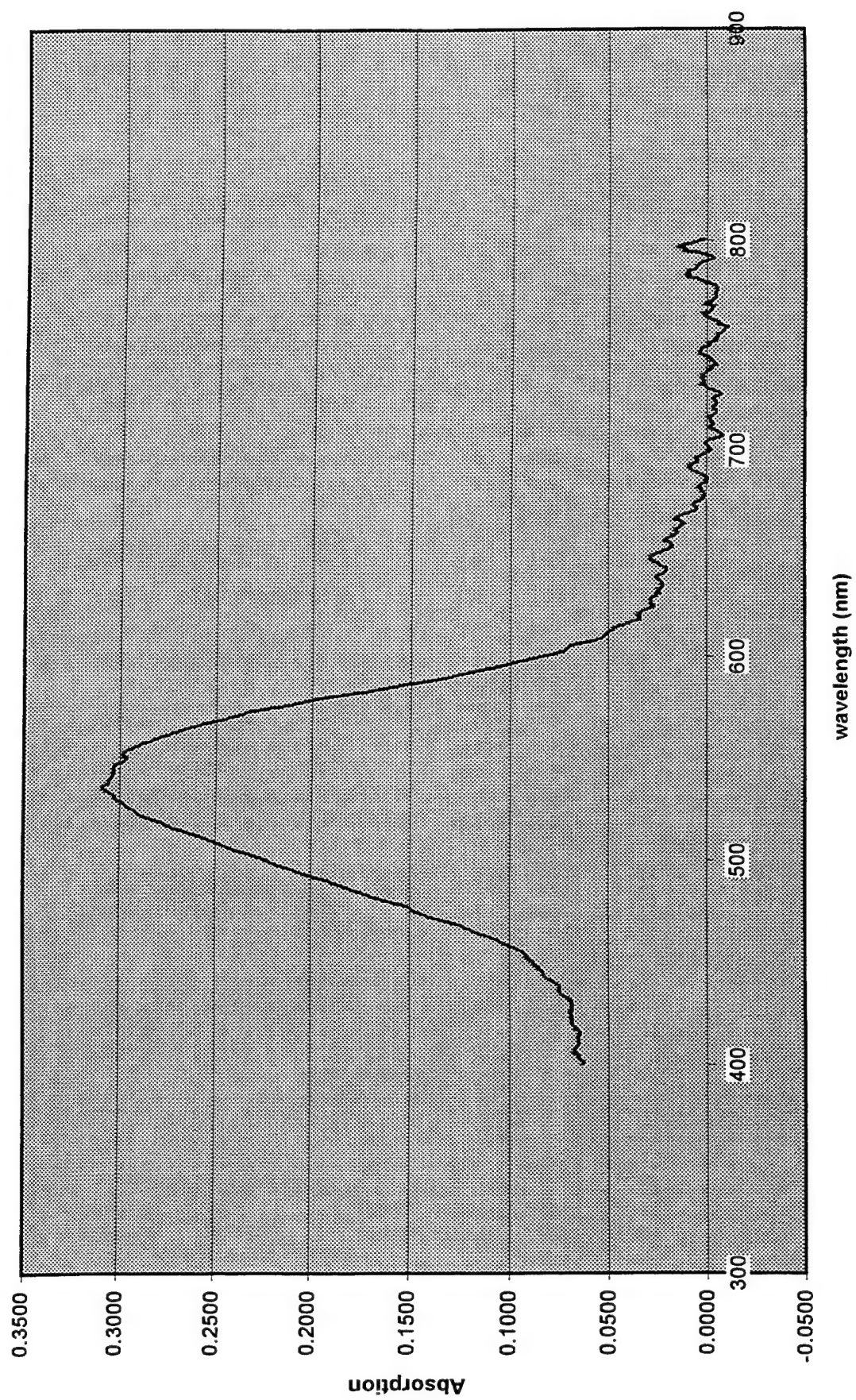
Sample us4



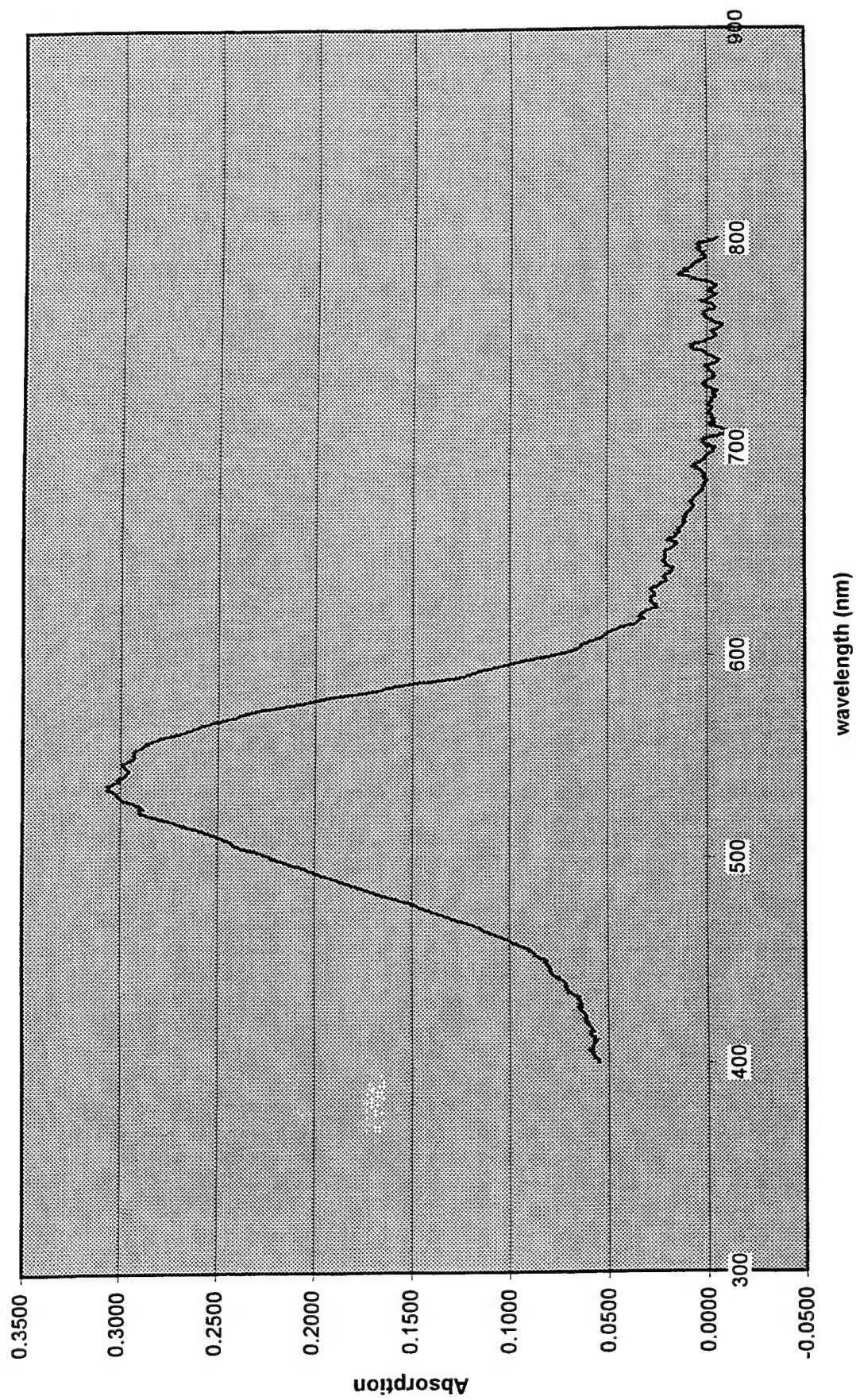
Sample us5



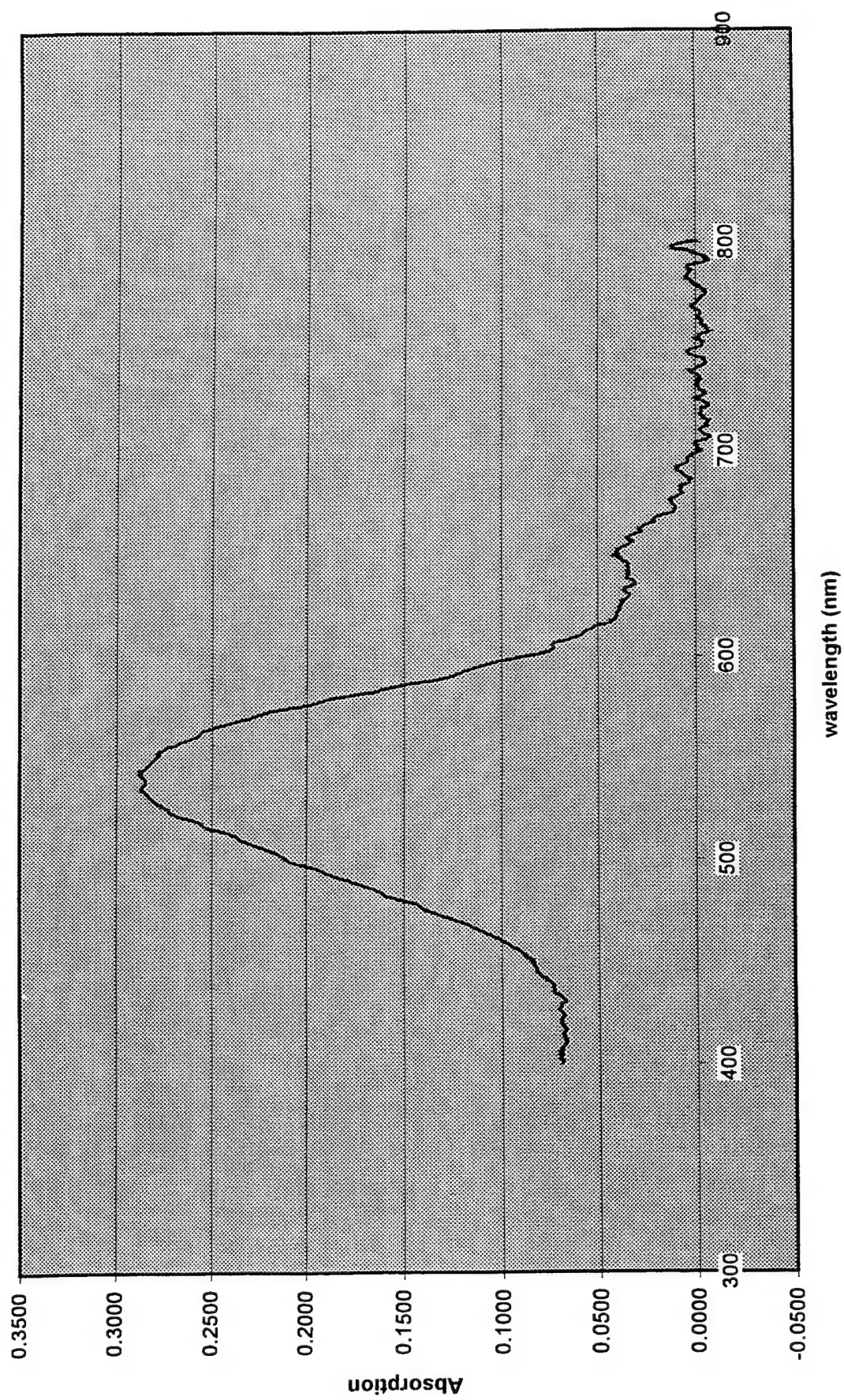
Sample us6



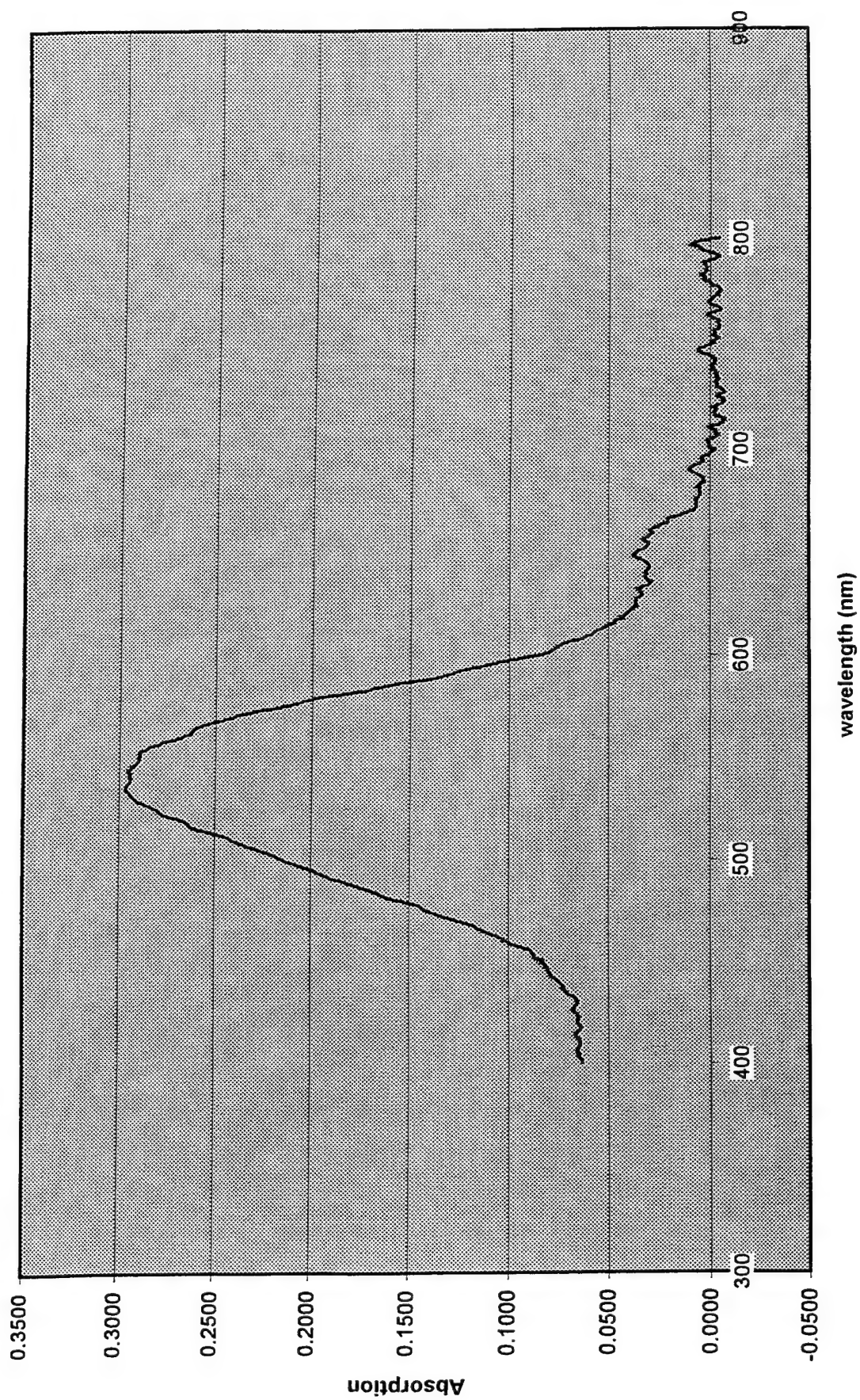
Sample us7



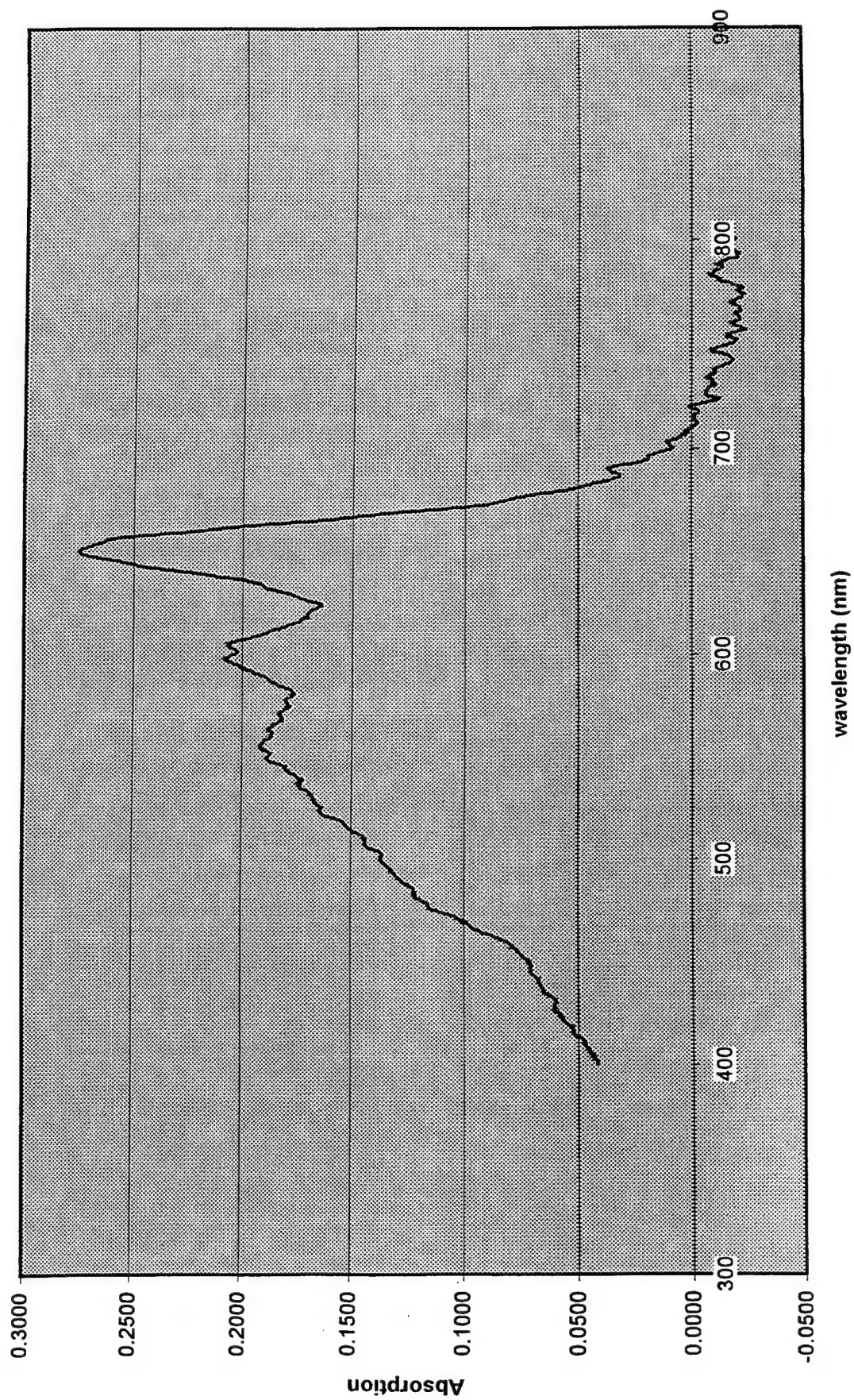
Sample us8



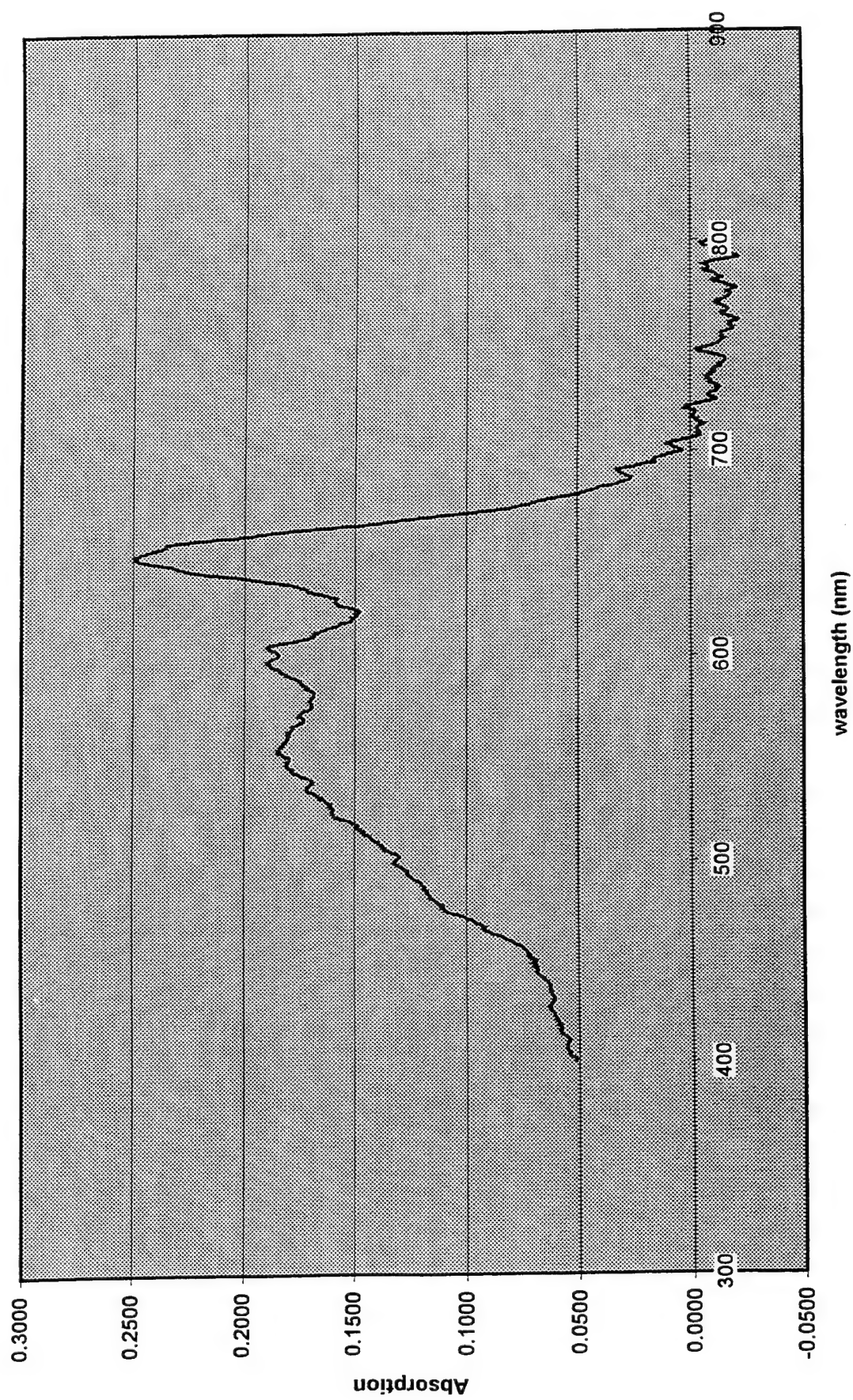
Sample us9



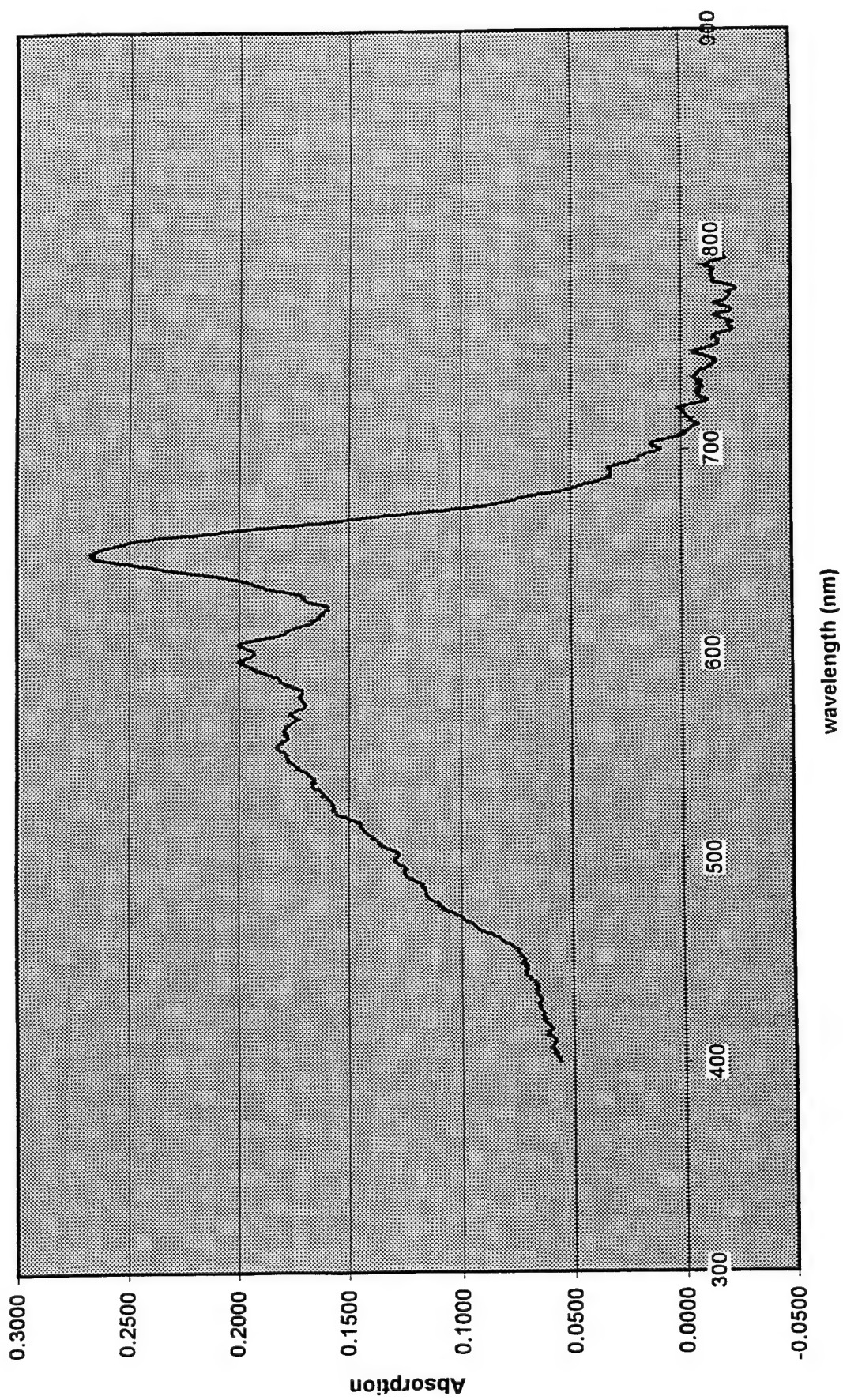
Sample us10



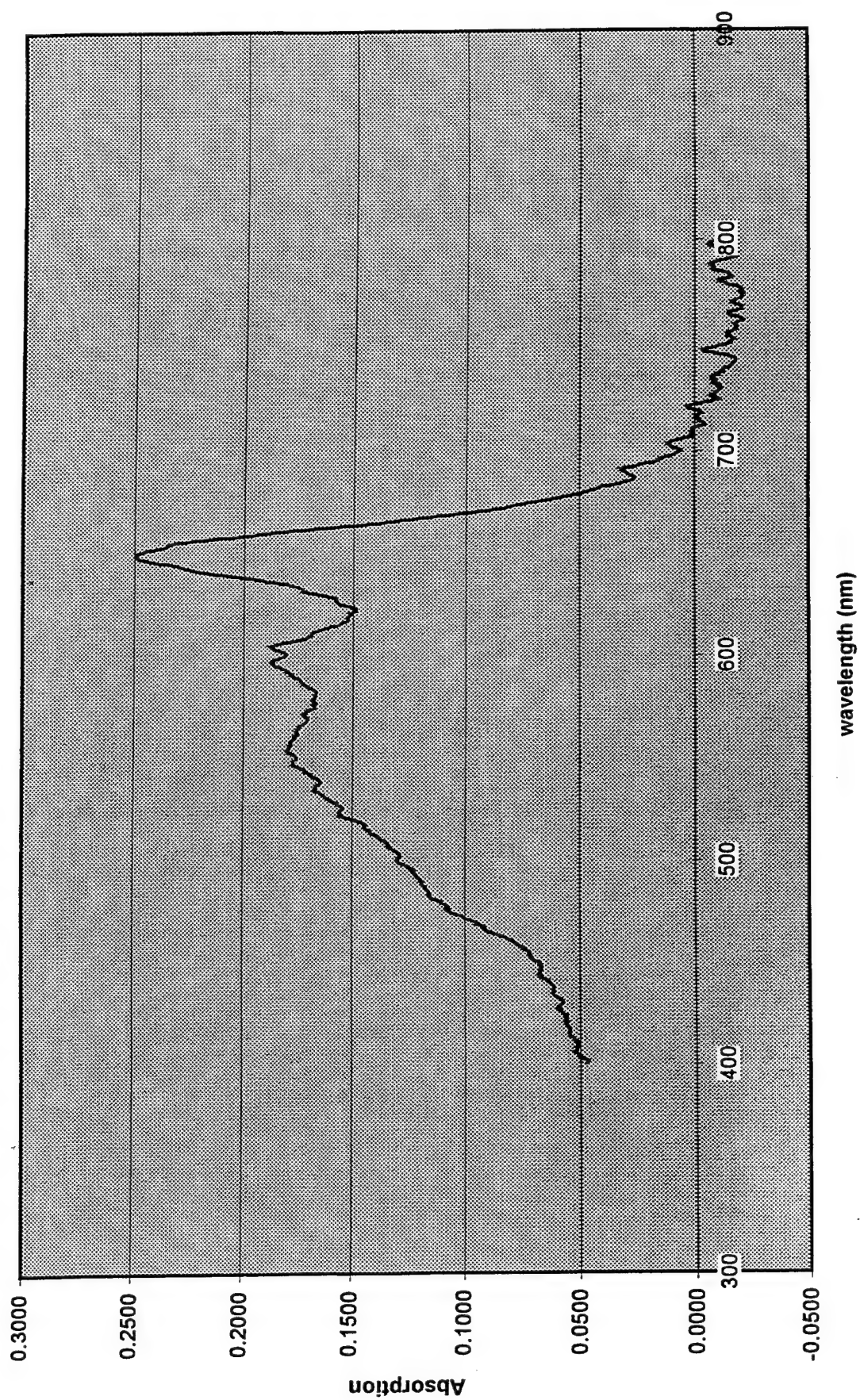
Sample us11



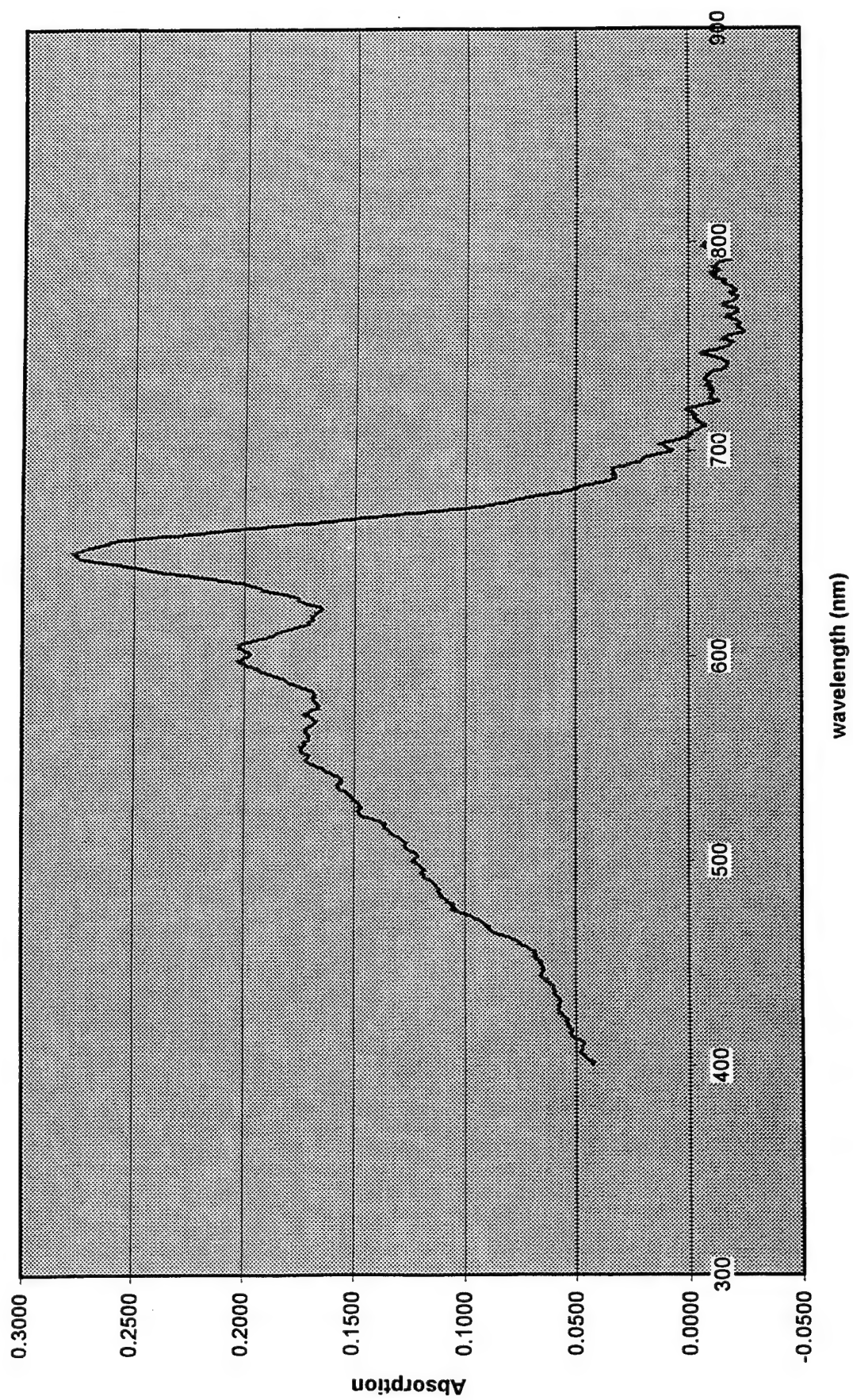
Sample us12



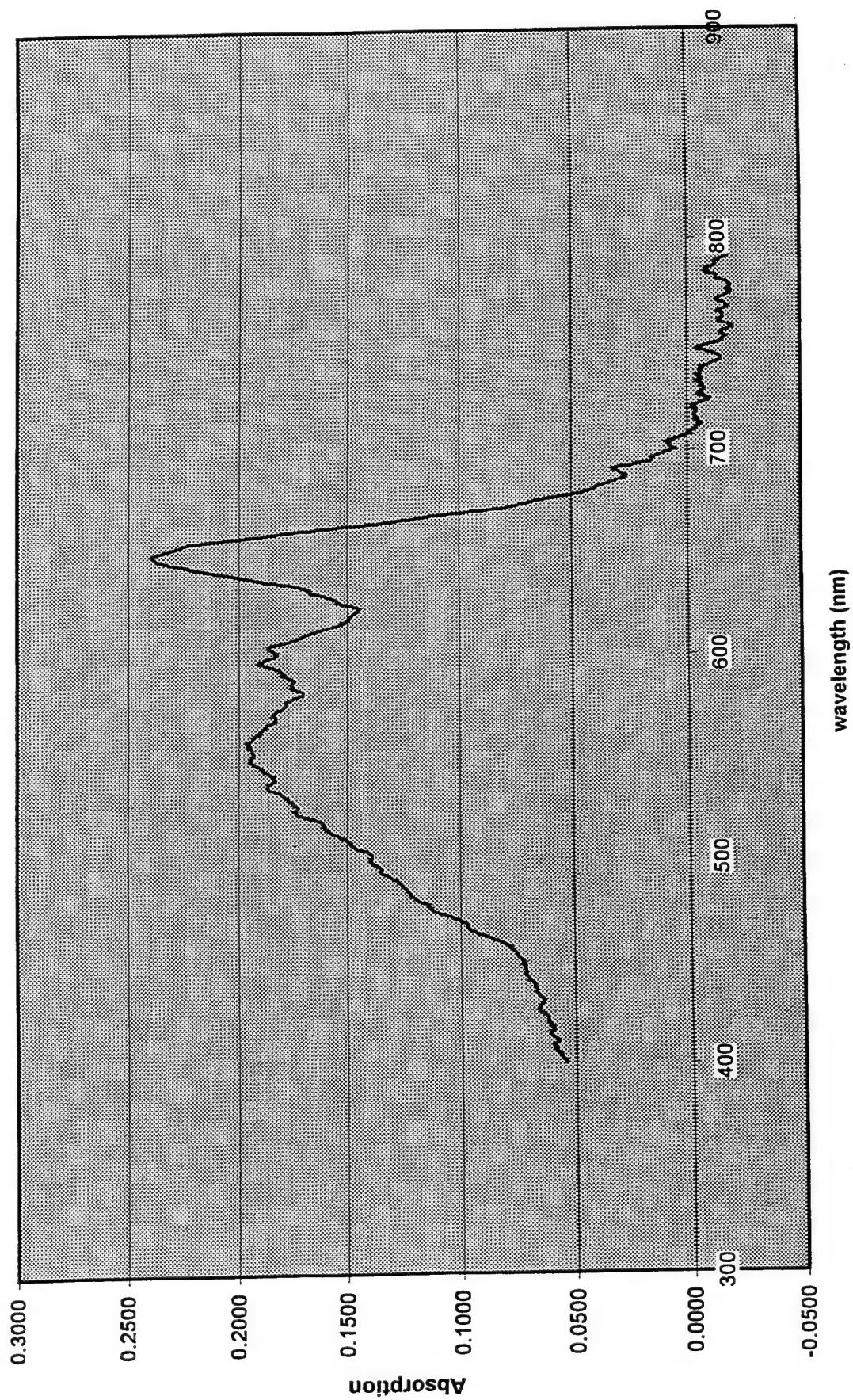
Sample us13



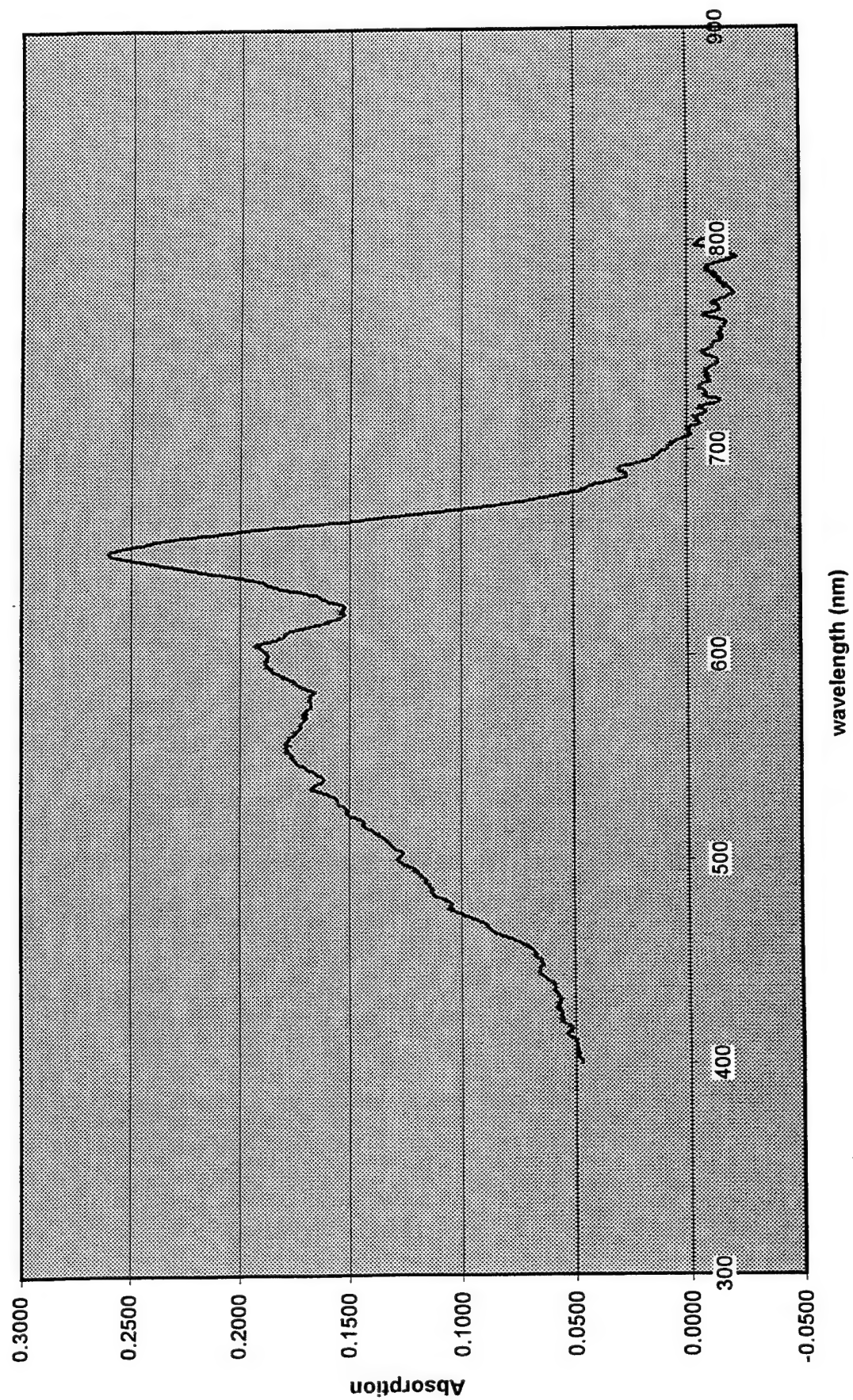
Sample us14



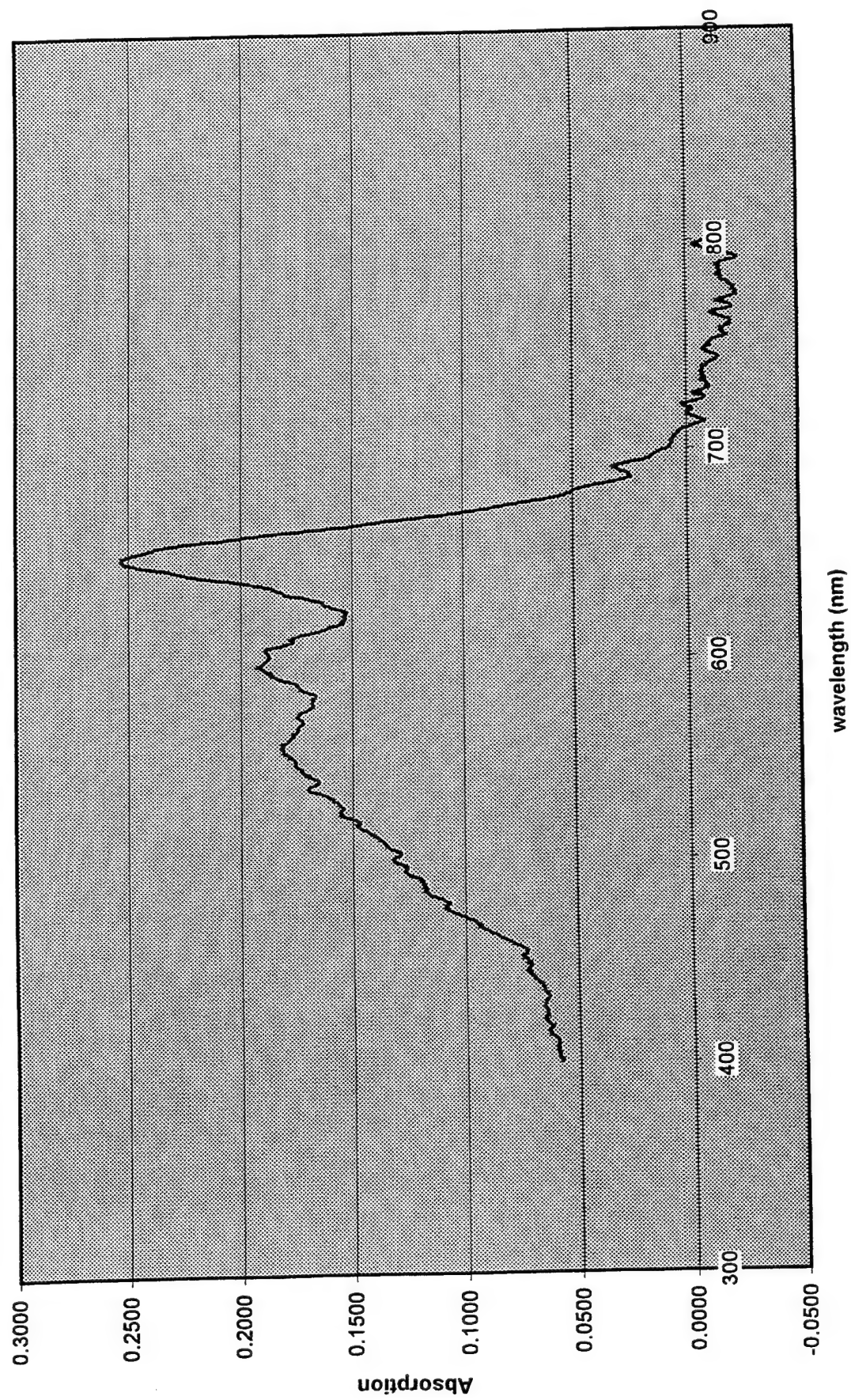
Sample us15



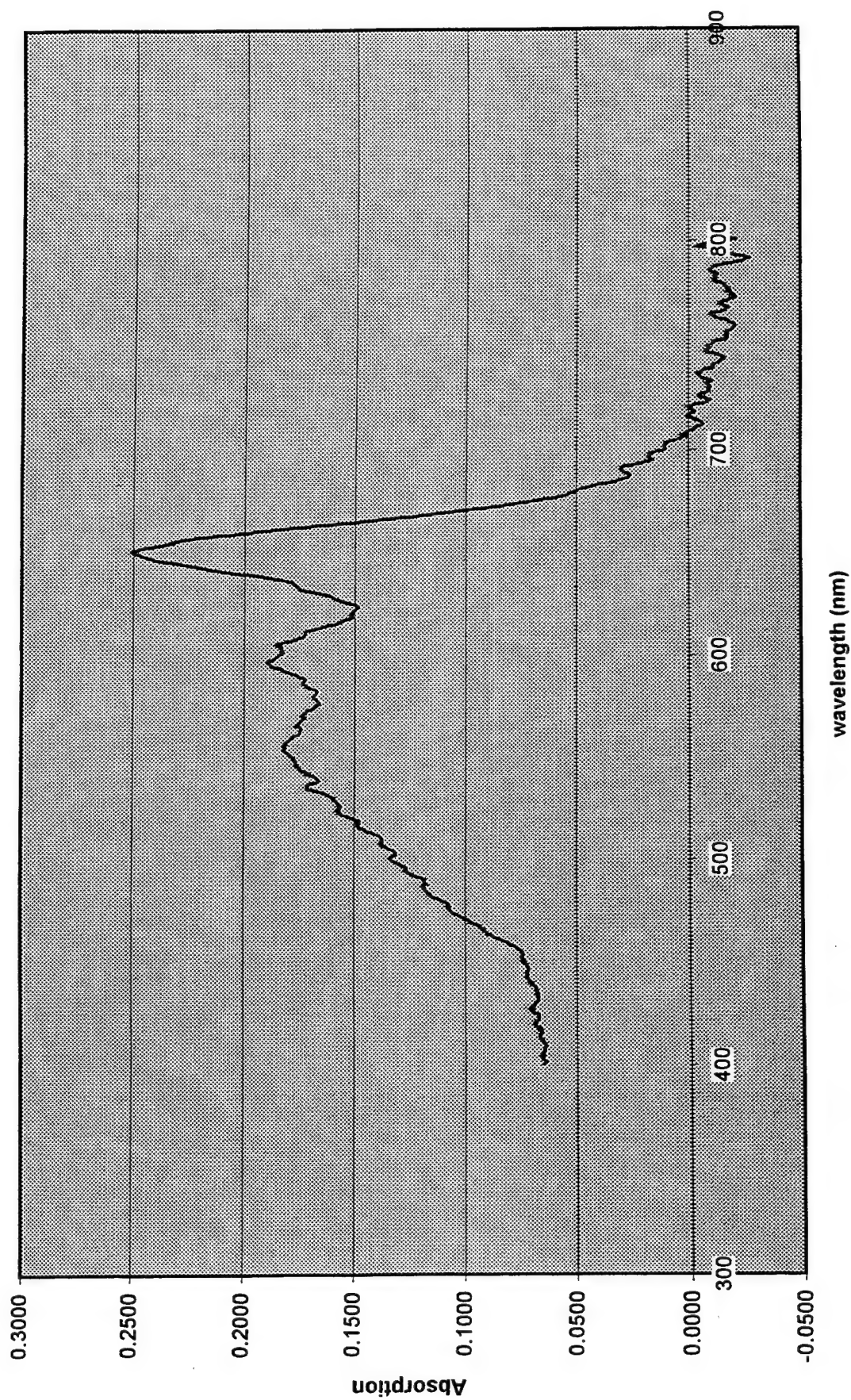
Sample us16



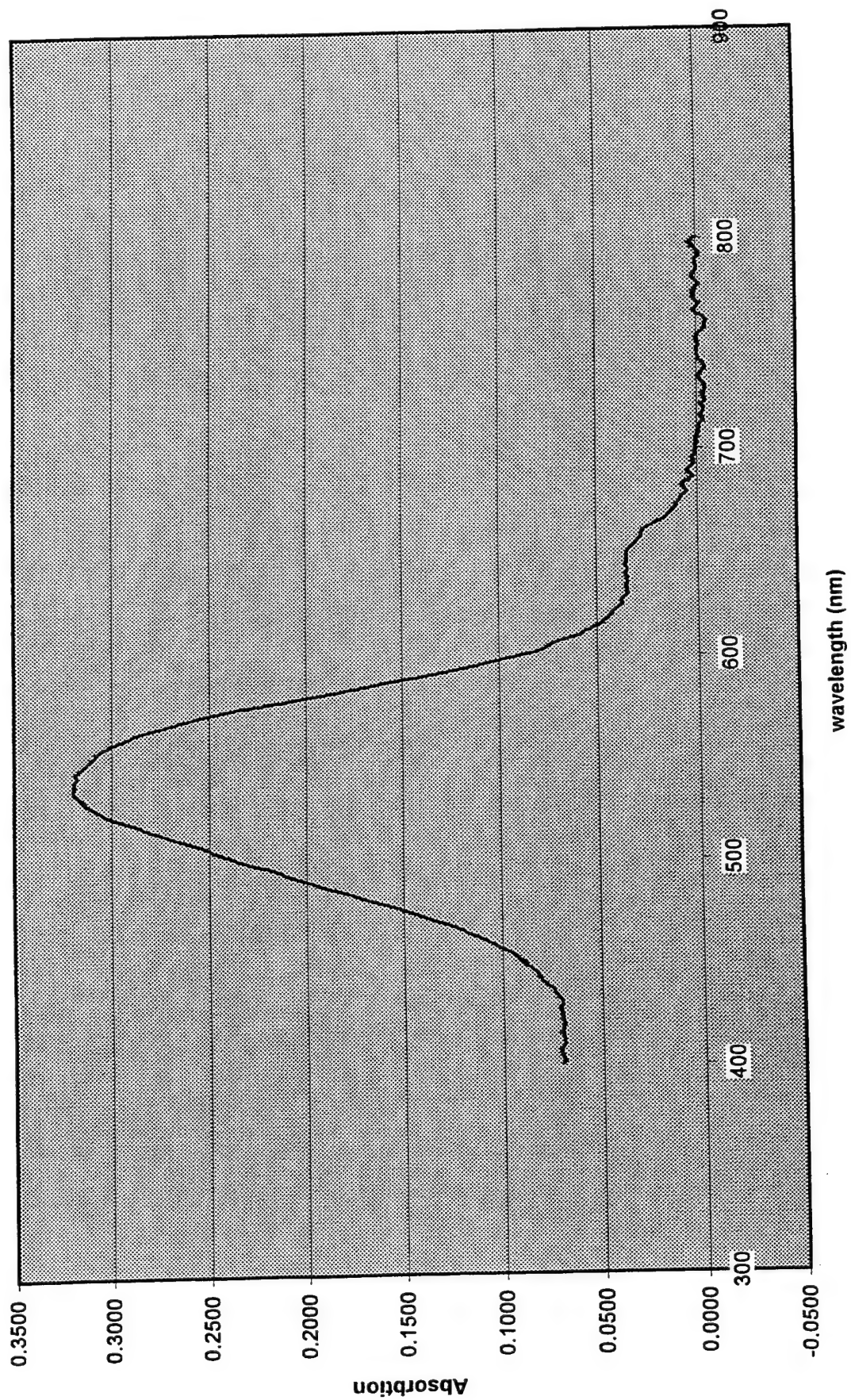
Sample us17



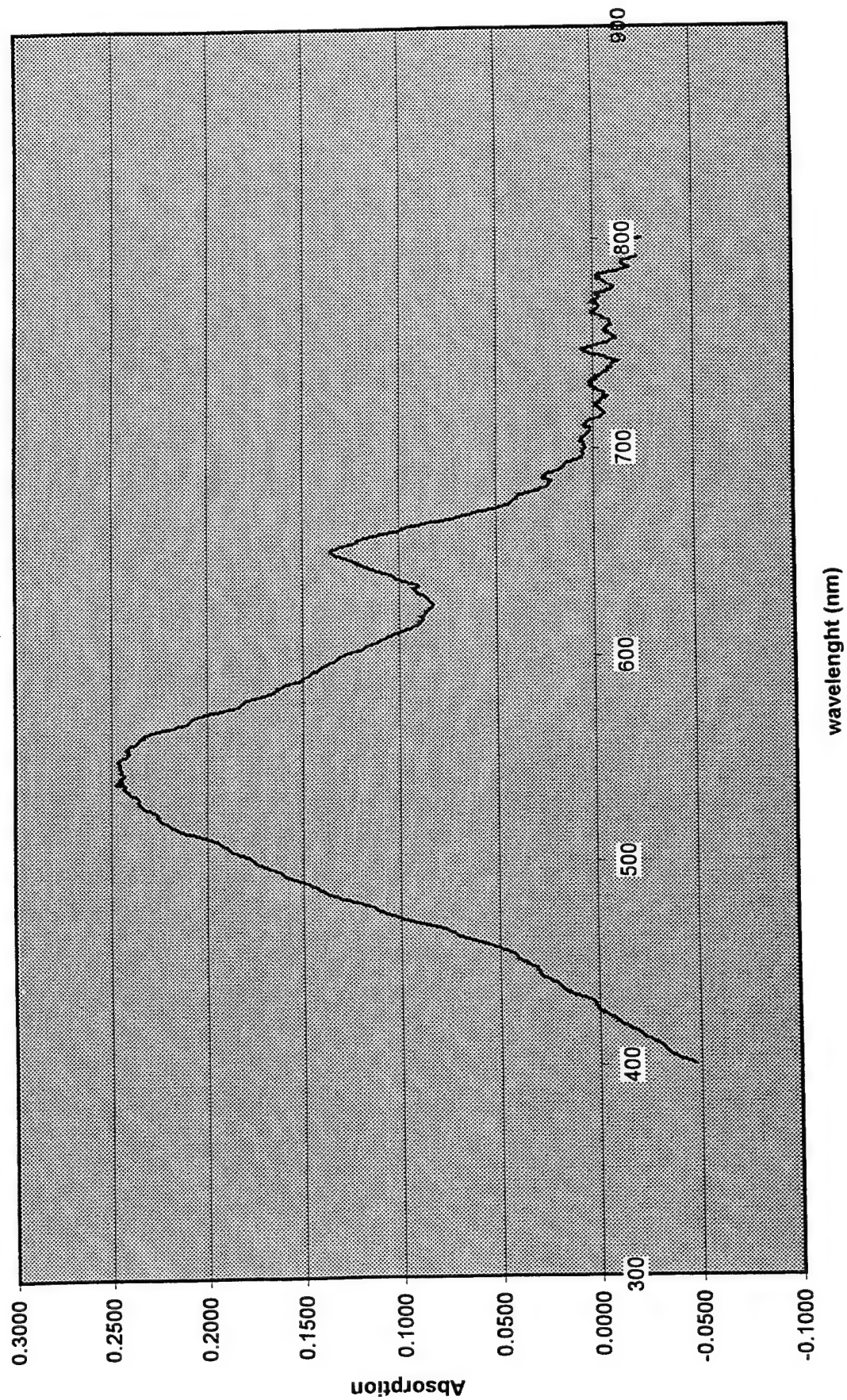
Sample us18



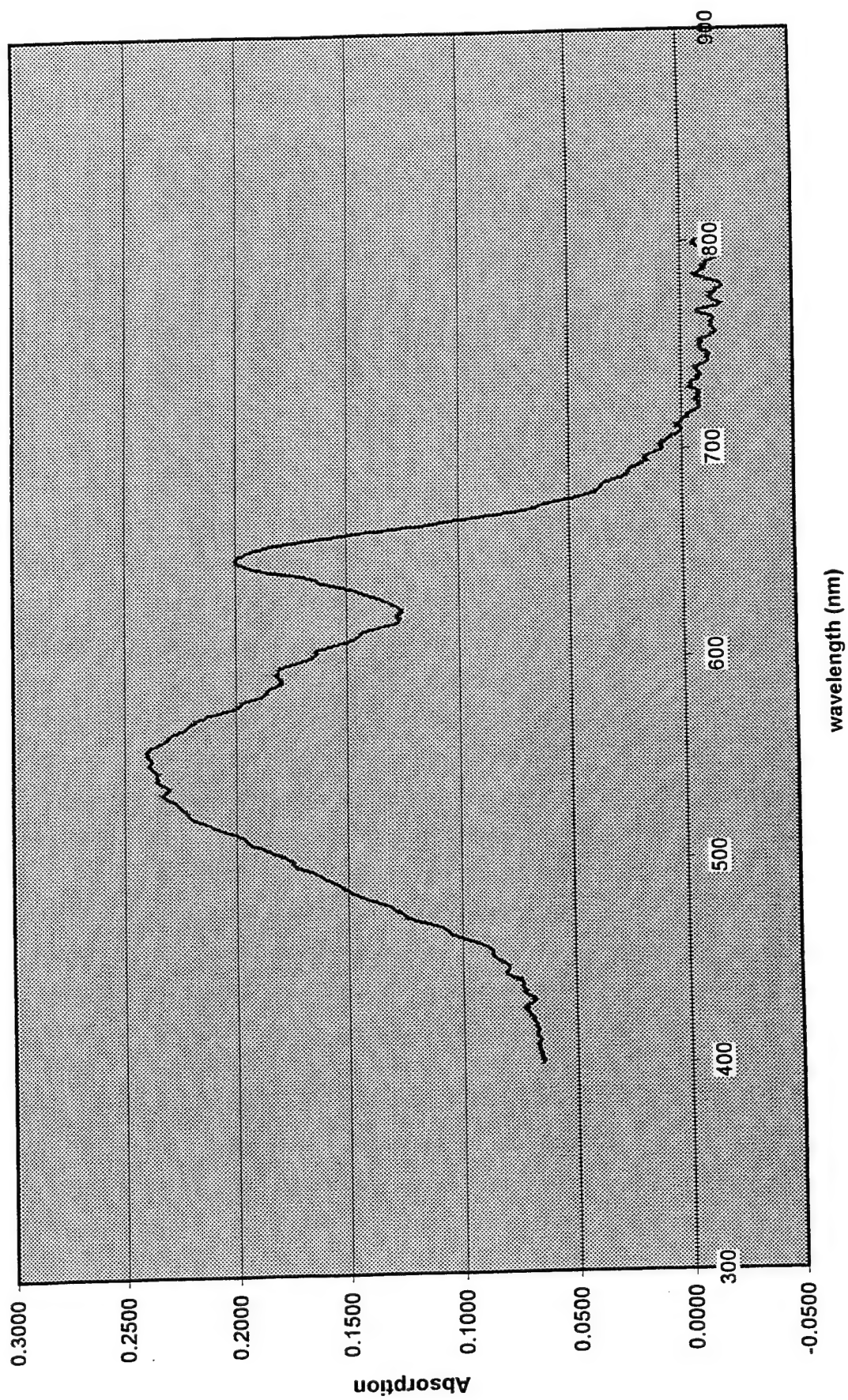
Standard #1 - 1e-6



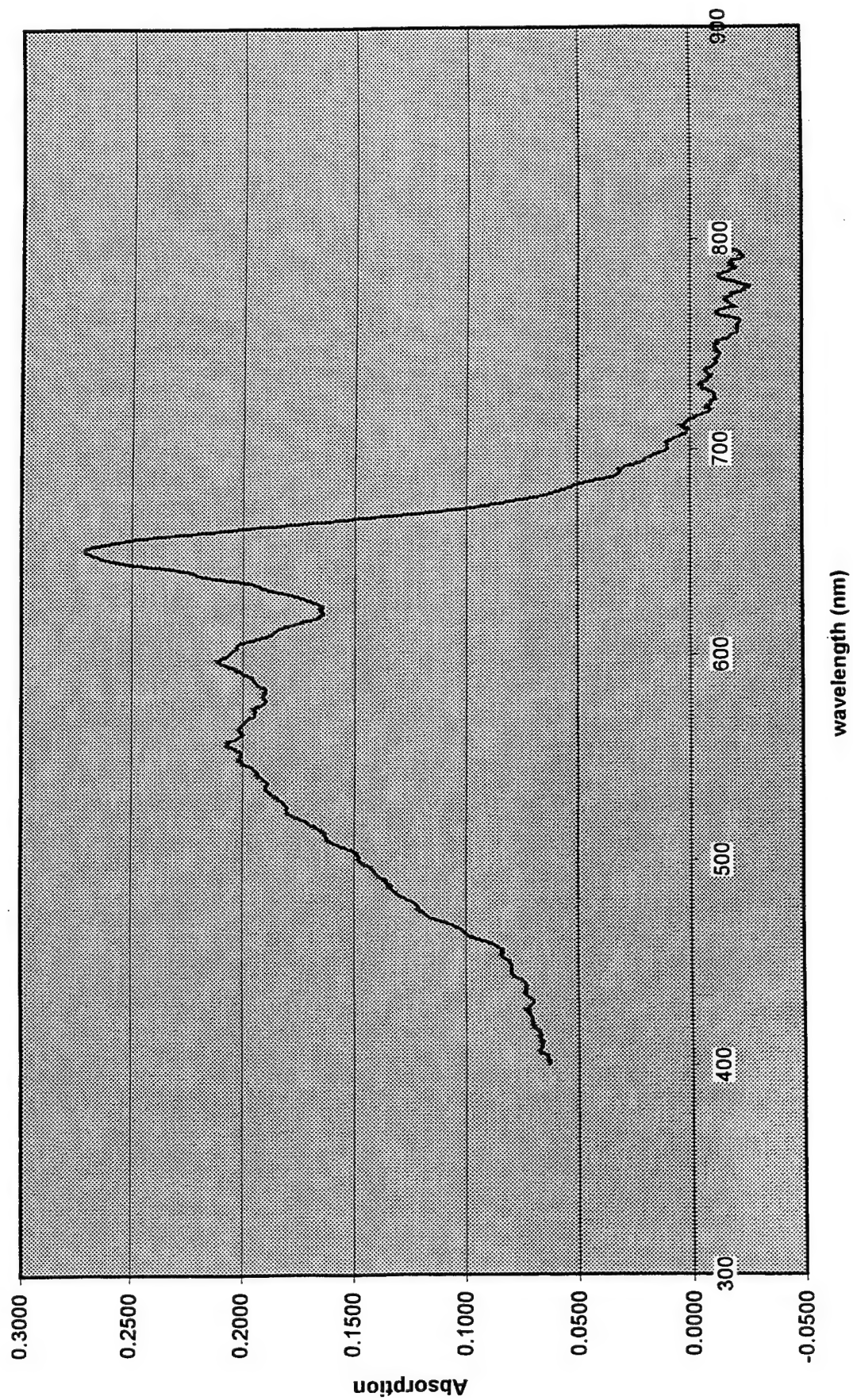
Standard #2 - 5e-6



Standard #3 - 7e-6



Standard #4 - 10e-6



Appendix C-2: Uranium Speciation Supporting Data

A	B	C	[NO ₃] ⁻			G	UO_2OH^+ $\text{UO}_2(\text{OH})_2^0$ $\text{UO}_2(\text{OH})_3^-$ $\text{UO}_2(\text{OH})_4^{2-}$ $(\text{UO}_2)_2\text{OH}^{3+}$ $(\text{UO}_2)_2(\text{OH})_2^{2+}$						
			[NO ₃] ⁻	pKa1co3	logKsum		pKw	logK10-10	logK10-20	logK10-30	logK10-40	logK20-10	logK20-20
			2.00E-05	6.30	-17.55		13.92	-5.40	-10.50	-19.20	-32.60	-2.90	-5.82
			D	E	F		H	I	J	K	L	M	N
pH	pp CO ₂	p[NO ₃] ⁻	[UO ₂] ²⁺	p[CO ₃] ²⁻	pM	[UO ₂] ²⁺	ΔpM	[UOH]	[U(OH) ₂]	[U(OH) ₃]	[U(OH) ₄]	[U ₂ OH]	[U ₂ (OH) ₂]
1.0	3.02E-04	4.70	1.00E-05	19.07	5.00	1.00E-05	0.00	3.98E-10	3.16E-14	6.31E-22	2.51E-34	1.26E-12	1.51E-14
1.1	3.02E-04	4.70	1.00E-05	18.87	5.00	1.00E-05	0.00	5.01E-10	5.01E-14	1.26E-21	6.31E-34	1.58E-12	2.40E-14
1.2	3.02E-04	4.70	1.00E-05	18.67	5.00	1.00E-05	0.00	6.31E-10	7.94E-14	2.51E-21	1.58E-33	2.00E-12	3.80E-14
1.3	3.02E-04	4.70	1.00E-05	18.47	5.00	1.00E-05	0.00	7.94E-10	1.26E-13	5.01E-21	3.98E-33	2.51E-12	6.02E-14
1.4	3.02E-04	4.70	1.00E-05	18.27	5.00	1.00E-05	0.00	1.00E-09	2.00E-13	1.00E-20	2.51E-32	3.98E-12	1.51E-13
1.5	3.02E-04	4.70	1.00E-05	18.07	5.00	1.00E-05	0.00	1.26E-09	3.16E-13	2.00E-20	2.51E-32	3.98E-12	2.40E-13
1.6	3.02E-04	4.70	1.00E-05	17.87	5.00	1.00E-05	0.00	1.58E-09	5.01E-13	3.98E-20	6.31E-32	5.01E-12	3.80E-13
1.7	3.02E-04	4.70	1.00E-05	17.67	5.00	1.00E-05	0.00	1.99E-09	7.94E-13	7.94E-20	1.58E-31	6.31E-12	6.02E-13
1.8	3.02E-04	4.70	1.00E-05	17.47	5.00	1.00E-05	0.00	2.51E-09	1.26E-12	1.58E-19	3.98E-31	7.94E-12	9.54E-13
1.9	3.02E-04	4.70	1.00E-05	17.27	5.00	1.00E-05	0.00	3.16E-09	1.99E-12	3.16E-19	1.00E-30	9.99E-12	1.51E-12
2.0	3.02E-04	4.70	1.00E-05	17.07	5.00	1.00E-05	0.00	3.98E-09	3.16E-12	6.31E-19	2.51E-30	1.26E-11	2.40E-12
2.1	3.02E-04	4.70	1.00E-05	16.87	5.00	9.99E-06	0.00	5.01E-09	5.01E-12	1.26E-18	6.31E-30	1.58E-11	3.80E-12
2.2	3.02E-04	4.70	1.00E-05	16.67	5.00	9.99E-06	0.00	6.31E-09	7.94E-12	2.51E-18	1.58E-29	1.99E-11	6.02E-12
2.3	3.02E-04	4.70	1.00E-05	16.47	5.00	9.99E-06	0.00	7.94E-09	1.26E-11	5.01E-18	3.98E-29	2.51E-11	9.53E-12
2.4	3.02E-04	4.70	1.00E-05	16.27	5.00	9.99E-06	0.00	9.99E-09	1.99E-11	9.99E-18	9.99E-29	3.16E-11	1.51E-11
2.5	3.02E-04	4.70	1.00E-05	16.07	5.00	9.99E-06	0.00	1.26E-08	3.16E-11	1.99E-17	2.51E-28	3.97E-11	2.39E-11
2.6	3.02E-04	4.70	1.00E-05	15.87	5.00	9.98E-06	0.00	1.58E-08	5.00E-11	3.97E-17	6.30E-28	5.00E-11	3.79E-11
2.7	3.02E-04	4.70	1.00E-05	15.67	5.00	9.98E-06	0.00	1.99E-08	7.93E-11	7.93E-17	1.58E-27	6.28E-11	5.99E-11
2.8	3.02E-04	4.70	1.00E-05	15.47	5.00	9.97E-06	0.00	2.51E-08	1.26E-10	1.58E-16	3.97E-27	7.90E-11	9.49E-11
2.9	3.02E-04	4.70	1.00E-05	15.27	5.00	9.97E-06	0.00	3.15E-08	1.99E-10	3.15E-16	9.97E-27	9.94E-11	1.50E-10
3.0	3.02E-04	4.70	1.00E-05	15.07	5.00	9.96E-06	0.00	3.96E-08	3.15E-10	6.28E-16	2.50E-26	1.25E-10	2.37E-10
3.1	3.02E-04	4.70	1.00E-05	14.87	5.00	9.95E-06	0.00	4.99E-08	4.99E-10	1.25E-15	6.28E-26	1.57E-10	3.75E-10
3.2	3.02E-04	4.70	1.00E-05	14.67	5.00	9.94E-06	0.00	6.27E-08	7.89E-10	2.50E-15	1.57E-25	1.97E-10	5.93E-10
3.3	3.02E-04	4.70	1.00E-05	14.47	5.00	9.92E-06	0.00	7.88E-08	1.25E-09	4.97E-15	3.95E-25	2.47E-10	9.35E-10
3.4	3.02E-04	4.70	1.00E-05	14.27	5.00	9.90E-06	0.00	9.90E-08	1.97E-09	9.90E-15	9.90E-25	3.10E-10	1.47E-09
3.5	3.02E-04	4.70	1.00E-05	14.07	5.01	9.87E-06	0.00	1.24E-07	3.12E-09	1.97E-14	2.48E-24	3.88E-10	2.32E-09
3.6	3.02E-04	4.70	1.00E-05	13.87	5.01	9.83E-06	0.00	1.56E-07	4.93E-09	3.91E-14	6.20E-24	4.85E-10	3.64E-09
3.7	3.02E-04	4.70	1.00E-05	13.67	5.01	9.79E-06	0.00	1.95E-07	7.78E-09	7.78E-14	1.55E-23	6.05E-10	5.70E-09
3.8	3.02E-04	4.70	1.00E-05	13.47	5.01	9.73E-06	0.00	2.44E-07	1.22E-08	1.54E-13	3.87E-23	7.52E-10	8.90E-09
3.9	3.02E-04	4.70	1.00E-05	13.27	5.02	9.66E-06	0.00	3.05E-07	1.93E-08	3.05E-13	9.66E-23	9.32E-10	1.38E-08
4.0	3.02E-04	4.70	1.00E-05	13.07	5.02	9.56E-06	0.00	3.81E-07	3.02E-08	6.03E-13	2.40E-22	1.15E-09	2.13E-08
4.1	3.02E-04	4.70	1.00E-05	12.87	5.03	9.43E-06	0.00	4.73E-07	4.73E-08	1.19E-12	5.95E-22	1.41E-09	3.27E-08
4.2	3.02E-04	4.70	1.00E-05	12.67	5.03	9.27E-06	0.00	5.85E-07	7.36E-08	2.33E-12	1.47E-21	1.72E-09	4.95E-08
4.3	3.02E-04	4.70	1.00E-05	12.47	5.04	9.06E-06	0.00	7.20E-07	1.14E-07	4.54E-12	3.61E-21	2.06E-09	7.38E-08
4.4	3.02E-04	4.70	1.00E-05	12.27	5.06	8.79E-06	0.00	8.79E-07	1.75E-07	8.79E-12	8.79E-21	2.44E-09	1.08E-07
4.5	3.02E-04	4.70	1.00E-05	12.07	5.07	8.44E-06	0.00	1.06E-06	2.67E-07	1.68E-11	2.12E-20	2.84E-09	1.54E-07
4.6	3.02E-04	4.70	1.00E-05	11.87	5.10	8.01E-06	0.00	1.27E-06	4.01E-07	3.19E-11	5.05E-20	3.21E-09	2.12E-07
4.7	3.02E-04	4.70	1.00E-05	11.67	5.13	7.47E-06	0.00	1.49E-06	5.94E-07	5.94E-11	1.18E-19	3.52E-09	2.81E-07
4.8	3.02E-04	4.70	1.00E-05	11.47	5.17	6.83E-06	0.00	1.72E-06	8.60E-07	1.08E-10	2.72E-19	3.71E-09	3.56E-07
4.9	3.02E-04	4.70	1.00E-05	11.27	5.21	6.11E-06	0.00	1.93E-06	1.22E-06	1.93E-10	6.11E-19	3.73E-09	4.27E-07
5.0	3.02E-04	4.70	1.00E-05	11.07	5.27	5.31E-06	0.00	2.11E-06	1.68E-06	3.35E-10	1.33E-18	3.55E-09	4.83E-07
5.1	3.02E-04	4.70	1.00E-05	10.87	5.35	4.49E-06	0.00	2.25E-06	2.25E-06	5.65E-10	2.83E-18	3.19E-09	5.13E-07
5.2	3.02E-04	4.70	1.00E-05	10.67	5.43	3.67E-06	0.00	2.32E-06	2.92E-06	9.23E-10	5.82E-18	2.69E-09	5.12E-07
5.3	3.02E-04	4.70	1.00E-05	10.47	5.54	2.91E-06	0.00	2.31E-06	3.67E-06	1.46E-09	1.16E-17	2.13E-09	4.79E-07
5.4	3.02E-04	4.70	1.00E-05	10.27	5.65	2.24E-06	0.00	2.24E-06	4.47E-06	2.24E-09	2.24E-17	1.59E-09	4.21E-07
5.5	3.02E-04	4.70	1.00E-05	10.07	5.78	1.67E-06	0.00	2.10E-06	5.28E-06	3.33E-09	4.19E-17	1.11E-09	3.50E-07
5.6	3.02E-04	4.70	1.00E-05	9.87	5.92	1.21E-06	0.00	1.91E-06	6.05E-06	4.81E-09	7.62E-17	7.31E-10	2.75E-07
5.7	3.02E-04	4.70	1.00E-05	9.67	6.07	8.51E-07	0.00	1.70E-06	6.76E-06	6.76E-09	1.35E-16	4.57E-10	2.07E-07
5.8	3.02E-04	4.70	1.00E-05	9.47	6.23	5.86E-07	0.00	1.47E-06	7.37E-06	9.28E-09	2.33E-16	2.72E-10	1.49E-07
5.9	3.02E-04	4.70	1.00E-05	9.27	6.40	3.95E-07	0.00	1.25E-06	7.89E-06	1.25E-08	3.95E-16	1.56E-10	1.04E-07
6.0	3.02E-04	4.70	1.00E-05	9.07	6.58	2.62E-07	0.00	1.04E-06	8.30E-06	1.66E-08	6.59E-16	8.67E-11	7.11E-08
6.1	3.02E-04	4.70	1.00E-05	8.87	6.76	1.72E-07	0.00	8.63E-07	8.63E-06	2.17E-08	1.09E-15	4.69E-11	4.75E-08
6.2	3.02E-04	4.70	1.00E-05	8.67	6.95	1.12E-07	0.00	7.05E-07	8.88E-06	2.81E-08	1.77E-15	2.49E-11	3.13E-08
6.3	3.02E-04	4.70	1.00E-05	8.47	7.14	7.20E-08	0.00	5.72E-07	9.07E-06	3.61E-08	2.87E-15	1.30E-11	2.03E-08
6.4	3.02E-04	4.70	1.00E-05	8.27	7.34	4.61E-08	0.00	4.61E-07	9.21E-06	4.61E-08	4.61E-15	6.73E-12	1.31E-08
6.5	3.02E-04	4.70	1.00E-05	8.07	7.53	2.94E-08	0.00	3.70E-07	9.30E-06	5.87E-08	7.39E-15	3.45E-12	8.38E-09
6.6	3.02E-04	4.70	1.00E-05	7.87	7.73	1.87E-08	0.00	2.96E-07	9.37E-06	7.44E-08	1.18E-14	1.75E-12	5.32E-09
6.7	3.02E-04	4.70	1.00E-05	7.67	7.93	1.18E-08	0.00	2.36E-07	9.40E-06	9.40E-08	1.87E-14	8.83E-13	3.35E-09
6.8	3.02E-04	4.70	1.00E-05	7.47	8.13	7.46E-09	0.00	1.87E-07	9.39E-06	1.18E-07	2.97E-14	4.42E-13	2.10E-09
6.9	3.02E-04	4.70	1.00E-05	7.27	8.33	4.68E-09	0.00	1.48E-07	9.35E-06	1.48E-07	4.68E-14	2.19E-13	1.30E-09
7.0	3.02E-04	4.70	1.00E-05	7.07	8.53	2.93E-09	0.00	1.16E-07	9.25E-06	1.85E-07	7.35E-14	1.08E-13	7.89E-10
7.1	3.02E-04	4.70	1.00E-05	6.87	8.74	1.81E-09	0.00	9.09E-08	9.09E-06	2.28E-07	1.14E-13	5.21E-14	4.70E-10
7.2	3.02E-04	4.70	1.00E-05	6.67	8.95	1.11E-09	0.00	7.02E-08	8.83E-06	2.79E-07	1.76E-13	2.47E-14	

	UO_2CO_3^0	$\text{UO}_2(\text{CO}_3)_2^{2-}$	$\text{UO}_2(\text{CO}_3)_3^{4-}$	UO_2NO_3^+	$\text{UO}_2(\text{NO}_3)_2^0$	$\text{UO}_2(\text{NO}_3)_3^-$						
	log β 1001	log β 1002	log β 1003	log β 1011	log β 1012	log β 1013						
	8.87	16.07	21.60	-0.43	-1.66	0.50						
A	O	P	Q	R	S	T	U	V	W	X	Y	
									0.9999599	0.231784	0.93960876	
pH	[UO $_2$]	[U(CO $_3$) $_2$]	[U(CO $_3$) $_3$]	[UNO $_3$]	[U(NO $_3$) $_2$]	[U(NO $_3$) $_3$]	% Mf	pMc	% Uf	% UOH	% U(OH) $_2$	
1.0	6.31E-16	8.51E-28	2.45E-41	7.43E-11	1.49E-15	2.97E-20	1.00E+00	5.00	1.00E+00	3.98E-05	3.16E-09	
1.1	1.00E-15	2.14E-27	9.77E-41	7.43E-11	1.49E-15	2.97E-20	1.00E+00	5.00	1.00E+00	5.01E-05	5.01E-09	
1.2	1.58E-15	5.37E-27	3.89E-40	7.43E-11	1.49E-15	2.97E-20	1.00E+00	5.00	1.00E+00	6.31E-05	7.94E-09	
1.3	2.51E-15	1.35E-26	1.55E-39	7.43E-11	1.49E-15	2.97E-20	1.00E+00	5.00	1.00E+00	7.94E-05	1.26E-08	
1.4	3.98E-15	3.39E-26	6.17E-39	7.43E-11	1.49E-15	2.97E-20	1.00E+00	5.00	1.00E+00	1.00E-04	2.00E-08	
1.5	6.31E-15	8.51E-26	2.45E-38	7.43E-11	1.49E-15	2.97E-20	1.00E+00	5.00	1.00E+00	1.26E-04	3.16E-08	
1.6	1.00E-14	2.14E-25	9.77E-38	7.43E-11	1.49E-15	2.97E-20	1.00E+00	5.00	1.00E+00	1.58E-04	5.01E-08	
1.7	1.58E-14	5.37E-25	3.89E-37	7.43E-11	1.49E-15	2.97E-20	1.00E+00	5.00	1.00E+00	1.99E-04	7.94E-08	
1.8	2.51E-14	1.35E-24	1.55E-36	7.43E-11	1.49E-15	2.97E-20	1.00E+00	5.00	1.00E+00	2.51E-04	1.26E-07	
1.9	3.98E-14	3.39E-24	6.16E-36	7.43E-11	1.49E-15	2.97E-20	1.00E+00	5.00	1.00E+00	3.16E-04	1.99E-07	
2.0	6.31E-14	8.51E-24	2.45E-35	7.43E-11	1.49E-15	2.97E-20	1.00E+00	5.00	1.00E+00	3.98E-04	3.16E-07	
2.1	9.99E-14	2.14E-23	9.77E-35	7.43E-11	1.49E-15	2.97E-20	9.99E-01	5.00	9.99E-01	5.01E-04	5.01E-07	
2.2	1.58E-13	5.37E-23	3.89E-34	7.43E-11	1.49E-15	2.97E-20	9.99E-01	5.00	9.99E-01	6.31E-04	7.94E-07	
2.3	2.51E-13	1.35E-22	1.55E-33	7.42E-11	1.48E-15	2.97E-20	9.99E-01	5.00	9.99E-01	7.94E-04	1.26E-06	
2.4	3.98E-13	3.39E-22	6.16E-33	7.42E-11	1.48E-15	2.97E-20	9.99E-01	5.00	9.99E-01	9.99E-04	1.99E-06	
2.5	6.30E-13	8.50E-22	2.45E-32	7.42E-11	1.48E-15	2.97E-20	9.99E-01	5.00	9.99E-01	1.26E-03	3.16E-06	
2.6	9.98E-13	2.13E-21	9.76E-32	7.42E-11	1.48E-15	2.97E-20	9.98E-01	5.00	9.98E-01	1.58E-03	5.00E-06	
2.7	1.58E-12	5.36E-21	3.88E-31	7.42E-11	1.48E-15	2.97E-20	9.98E-01	5.00	9.98E-01	1.99E-03	7.93E-06	
2.8	2.51E-12	1.35E-20	1.54E-30	7.41E-11	1.48E-15	2.96E-20	9.97E-01	5.00	9.97E-01	2.51E-03	1.26E-05	
2.9	3.97E-12	3.38E-20	6.15E-30	7.41E-11	1.48E-15	2.96E-20	9.97E-01	5.00	9.97E-01	3.15E-03	1.99E-05	
3.0	6.28E-12	8.48E-20	2.44E-29	7.40E-11	1.48E-15	2.96E-20	9.96E-01	5.00	9.96E-01	3.96E-03	3.15E-05	
3.1	9.95E-12	2.13E-19	9.72E-29	7.39E-11	1.48E-15	2.96E-20	9.95E-01	5.00	9.95E-01	4.99E-03	4.99E-05	
3.2	1.57E-11	5.34E-19	3.87E-28	7.38E-11	1.48E-15	2.95E-20	9.94E-01	5.00	9.94E-01	6.27E-03	7.89E-05	
3.3	2.49E-11	1.34E-18	1.54E-27	7.37E-11	1.47E-15	2.95E-20	9.92E-01	5.00	9.92E-01	7.88E-03	1.25E-04	
3.4	3.94E-11	3.35E-18	6.10E-27	7.35E-11	1.47E-15	2.94E-20	9.90E-01	5.00	9.90E-01	9.90E-03	1.97E-04	
3.5	6.23E-11	8.40E-18	2.42E-26	7.33E-11	1.47E-15	2.93E-20	9.87E-01	5.01	9.87E-01	1.24E-02	3.12E-04	
3.6	9.83E-11	2.10E-17	9.61E-26	7.31E-11	1.46E-15	2.92E-20	9.83E-01	5.01	9.83E-01	1.56E-02	4.93E-04	
3.7	1.55E-10	5.26E-17	3.81E-25	7.27E-11	1.45E-15	2.91E-20	9.79E-01	5.01	9.79E-01	1.95E-02	7.78E-04	
3.8	2.44E-10	1.31E-16	1.51E-24	7.23E-11	1.45E-15	2.89E-20	9.73E-01	5.01	9.73E-01	2.44E-02	1.22E-03	
3.9	3.84E-10	3.27E-16	5.95E-24	7.17E-11	1.43E-15	2.87E-20	9.66E-01	5.02	9.66E-01	3.05E-02	1.93E-03	
4.0	6.03E-10	8.14E-16	2.35E-23	7.10E-11	1.42E-15	2.84E-20	9.56E-01	5.02	9.56E-01	3.81E-02	3.02E-03	
4.1	9.43E-10	2.02E-15	9.22E-23	7.01E-11	1.40E-15	2.80E-20	9.43E-01	5.03	9.43E-01	4.73E-02	4.73E-03	
4.2	1.47E-09	4.98E-15	3.61E-22	6.89E-11	1.38E-15	2.76E-20	9.27E-01	5.03	9.27E-01	5.85E-02	7.36E-03	
4.3	2.28E-09	1.22E-14	1.40E-21	6.73E-11	1.35E-15	2.69E-20	9.06E-01	5.04	9.06E-01	7.20E-02	1.14E-02	
4.4	3.50E-09	2.98E-14	5.42E-21	6.53E-11	1.31E-15	2.61E-20	8.79E-01	5.06	8.79E-01	8.79E-02	1.75E-02	
4.5	5.33E-09	7.19E-14	2.07E-20	6.27E-11	1.25E-15	2.51E-20	8.44E-01	5.07	8.44E-01	1.06E-01	2.67E-02	
4.6	8.01E-09	1.71E-13	7.83E-20	5.95E-11	1.19E-15	2.38E-20	8.01E-01	5.10	8.01E-01	1.27E-01	4.01E-02	
4.7	1.18E-08	4.01E-13	2.91E-19	5.55E-11	1.11E-15	2.22E-20	7.47E-01	5.13	7.47E-01	1.49E-01	5.94E-02	
4.8	1.72E-08	9.22E-13	1.06E-18	5.08E-11	1.02E-15	2.03E-20	6.83E-01	5.17	6.83E-01	1.72E-01	8.60E-02	
4.9	2.43E-08	2.07E-12	3.77E-18	4.54E-11	9.08E-16	1.82E-20	6.11E-01	5.21	6.11E-01	1.93E-01	1.22E-01	
5.0	3.35E-08	4.52E-12	1.30E-17	3.95E-11	7.89E-16	1.58E-20	5.31E-01	5.27	5.31E-01	2.11E-01	1.68E-01	
5.1	4.49E-08	9.59E-12	4.38E-17	3.33E-11	6.67E-16	1.33E-20	4.49E-01	5.35	4.49E-01	2.25E-01	2.25E-01	
5.2	5.82E-08	1.97E-11	1.43E-16	2.73E-11	5.46E-16	1.09E-20	3.67E-01	5.43	3.67E-01	2.32E-01	2.92E-01	
5.3	7.32E-08	3.93E-11	4.51E-16	2.17E-11	4.33E-16	8.66E-21	2.91E-01	5.54	2.91E-01	2.31E-01	3.67E-01	
5.4	8.92E-08	7.59E-11	1.38E-15	1.66E-11	3.33E-16	6.66E-21	2.24E-01	5.65	2.24E-01	2.24E-01	4.47E-01	
5.5	1.05E-07	1.42E-10	4.10E-15	1.24E-11	2.48E-16	4.96E-21	1.67E-01	5.78	1.67E-01	2.10E-01	5.28E-01	
5.6	1.21E-07	2.58E-10	1.18E-14	8.97E-12	1.79E-16	3.59E-21	1.21E-01	5.92	1.21E-01	1.91E-01	6.05E-01	
5.7	1.35E-07	4.57E-10	3.31E-14	6.32E-12	1.26E-16	2.53E-21	8.51E-02	6.07	8.51E-02	1.70E-01	6.76E-01	
5.8	1.47E-07	7.90E-10	9.07E-14	4.35E-12	8.70E-17	1.74E-21	5.86E-02	6.23	5.86E-02	1.47E-01	7.37E-01	
5.9	1.57E-07	1.34E-09	2.44E-13	2.94E-12	5.87E-17	1.17E-21	3.95E-02	6.40	3.95E-02	1.25E-01	7.89E-01	
6.0	1.66E-07	2.23E-09	6.44E-13	1.95E-12	3.90E-17	7.80E-22	2.62E-02	6.58	2.62E-02	1.04E-01	8.30E-01	
6.1	1.72E-07	3.68E-09	1.68E-12	1.28E-12	2.56E-17	5.12E-22	1.72E-02	6.76	1.72E-02	8.63E-02	8.63E-01	
6.2	1.77E-07	6.00E-09	4.35E-12	8.30E-13	1.66E-17	3.32E-22	1.12E-02	6.95	1.12E-02	7.05E-02	8.88E-01	
6.3	1.81E-07	9.72E-09	1.12E-11	5.35E-13	1.07E-17	2.14E-22	7.20E-03	7.14	7.20E-03	5.72E-02	9.07E-01	
6.4	1.84E-07	1.56E-08	2.85E-11	3.43E-13	6.86E-18	1.37E-22	4.61E-03	7.34	4.61E-03	4.61E-02	9.21E-01	
6.5	1.86E-07	2.50E-08	7.22E-11	2.19E-13	4.37E-18	8.75E-23	2.94E-03	7.53	2.94E-03	3.70E-02	9.30E-01	
6.6	1.87E-07	4.00E-08	1.83E-10	1.39E-13	2.78E-18	5.56E-23	1.87E-03	7.73	1.87E-03	2.96E-02	9.37E-01	
6.7	1.87E-07	6.35E-08	4.60E-10	8.79E-14	1.76E-18	3.52E-23	1.18E-03	7.93	1.18E-03	2.36E-02	9.40E-01	
6.8	1.87E-07	1.01E-07	1.16E-09	5.54E-14	1.11E-18	2.22E-23	7.46E-04	8.13	7.46E-04	1.87E-02	9.39E-01	
6.9	1.86E-07	1.59E-07	2.89E-09	3.48E-14	6.96E-19	1.39E-23	4.68E-04	8.33	4.68E-04	1.48E-02	9.35E-01	
7.0	1.85E-07	2.49E-07	7.18E-09	2.17E-14	4.35E-19	8.70E-24	2.93E-04	8.53	2.93E-04	1.16E-02	9.25E-01	
7.1	1.81E-07	3.88E-07	1.77E-08	1.35E-14	2.70E-19	5.39E-24	1.81E-04	8.74	1.81E-04	9.09E-03	9.09E-01	
7.2	1.76E-07	5.97E-07	4.33E-08	8.26E-15	1.65E-19	3.30E-24	1.11E-04	8.95	1.11E-04	7.02E-03	8.83E-01	

A	Z	AA	AB	AC	AD	AE	AF	AG	AH	AI	AJ
	0.04607	9.2E-08	0.000746	0.102611	0.01875	0.310618	0.99997	7.43E-06	1.486E-10	2.97E-15	
pH	% U(OH) ₂	% U(OH) ₄	% U ₂ OH	% U ₂ (OH) ₂	% UCO ₂	% U(CO ₂) ₂	% U(CO ₂) ₂	% UNO ₂	% U(NO ₂) ₂	% U(NO ₂) ₂	% sum
1.0	6.31E-17	2.51E-29	2.52E-07	3.03E-09	6.31E-11	8.51E-23	2.45E-36	7.43E-06	1.49E-10	2.97E-15	1.00E+00
1.1	1.26E-16	6.31E-29	3.17E-07	4.80E-09	1.00E-10	2.14E-22	9.77E-36	7.43E-06	1.49E-10	2.97E-15	1.00E+00
1.2	2.51E-16	1.58E-28	3.99E-07	7.60E-09	1.58E-10	5.37E-22	3.89E-35	7.43E-06	1.49E-10	2.97E-15	1.00E+00
1.3	5.01E-16	3.98E-28	5.02E-07	1.20E-08	2.51E-10	1.35E-21	1.55E-34	7.43E-06	1.49E-10	2.97E-15	1.00E+00
1.4	1.00E-15	1.00E-27	6.32E-07	1.91E-08	3.98E-10	3.39E-21	6.17E-34	7.43E-06	1.49E-10	2.97E-15	1.00E+00
1.5	2.00E-15	2.51E-27	7.96E-07	3.03E-08	6.31E-10	8.51E-21	2.45E-33	7.43E-06	1.49E-10	2.97E-15	1.00E+00
1.6	3.98E-15	6.31E-27	1.00E-06	4.80E-08	1.00E-09	2.14E-20	9.77E-33	7.43E-06	1.49E-10	2.97E-15	1.00E+00
1.7	7.94E-15	1.58E-26	1.26E-06	7.60E-08	1.58E-09	5.37E-20	3.89E-32	7.43E-06	1.49E-10	2.97E-15	1.00E+00
1.8	1.58E-14	3.98E-26	1.59E-06	1.20E-07	2.51E-09	1.35E-19	1.55E-31	7.43E-06	1.49E-10	2.97E-15	1.00E+00
1.9	3.16E-14	1.00E-25	2.00E-06	1.91E-07	3.98E-09	3.39E-19	6.16E-31	7.43E-06	1.49E-10	2.97E-15	1.00E+00
2.0	6.31E-14	2.51E-25	2.52E-06	3.02E-07	6.31E-09	8.51E-19	2.45E-30	7.43E-06	1.49E-10	2.97E-15	1.00E+00
2.1	1.26E-13	6.31E-25	3.17E-06	4.79E-07	9.99E-09	2.14E-18	9.77E-30	7.43E-06	1.49E-10	2.97E-15	1.00E+00
2.2	2.51E-13	1.58E-24	3.99E-06	7.59E-07	1.58E-08	5.37E-18	3.89E-29	7.43E-06	1.49E-10	2.97E-15	1.00E+00
2.3	5.01E-13	3.98E-24	5.02E-06	1.20E-06	2.51E-08	1.35E-17	1.55E-28	7.42E-06	1.48E-10	2.97E-15	1.00E+00
2.4	9.99E-13	9.99E-24	6.31E-06	1.91E-06	3.98E-08	3.39E-17	6.16E-28	7.42E-06	1.48E-10	2.97E-15	1.00E+00
2.5	1.99E-12	2.51E-23	7.94E-06	3.02E-06	6.30E-08	8.50E-17	2.45E-27	7.42E-06	1.48E-10	2.97E-15	1.00E+00
2.6	3.97E-12	6.30E-23	9.99E-06	4.78E-06	9.98E-08	2.13E-16	9.76E-27	7.42E-06	1.48E-10	2.97E-15	1.00E+00
2.7	7.93E-12	1.58E-22	1.26E-05	7.57E-06	1.58E-07	5.36E-16	3.88E-26	7.42E-06	1.48E-10	2.97E-15	1.00E+00
2.8	1.58E-11	3.97E-22	1.58E-05	1.20E-05	2.51E-07	1.35E-15	1.54E-25	7.41E-06	1.48E-10	2.96E-15	1.00E+00
2.9	3.15E-11	9.97E-22	1.99E-05	1.90E-05	3.97E-07	3.38E-15	6.15E-25	7.41E-06	1.48E-10	2.96E-15	1.00E+00
3.0	6.28E-11	2.50E-21	2.50E-05	3.00E-05	6.28E-07	8.48E-15	2.44E-24	7.40E-06	1.48E-10	2.96E-15	1.00E+00
3.1	1.25E-10	6.28E-21	3.14E-05	4.75E-05	9.95E-07	2.13E-14	9.72E-24	7.39E-06	1.48E-10	2.96E-15	1.00E+00
3.2	2.50E-10	1.57E-20	3.94E-05	7.51E-05	1.57E-06	5.34E-14	3.87E-23	7.38E-06	1.48E-10	2.95E-15	1.00E+00
3.3	4.97E-10	3.95E-20	4.94E-05	1.19E-04	2.49E-06	1.34E-13	1.54E-22	7.37E-06	1.47E-10	2.95E-15	1.00E+00
3.4	9.90E-10	9.90E-20	6.19E-05	1.87E-04	3.94E-06	3.35E-13	6.10E-22	7.35E-06	1.47E-10	2.94E-15	1.00E+00
3.5	1.97E-09	2.48E-19	7.75E-05	2.95E-04	6.23E-06	8.40E-13	2.42E-21	7.33E-06	1.47E-10	2.93E-15	1.00E+00
3.6	3.91E-09	6.20E-19	9.69E-05	4.64E-04	9.83E-06	2.10E-12	9.61E-21	7.31E-06	1.46E-10	2.92E-15	1.00E+00
3.7	7.78E-09	1.55E-18	1.21E-04	7.29E-04	1.55E-05	5.26E-12	3.81E-20	7.27E-06	1.45E-10	2.91E-15	1.00E+00
3.8	1.54E-08	3.87E-18	1.50E-04	1.14E-03	2.44E-05	1.31E-11	1.51E-19	7.23E-06	1.45E-10	2.89E-15	1.00E+00
3.9	3.05E-08	9.66E-18	1.86E-04	1.78E-03	3.84E-05	3.27E-11	5.95E-19	7.17E-06	1.43E-10	2.87E-15	1.00E+00
4.0	6.03E-08	2.40E-17	2.30E-04	2.77E-03	6.03E-05	8.14E-11	2.35E-18	7.10E-06	1.42E-10	2.84E-15	1.00E+00
4.1	1.19E-07	5.95E-17	2.82E-04	4.27E-03	9.43E-05	2.02E-10	9.22E-18	7.01E-06	1.40E-10	2.80E-15	1.00E+00
4.2	2.33E-07	1.47E-16	3.43E-04	6.54E-03	1.47E-04	4.98E-10	3.61E-17	6.89E-06	1.38E-10	2.76E-15	1.00E+00
4.3	4.54E-07	3.61E-16	4.12E-04	9.89E-03	2.28E-04	1.22E-09	1.40E-16	6.73E-06	1.35E-10	2.69E-15	1.00E+00
4.4	8.79E-07	8.79E-16	4.89E-04	1.48E-02	3.50E-04	2.98E-09	5.42E-16	6.53E-06	1.31E-10	2.61E-15	1.00E+00
4.5	1.68E-06	2.12E-15	5.68E-04	2.16E-02	5.33E-04	7.19E-09	2.07E-15	6.27E-06	1.25E-10	2.51E-15	1.00E+00
4.6	3.19E-06	5.05E-15	6.43E-04	3.08E-02	8.01E-04	1.71E-08	7.83E-15	5.95E-06	1.19E-10	2.38E-15	1.00E+00
4.7	5.94E-06	1.18E-14	7.05E-04	4.25E-02	1.18E-03	4.01E-08	2.91E-14	5.55E-06	1.11E-10	2.22E-15	1.00E+00
4.8	1.08E-05	2.72E-14	7.42E-04	5.63E-02	1.72E-03	9.22E-08	1.06E-13	5.08E-06	1.02E-10	2.03E-15	1.00E+00
4.9	1.93E-05	6.11E-14	7.46E-04	7.12E-02	2.43E-03	2.07E-07	3.77E-13	4.54E-06	9.08E-11	1.82E-15	1.00E+00
5.0	3.35E-05	1.33E-13	7.10E-04	8.54E-02	3.35E-03	4.52E-07	1.30E-12	3.95E-06	7.89E-11	1.58E-15	1.00E+00
5.1	5.65E-05	2.83E-13	6.38E-04	9.65E-02	4.49E-03	9.59E-07	4.38E-12	3.33E-06	6.67E-11	1.33E-15	1.00E+00
5.2	9.23E-05	5.82E-13	5.39E-04	1.03E-01	5.82E-03	1.97E-06	1.43E-11	2.73E-06	5.46E-11	1.09E-15	1.00E+00
5.3	1.46E-04	1.16E-12	4.27E-04	1.02E-01	7.32E-03	3.93E-06	4.51E-11	2.17E-06	4.33E-11	8.66E-16	1.00E+00
5.4	2.24E-04	2.24E-12	3.17E-04	9.58E-02	8.92E-03	7.59E-06	1.38E-10	1.66E-06	3.33E-11	6.66E-16	1.00E+00
5.5	3.33E-04	4.19E-12	2.22E-04	8.43E-02	1.05E-02	1.42E-05	4.10E-10	1.24E-06	2.48E-11	4.96E-16	1.00E+00
5.6	4.81E-04	7.62E-12	1.46E-04	7.00E-02	1.21E-02	2.58E-05	1.18E-09	8.97E-07	1.79E-11	3.59E-16	1.00E+00
5.7	6.76E-04	1.35E-11	9.13E-05	5.50E-02	1.35E-02	4.57E-05	3.31E-09	6.32E-07	1.26E-11	2.53E-16	1.00E+00
5.8	9.28E-04	2.33E-11	5.45E-05	4.13E-02	1.47E-02	7.90E-05	9.07E-09	4.35E-07	8.70E-12	1.74E-16	1.00E+00
5.9	1.25E-03	3.95E-11	3.12E-05	2.98E-02	1.57E-02	1.34E-04	2.44E-08	2.94E-07	5.87E-12	1.17E-16	1.00E+00
6.0	1.66E-03	6.59E-11	1.73E-05	2.09E-02	1.66E-02	2.23E-04	6.44E-08	1.95E-07	3.90E-12	7.80E-17	1.00E+00
6.1	2.17E-03	1.09E-10	9.39E-06	1.42E-02	1.72E-02	3.68E-04	1.68E-07	1.28E-07	2.56E-12	5.12E-17	1.00E+00
6.2	2.81E-03	1.77E-10	4.98E-06	9.50E-03	1.77E-02	6.00E-04	4.35E-07	8.30E-08	1.66E-12	3.32E-17	1.00E+00
6.3	3.61E-03	2.87E-10	2.61E-06	6.25E-03	1.81E-02	9.72E-04	1.12E-06	5.35E-08	1.07E-12	2.14E-17	1.00E+00
6.4	4.61E-03	4.61E-10	1.35E-06	4.07E-03	1.84E-02	1.56E-03	2.85E-06	3.43E-08	6.86E-13	1.37E-17	1.00E+00
6.5	5.87E-03	7.39E-10	6.89E-07	2.62E-03	1.86E-02	2.50E-03	7.22E-06	2.19E-08	4.37E-13	8.75E-18	1.00E+00
6.6	7.44E-03	1.18E-09	3.50E-07	1.68E-03	1.87E-02	4.00E-03	1.83E-05	1.39E-08	2.78E-13	5.56E-18	1.00E+00
6.7	9.40E-03	1.87E-09	1.77E-07	1.06E-03	1.87E-02	6.35E-03	4.60E-05	8.79E-09	1.76E-13	3.52E-18	1.00E+00
6.8	1.18E-02	2.97E-09	8.84E-08	6.71E-04	1.87E-02	1.01E-02	1.16E-04	5.54E-09	1.11E-13	2.22E-18	1.00E+00
6.9	1.48E-02	4.68E-09	4.39E-08	4.19E-04	1.86E-02	1.59E-02	2.89E-04	3.48E-09	6.96E-14	1.39E-18	1.00E+00
7.0	1.85E-02	7.35E-09	2.16E-08	2.59E-04	1.85E-02	2.49E-02	7.18E-04	2.17E-09	4.35E-14	8.70E-19	1.00E+00
7.1	2.28E-02	1.14E-08	1.04E-08	1.58E-04	1.81E-02	3.88E-02	1.77E-03	1.35E-09	2.70E-14	5.39E-19	1.00E+00
7.2	2.79E-02	1.76E-08	4.93E-09	9.40E-05	1.76E-02	5.97E-02	4.33E-03	8.26E-10	1.65E-14	3.30E-19	1.00E+00

Appendix C-3: Cell Formulas for Uranium Speciation Data

Column A: pH = independent variable

Column B: $ppCO_2 = 10^{-3.52}$

Column C: $p[NO_3^-]f = -1 * \log[NO_3^-]$

Column D: $[UO_2]_T = 1 \times 10^{-5}$

Column E: $p[CO_3]f = -1 * (\log K_{sum} + \log(ppCO_2) + 2pH)$

Column F: $pM = pM_c$

Column G: $[UO_2^{2+}] = 10^{-pM}$

Column H: $\Delta pM = pM - pM_c$

Column I: $[UOH] = 10 \exp(-)[pM + (pK_w - pH) - (\log K_{10-10} + pK_w)]$

Column J: $[U(OH)_2] = 10 \exp(-)[pM + 2(pK_w - pH) - (\log K_{10-20} + 2pK_w)]$

Column K: $[U(OH)_3] = 10 \exp(-)[pM + 3(pK_w - pH) - (\log K_{10-30} + 3pK_w)]$

Column L: $[U(OH)_4] = 10 \exp(-)[pM + 4(pK_w - pH) - (\log K_{10-40} + 4pK_w)]$

Column M: $[U_2OH] = 10 \exp(-)[2pM + (pK_w - pH) - (\log K_{20-10} + pK_w)]$

Column N: $[U_2(OH)_2] = 10 \exp(-)[2pM + 2(pK_w - pH) - (\log K_{20-20} + 2pK_w)]$

Column O: $[UCO_3] = 10 \exp(-)[pM + p[CO_3]f - \log \beta_{10-01}]$

Column P: $[U(CO_3)_2] = 10 \exp(-)[pM + 2p[CO_3]f - \log \beta_{10-02}]$

Column Q: $[U(CO_3)_3] = 10 \exp(-)[pM + 3p[CO_3]f - \log \beta_{10-03}]$

Column R: $[UNO_3] = 10 \exp(-)[pM + p[NO_3]f - \log \beta_{10-11}]$

Column S: $[U(NO_3)_2] = 10 \exp(-)[pM + 2p[NO_3]f - \log \beta_{10-12}]$

Column T: $[U(NO_3)_3] = 10 \exp(-)[pM + 3p[NO_3]f - \log \beta_{10-13}]$

Column U:
$$\%M_f = \frac{10^{-pM}}{\left[10^{-pM} + \sum_{x=1}^4 [U(OH)_x] + 2 \sum_{y=1}^2 [U_2(OH)_y] + \sum_{z=1}^3 [U(CO_3)_z] + \sum_{w=1}^3 [U(NO_3)_w] \right]}$$

Column V: $pM_c = -\log(\%M_f * [UO_2]_T)$

Column W: $\%U_f = \frac{10^{-pM}}{[UO_2]_T}$

Column X: $\%UOH = \frac{[UOH]}{[UO_2]_T}$

Column Y: $\%U(OH)_2 = \frac{[U(OH)_2]}{[UO_2]_T}$

Column Z: $\%U(OH)_3 = \frac{[U(OH)_3]}{[UO_2]_T}$

Column AA: $\%U(OH)_4 = \frac{[U(OH)_4]}{[UO_2]_T}$

Column AB: $\%U_2OH = \frac{[U_2OH]}{[UO_2]_T}$

Column AC: $\%U_2(OH)_2 = \frac{[U_2(OH)_2]}{[UO_2]_r}$

Column AD: $\%UCO_3 = \frac{[UCO_3]}{[UO_2]_r}$

Column AE: $\%U(CO_3)_2 = \frac{[U(CO_3)_2]}{[UO_2]_r}$

Column AF: $\%U(CO_3)_3 = \frac{[U(CO_3)_3]}{[UO_2]_r}$

Column AG: $\%UNO_3 = \frac{[UNO_3]}{[UO_2]_r}$

Column AH: $\%U(NO_3)_2 = \frac{[U(NO_3)_2]}{[UO_2]_r}$

Column AI: $\%U(NO_3)_3 = \frac{[U(NO_3)_3]}{[UO_2]_r}$

Column AJ:

$$\%sum = \left[\%U_f + \sum_{x=1}^4 \%U(OH)_n + \sum_{y=1}^2 \%U_2(OH)_n + \sum_{z=1}^3 \%U(CO_3)_n + \sum_{w=1}^3 \%U(NO_3)_n \right]$$

Definition of Constants:

$[NO_3^-] = 2 \times 10^{-5}$	= concentration of free nitrate ions [experiment].
$pK_{a1_{CO_3}} = 6.3$	= equilibrium constant for carbonate ions [5-3].
$\log K_{sum} = -17.55$	= summation of equilibrium constants for hydroxide [5-3].
$pK_w = 13.92$	= $pOH^- + pH^+$ [5-3].
$\log K_{10-10} = -5.40$	= equilibrium constant for UO_2OH^+
$\log K_{10-20} = -10.50$	= equilibrium constant for $UO_2(OH)_2^0$
$\log K_{10-30} = -19.20$	= equilibrium constant for $UO_2(OH)_3^-$
$\log K_{10-40} = -32.60$	= equilibrium constant for $UO_2(OH)_4^{2-}$
$\log K_{20-10} = -2.90$	= equilibrium constant for $(UO_2)_2OH^{3-}$
$\log K_{20-20} = -5.82$	= equilibrium constant for $(UO_2)_2(OH)_2^{2-}$
$\log \beta_{10-01} = 8.87$	= stability constant for $UO_2CO_3^0$
$\log \beta_{10-02} = 16.07$	= stability constant for $UO_2(CO_3)_2^{2-}$
$\log \beta_{10-03} = 21.60$	= stability constant for $UO_2(CO_3)_3^{4-}$
$\log \beta_{10-11} = -0.43$	= stability constant for $UO_2NO_3^+$
$\log \beta_{10-12} = -1.66$	= stability constant for $UO_2(NO_3)_2^0$
$\log \beta_{10-13} = 0.50$	= stability constant for $UO_2(NO_3)_3^-$